The footwall to the West Cycladic Detachment System on Kythnos, Western Cyclades, Greece; a field guide

A. Hugh N. Rice, Bernhard Grasemann

Journal of the VIRTUAL EXPLORER, Electronic Edition, ISSN 1441-8142, volume 50, Paper 2, In: (Eds.) Adamantios Kilias, Stylianos Lozios, Geological field trips in the Hellenides, 2018

Journal of the VIRTUAL EXPLORER

A dynamic review electronic Earth Science journal publishing material from all continents

The footwall to the West Cycladic Detachment System on Kythnos, Western Cyclades, Greece; a field guide

A. Hugh N. Rice, Bernhard Grasemann

[1]University of Vienna, Dept. Geodynamics & Sedimentology, Geozentrum, Althanstrasse 14, 1090 Vienna, Austria

GUIDE INFO

Keywords
Hellenides
Cyclades
West Cycladic Detachment
Kythnos

Citation
Rice, A.H.N., Grasemann, B., 2018. The footwall to the West Cycladic Detachment System on Kythnos, Western Cyclades, Greece; a field guide In: (Eds.) Kilias, A., Lozios, S., Geological field trips in the Hellenides, Journal of the Virtual Explorer, Electronic Edition, ISSN 1441-8142, volume 50, paper 2, doi: 10.3809/jvirtex.2016.08692

Correspondence to:
alexander.hugh.rice@univie.ac.at

IN THIS GUIDE

Kythnos lies between Kea and Serifos in the Western Cyclades, both of which were critical in developing an understanding of the Miocene top-to-the-SSW deformation associated with the West Cycladic Detachment System (WCDS). On Kythnos, the Cycladic Blueschist Unit (CBU; WCDS footwall; probable metamorphosed equivalent to the Pindos Unit) preserves relict parageneses of an M1 Eocene blueschist-facies peak metamorphism within retrograde greenschist facies assemblages. The north and east of the island have an ENE-WSW trending structural grain of M1 age; this gradually rotates to a NNE-SSW trend in the south and west, associated with Miocene M2 movement on the WCDS. The structural evolution also reflects extensional deformation during cooling, from the ductile to brittle fields.

Southern Kythnos has a well-defined lithostratigraphy (de Smeth 1975) of epidote schists with rare marble conglomerates (Kanala Formation) overlain by sericite-quartz-albite-graphite schists with some Cr-rich mica/chlorite layers (Upper & Lower Flabouria Formations). Between these sericite-quartz-albite-graphite schist formations, blue-grey calcite marble mylonites and quartz–white-mica–calcite schists/mylonites occur (Petroussa Formation); the blue-grey marble thins from ~14 m thick in SE Kythnos to one or more layers, each <0.75 m thick, near the WCDS in SW Kythnos.

Another unit of quartz–white-mica–calcite schists/mylonites with lenses/boudins of blue-grey marble mylonites/ultramylonites (Mavrianou Formation) occurs along the west coast of southern Kythnos, overlying the Upper Flabouria Formation; these are similar to the high-strain part of the Petroussa Formation and are locally overlain by epidote schists (Episkopi Formation). However, the distribution of the Mavrianou Formation on the crest of southern Kythnos is different to that proposed by de Smeth (1975), with several isolated small outcrops.

An impure grey-brown to blue-grey calcite marble (ultra)mylonite (Rizou Formation) lies directly under the WCDS in SW Kythnos, underlain by albite "gneisses" (Laner 2009, Lenauer 2009); this is possibly equivalent to the Mavrianou Formation.

The application of this stratigraphy becomes more uncertain in the northern half of the island.

The WCDS comprises marble ultramylonites (Rizou Formation), with top-to-the-SSW shear criteria, overlain on a sharp detachment surface by brittle-deformed quartzites (Aghios Dimitrios Formation), taken to be part of the Upper Cycladic Unit (Pelagonian Unit; although it might be an imbricate of the Cycladic Blueschist Unit). Calcite-quartzite ultracataclasites are locally developed at the detachment surface

INTRODUCTION

This field guide comprises six one-day excursions that show both the regional lithostratigraphy of the Upper Cycladic Unit and Cycladic Blueschist Unit (CBU) on Kythnos and the structures that formed within them during exhumation of the latter from HP-conditions and subsequent extension under and within the WCDS. The excursion Stops are also given in the attached *Excursion.kmz file.* Further outcrop descriptions, including some outcrops viewed from the inter-island ferries, are given in an appendix excursion guide; these are also available on-line (*a-Excursion.kmz*).

Note that Figs. A-H refer to figures described in the introductory text; Figs. 1 to 6.8 and a-Fig. 1.8 to a-Fig. 7.7 refer to those described in the excursion guide and appendix-excursion guide, respectively, with the figure number being the same as the stop number in the text.

GEOLOGY OF THE CYCLADES

The Cycladic islands, which lie in the central to southern part of the Aegean Sea, belong to the polymetamorphic terranes of the Attic-Cycladic Crystalline Complex, within the central part of the Hellenide-Tauride mountain belt (Fig. A). This formed due to the essentially continuous convergence of Africa and Eurasia since the Late Cretaceous (Bonneau & Kienast 1982, Jolivet & Brun 2010, Ring et al. 2010, Menant et al. 2016). The Cyclades are characterized by two tectono-metamorphic episodes. The first event, M1, comprised crustal thickening and high-pressure/low-temperature metamorphism associated with the Eocene subduction of the Adriatic continental micro-plate below the Eurasian plate (Altherr et al. 1979, 1982, Maluski et al. 1987, Wijbrans et al. 1988, Bröcker & Enders 1999). The second event, M2, corresponds to Oligocene and Miocene back-arc extension, caused by the southwards retreat of the Hellenic subduction zone, which now lies south of Crete. M2 was characterized by crustal thinning, due to the development of three crustal-scale low-angled normal faults (Fig. A): the Naxos-Paros Detachment (Lister et al. 1984, Gautier et al. 1993) and the North and West Cycladic Detachment Systems (Jolivet et al. 2010, Grasemann et al. 2012). Ring et al. (2011) proposed the existence of a South Cycladic Detachment System on Sifnos; this might be a lateral extension of the West Cycladic Detachment System.

In the Cyclades, three major tectono-metamorphic units have been described (Bonneau 1984; Fig. A): (i) The Cycladic Basement Unit, which consists of granite, paragneiss and orthogneiss, shows a complex polyphase pre-Alpine metamorphic history (Andriessen et al. 1987). (ii) The CBU, which consists of a sequence of metapelites, metabasites and marbles. This is believed to be equivalent to the Pindos Zone, which corresponds to a basin on the northern margin of the Adriatic plate, with thinned continental and also partly oceanic crust (Bonneau & Kienast 1982). (iii) The Upper Cycladic Unit, which consists of various lithologies, including ophiolitic material partly metamorphosed by a probable early late Cretaceous HP-episode (Huet et al. 2015) and a well-documented latest Cretaceous HT event; this unit has been correlated with the Pelagonian Unit (Maluski et al. 1987, Katzir et al. 1996, Soukis & Stockli 2013).

Grasemann et al. (2018; Jolivet pers. comm. 2018) divided the CBU into two parts, separated by the Trans Cycladic Thrust (Fig. A), which formed during exhumation from the Eocene subduction-channel. The footwall to this thrust, the Lower Cycladic Blueschist Nappe, including Kythnos, occurs in the southwest of the Cyclades and underwent M1 P-T conditions of 400 ±20°C, 10 ±2 kbar. The hanging wall, the Upper Cycladic Blueschist Nappe, which lies in the northwest, underwent P-T conditions of 550 ±50°C, 20 ±2 kbar, reflecting burial to, and subsequent exhumation from a deeper level.

The WCDS, which can be traced over a length of more than 100 km, from Lavrion (Attica) to Sifnos, is exposed on the intervening islands of Makronisos, Kea, Kythnos and Serifos (Grasemann & Petrakakis 2007, Bricheau et al. 2010, Iglseder et al. 2011, Grasemann et al. 2012, 2017, Berger et al. 2013, Rice et al. 2012, Scheffer et al. 2016, Huet et al. 2013; Fig. A). A typical structural profile across the WCDS reveals an increasing strain gradient upwards in the footwall, towards the detachment surface. Whereas this strain gradient is localized to within a few tens of metres of the WCDS on Serifos, it is much more distributed on Makronisos, Kea and to a lesser degree on Kythnos. Close to the detachment surface, the deformation occurs within marble ultramylonites up to several tens of metres thick, topped by a knife-sharp detachment surface, with evidence for brittle-ductile deformation mechanisms. Above this surface, there is an up to 0.5 m thick zone of polyphase ultracataclasites. The hanging wall consists of protocataclasites of various lithologies, in-

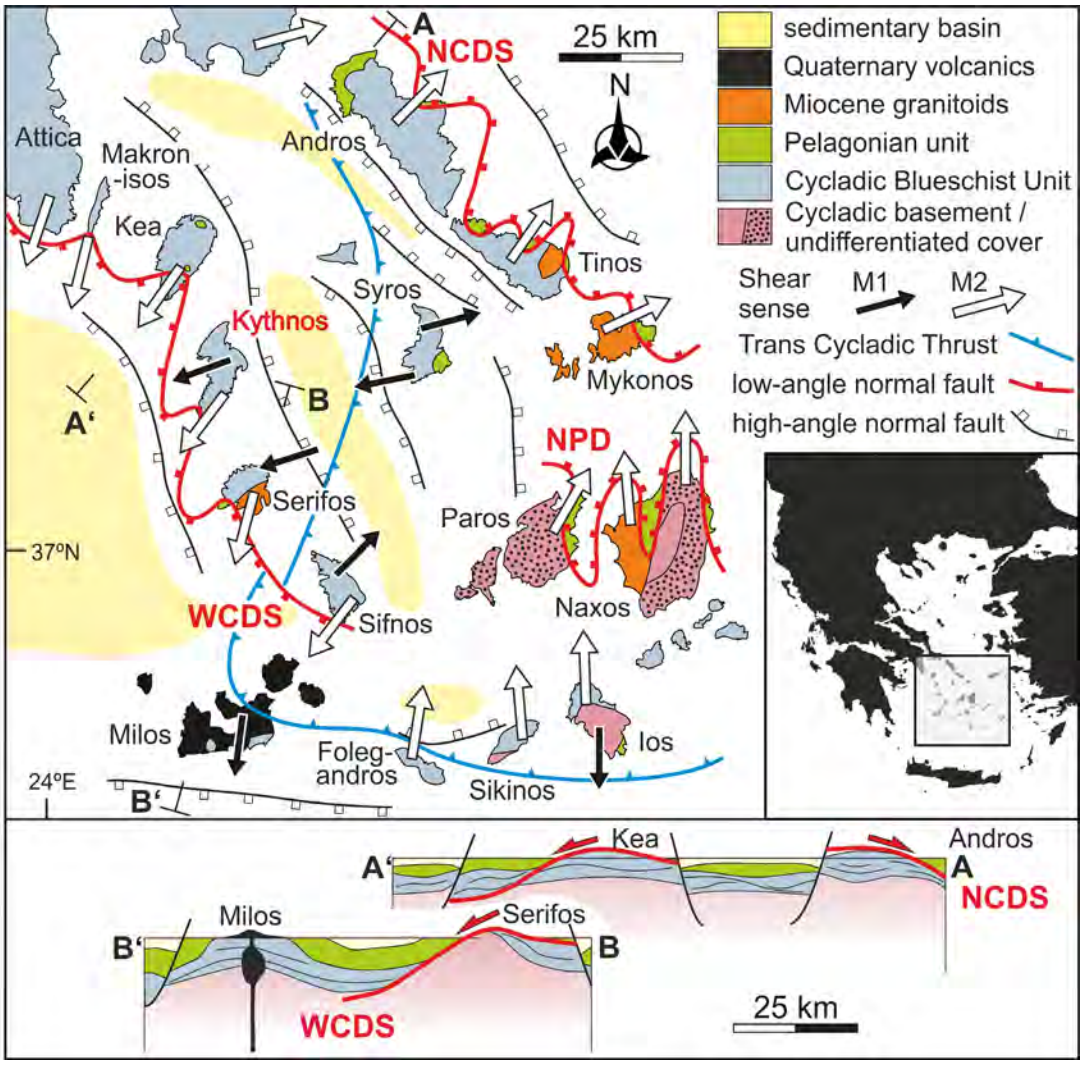

Figure A
Tectonic map of the Cyclades, showing the main tectono-metamorphic units (Gautier & Brun 1994, Huet et al. 2009, Jolivet et al. 2010, Grasemann et al. 2012, 2017, Jolivet et al. 2015). NCDS: North Cycladic Detachment System. WCDS: West Cycladic Detachment System. NPD: Naxos-Paros Detachment: Black arrows: Eocene crustal thickening kinematics. White arrows: Miocene crustal thinning kinematics.

cluding dolostones and occasional serpentinites, partly overprinted by hydrothermal alteration and mineralization (Berger et al. 2013, Rabillard et al. 2015). The kinematics of all brittle and ductile indicators reveal a very consistent top-to-the-SW to -SSW shear-sense. The exact time of the onset of extension is unclear, but c. 20-17 Ma $^{40}Ar/^{39}Ar$ ages on fabric-forming white-micas from Kea and Kythnos suggest that ductile movement along the WCDS was active in the Early Miocene (Grasemann et al. 2012). Timing of the activity of the WCDS is also constrained by the emplacement of the Serifos granodiorite between 11.6 and 9.5 Ma (Iglseder et al. 2009), which pierced a structurally deeper branch of the detachment (Grasemann & Tschegg 2012) whilst the roof of the pluton is cut by a structurally higher branch, post-dating the intrusion (Tschegg & Grasemann 2009, Rabillard et al. 2015).

GEOLOGY OF KYTHNOS

The Kythnos lies in the central part of the Western Cyclades, with Serifos to the southeast and Kea to the northwest, with a coastline that almost seems 'fjord-like' in places. The island is 21 km long N-S and 11 km wide E-W, with an area of 100.2 km^2 and a maximum altitude of 297 m a.s.l. The southern and eastern parts of the island are relatively well-developed, with a good road network, whilst the north and northwest is more difficult to access and topographically very steep in the coastal parts. The resident population is ~700 persons.

Although the neighbouring islands have received some geological attention in the past few years (Kea: Iglseder et al. 2011, Rice et al. 2013, Serifos: Grasemann & Petrakakis 2007, Tschegg & Grasemann 2009, Iglseder et al. 2009, Brichau et al. 2010, Grasemann & Tschegg 2012, Rabillard

et al. 2015), Kythnos has been mentioned in recent literature only in a reconnaissance structural study (Keiter et al. 2008), an overview of the Western Cyclades (Grasemann et al. 2012) and a few conference presentations (e.g. Lenauer et al. 2009, Rice & Grasemann 2012). Older sources of information include Chrysanthaki et al. (2003) and Schliestedt et al. (1994) and the geological map of de Smeth (1975; Fig. B). This map has been modified in the extreme southwest by Laner (2009) and Lenauer (2009) and elsewhere by our observations (Fig. C).

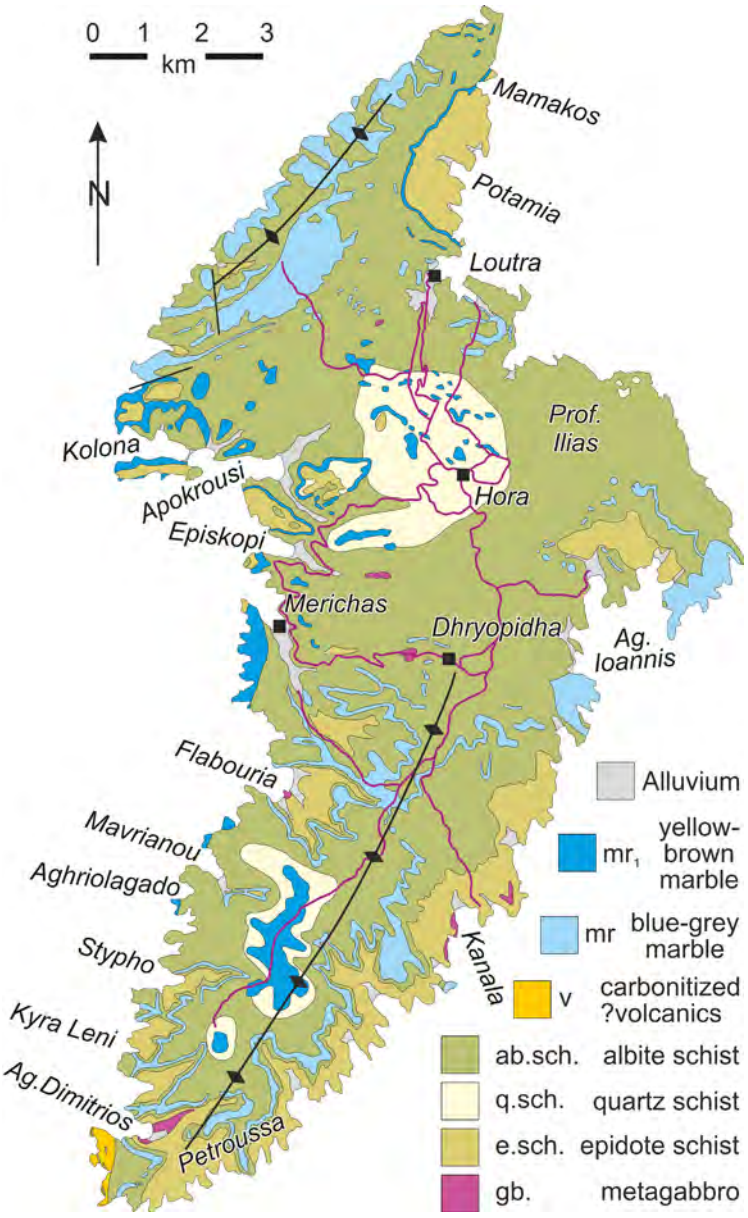

Figure B
Geological map of Kythnos by de Smeth (1975). Main roads in 1975 shown.

The outcrop pattern of Kythnos, which is predominantly composed of metapelitic schists and blue-grey marbles of the Cycladic Blueschist Unit (de Smeth 1975), is dominated by two NNW-SSE trending large-scale en-echelon antiforms (de Smeth 1975); the southeastern structure is here termed the Merovighli Antiform and the northwestern structure the Kakovolo Antiform (Fig. C). In the southern part of the island, de Smeth (1975; Fig. B) shows six lithologies (apart from Alluvium; Table 1), that only in part form a lithostratigraphy. The revisions proposed here are given in Table 2.

The epidote schists (here the Kanala Formation) forming the base of the succession have not been studied in detail by us. Generally, they are green coloured, reflecting a high epidote/chlorite content, and well foliated. In some areas, the rock comprises layers of coarse (<1cm) subidioblastic to idioblastic epidote porphyroblasts (Fig. D; Stop a-5.9). These are randomly oriented (no stretching or mineral lineation developed) and are not, or are only weakly wrapped by the main foliation. The matrix compositional banding of epidote rich and poor bands (or of epidote porphyroblast grain sizes) is parallel to the foliation, where discernable. White to medium grey carbonate layers occur within the Kanala Formation. More rarely, a marble conglomerate is present; prolate clasts of calcite marble with the X and Y-directions up to 2 cm in size and Z up to perhaps 20 cm long lie within a foliated and compositionally layered greenschist matrix (Stops 3.2, 4.4). Clast long-axes are parallel to the matrix stretching lineation direction. The three known outcrops of the marble conglomerate are shown on Fig. C. Although similar conglomerates also occur in the Northern Cyclades and on Serifos in the Western Cyclades, they have not yet been found on Kea.

The schists in the Kanala Formation are interpreted to have an intermediate to mafic volcanoclastic origin, most likely (partially) reworked/redeposited from other volcanic deposits. Correlation of the marble conglomerate outcrops is unlikely; thin conglomerate layers within volcanoclastic rocks are probably not laterally persistent but represent local, high-energy deposits from a relatively proximal coarse-grained source. If this is the case, then the rhythmic mineral layering within the matrix schists must have been tectonically/metamorphically induced.

A lithologically identical unit of epidote schists (here the Episkopi Formation; Fig. C), including one marble conglomerate outcrop, occurs in the Merichas-Kolona-Potamia area, at the highest

Table 1
Lithologies of de Smeth (1975; Fig. B)

UNIT	LITHOLOGY
mr1	Marbles : yellow-brown marbles; calcite with large amounts of muscovite, quartz, albite etc.
mr	Marbles : grey-blue marbles with only small quantities of muscovite and quartz. Frequently iron mineralisation along joints.
v	Carbonatized (Volcanic?) rocks : iron-rich rocks with quartz and chlorite. Only on the southern tip of the island.
ab. sch	Albite-quartz-muscovite-chlorite schists : the principal type is chlorite-sericite schists and small horizons of dark purple albite-chlorite-sericite schists, all with calcite, sphene, magnetite etc.
q. sch	Quartz-muscovite and chlorite schists : small horizon directly below the yellow-brown marble, which occupy the central part of the island.
e. sch	Epidote-zoisite schists : with light purple albite, chlorite, sericite, quartz, calcite, hematite and tourmaline.
gb.	Metamorphic gabbroic rocks: for the most part, completely serpentinized and chloritized with asbestos veins and talc: sometimes with relics of brown hornblende or completely altered to talc-chlorite schists with idiomorphic magnetite crystals.

lithostratigraphic level (Stops 1.5, 1.6).

The albite schists (here the Upper and Lower Flabouria Formations, separated by a marble/calc-schist unit; Fig. C) consist of medium to dark grey, white-mica-rich (or sericite where fine-grained) metapelitic schists. Graphite is ubiquitous and in some places is highly concentrated, forming layers up to 2 cm thick. Xenoblastic to subidioblastic albite porphyroblasts up to 2 mm in size are often extremely abundant (Stops 1.1, 2.3); these are black, due to graphite inclusions. Locally, chlorite schists also occur within the albite schists (Stop 1.3). Thin layers (1 mm to rarely 2 cm) of bright green schist occur frequently within the grey schists (Stop 1.1); the colour suggests a high Cr content, either within white-mica or chlorite. Despite their thinness, these layers can often be followed for several metres before dying out (Stop 1.2). Small lenses (metre scale), likely boudins, of grey to white marble, sometimes mylonitic and with thin quartzite layers also occur within the Upper and Lower Flabouria Formations (a-Stop 1.9, Stops 2.6. 4.6). Several generations of quartz-veins are present, from foliation parallel early veins, typically deformed into pinch-and-swell boudins with an obvious stretching lineation, to thick, foliation-oblique late veins that have a blocky appearance and do not carry a stretching lineation.

The thin quartz schist described by de Smeth (1975; Fig. B, Table 1) is problematic. In the south of the island, much of the area shown as this unit comprises grey metapelitic schists; differentiating these (assuming there is a difference) from the underlying albite schists of the Upper Flabouria Formation, on the basis of a lack of albite, is difficult, as not all of the Upper Flabouria Formation has macroscopic albite porphyroblasts. Further, the mapped boundary between the quartz schist and albite schists in the south is in some places parallel and elsewhere at a high angle to the contours (de Smeth 1975; Fig. B), implying either undocumented folding/boudinage or that the mapped boundary is not parallel to an originally sub-horizontal bedding. Thus much of the quartz schist of de Smeth (1975) is here included in the Upper Flabouria Formation, if they appear similar (Fig. C); the rest is discussed further with the marbles.

Elsewhere, especially around Hora and to the northwest and northeast, the quartz schists of de Smeth (1975) comprise yellow-weathered quartz–white-mica–calcite schists (Stop 1.1a). These are, again, discussed further with the marbles.

The greatest difficulties with the map of de Smeth (1975) lie with the marbles; the problems are documented in some detail here, since they are referred to in the guide. de Smeth (1975) defined two marble units (Fig. B, Table 1).

(a) A lower marble (mr of de Smeth 1975; here the Petroussa Formation) that includes a distinctive blue-grey marble. The outcrop pattern of this unit highlights the Merovighli Antiform of southern Kythnos and forms large outcrops along northwestern and eastern Kythnos on the map of de Smeth (1975; Fig. B). In the north of the island, and seemingly also sometimes in the south (but not always), de Smeth (1975) included in mr the yellow-weathered quartz–white-mica–calcite

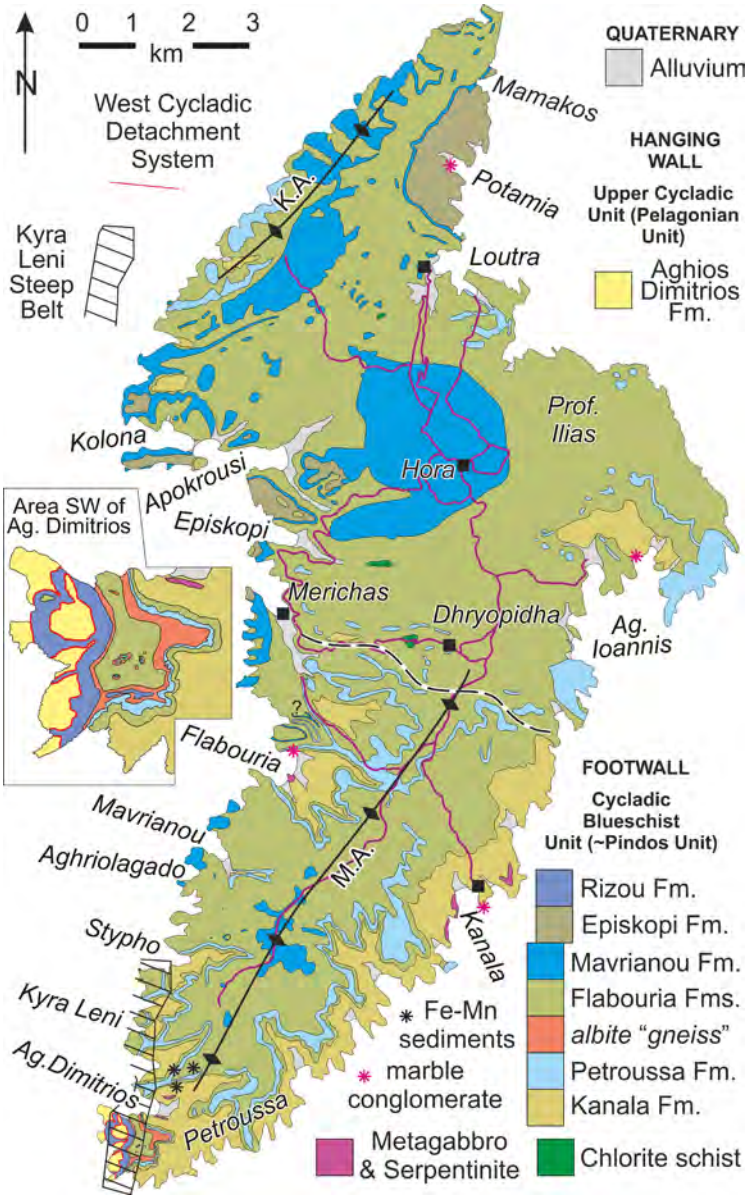

Figure C
Modified geological map of Kythnos, based on a combination of de Smeth's (1975) map, our recent work and limited satellite image interpretation. The area southwest of Aghios Dimitrios was remapped by Laner (2009) and Lenauer (2009). Fold-axes are from de Smeth (1975): K.A. - Kakovolo Antiform, M.A. - Merovighli Antiform.

schists that under- and overly the blue-grey marble (Stops 1.4, 6.1). Where de Smeth (1975) found quartz–white-mica–calcite schists without any blue-grey marble (e.g. NE of Prophitis Ilias; Stop 1.1, Fig. 1.1a) or where it was possible to map it separately from the blue-grey marbles it is shown as quartz schists (Fig. B). These schists, which are without graphite, are here always included in the Petroussa Formation, or in some cases in an upper marble/calc-schist unit (e.g. around Hora - see below; Fig. C).

Mapping the Petroussa Formation across southern Kythnos reveals an initially gradual and then sudden decrease in thickness, accompanied by evidence of an increasing strain. In the southeast, it is a single layer of marble ~14 m thick (Stop 5.2), with a few thin internal quartzite layers, and a few metres of under- and overlying quartz–white-mica–calcite schists. These schists are underlain by albite schists of the Lower Flabouria Formation, with occasional small quartz boudins. In contrast, on the south side of Aghios Dimitrios Bay, the Petroussa Formation consists of two layers of pinch-and-swelled blue-grey marble mylonite, each <0.5 m thick, associated with ~8 m of yellow-weathered quartz–white-mica–calcite schist/mylonite (Stop 6.1, see also Stop 5.6). On the north side of the bay, the underlying Lower Flabouria Formation is characterised by abundant large quartz boudins with a very strong/coarse quartz stretching lineation and a (sub-) parallel crenulation lineation in the schists. This westward thinning of the Petroussa Formation can also be seen in many bays to the north, up to the north side of Flabouria Bay (Fig. B; Stop 4.3).

Along the northwest coast of Kythnos (Fig. B), mr of de Smeth (1975) comprises exposures some tens of metres thick of yellow-weathered quartz–white-mica–calcite schists with several thick layers of blue-grey marble (Stop 1.4). Whether these rocks are part of the Petroussa Formation is discussed below.

(b) An upper marble/calc-schist unit (mr1), near the top of the stratigraphy of de Smeth (1975), forming (Fig. B):

(i). A series of small outcrops at the west end of several peninsulas along the southwest coast, from Aghriolagadho Bay to Merichas;

(ii). Two large outcrops on the ridge of the southern part of the island, above the quartz-schists (Fig. C);

(iii). A series of outcrops in the central to central-western part of the island (Merichas-Hora-Kolona area).

(iv). A thin layer towards the east coast in the north of the island (Loutra-Mamakos area).

Taking each of these in detail:

(i) On the peninsula south of Aghriolagadho Bay, layers and boudins of blue-grey marble mylonites, from a few centimetres to <1 m thick, crop out within ~5 m of yellow-weathered quartz–white-mica–calcite mylonite (Stop 4.7). This succession is here termed the Mavrianou Formation.

Table 2
Tectono/Lithostratigraphy used here (Fig. C)

FORMATION	LITHOLOGY (With de Smeth's 1975 equivalents.)
UPPER CYCLADIC UNIT – HANGING WALL (PELAGONIAN UNIT)	
Aghios Dimitrios	Quartzite, generally strongly brecciated. (*Formerly part of* ***v***.)
CYCLADIC BLUESCHIST UNIT – FOOTWALL (PINDOS UNIT)	
Rizou	Grey-brown to blue-grey or white or yellow marble (ultra)-mylonites with variable amounts of quartzite/quartz sigmoids/porphyroclasts on all scales from a few cm down to (sub)-microscopic. (*Formerly part of* ***v***.)
Episkopi	Chlorite and coarse grained epidote-zoisite schists (metavolcanics), rarely with marble conglomerate. (Formerly ***e. sch.***)
Mavrianou	Blue-grey marble within yellow-weathered quartz–white-mica–calcite schists. In the south, these are mylonitic with only < 1 m thick boudins of marble; in the north the layering is more persistent, with marbles up to a few metres thick. (*Formerly parts of* ***mr1*** *or* ***mr*** *and* ***q. sch***.)
Upper Flabouria	Albite-white-mica-quartz-chlorite-graphite schists, locally with graphite concentrated into layers up to 2 cm thick and with bright green Cr-rich layers. (*Formerly* ***ab. sch***.)
Petroussa	Blue-grey marbles up to 14 m thick with associated yellow-weathered quartz–white-mica–calcite schists. At higher strains, the marbles thin to irregular mylonitic boudins < 0.75 m thick within much thicker (8 m) quartz–white-mica–calcite schist mylonites. (*Formerly mr, although the inclusion of the* ***q. sch*** *quartz–white-mica–calcite schists within the unit was variable*.)
Lower Flabouria	Albite-white-mica-quartz-chlorite-graphite schists, locally with the graphite concentrated into layers up to 2 cm thick and with bright green Cr-rich layers. (*Formerly* ***ab. sch***.)
Kanala	Chlorite and coarse grained epidote-zoisite schists (metavolcanics), rarely with marble conglomerate. (*Formerly* ***e. sch***.)
Metagabbro	Metamorphic gabbroic rocks: for the most part, completely serpentinized and chloritized, with asbestos veins and talc: sometimes with relics of brown hornblende or completely altered to talc-chlorite schists with idiomorphic magnetite crystals.

The mylonites overlie several metres of the Upper Flabouria Formation that here contains abundant large quartz boudins with a coarse stretching/crenulation lineation. This outcrop is very similar to the outcrop of the Petroussa Formation NW of Aghios Dimitrios (Stop 5.6). The Mavrianou Formation also crops out on the peninsula southwest of Stypho Bay, only 2 km north of Aghios Dimitrios Bay (Fig. C). It also crops out directly north of Aghriolagadho Bay and also on the small peninsula on the northeast side of Flabouria Bay (Fig. C) and then farther north to Merichas and Kolona Bay.

(ii) Outcrops of mr1 in the south of the island are more extensive than shown by de Smeth (1975; Figs. B & C). For both outcrops shown by de Smeth (1975), most of the rocks comprise yellow-weathered quartz–white-mica–calcite schists, with only occasional lenses/boudins of blue-grey to white marble mylonites with abundant quartzite layers and porphyroclasts. Elsewhere, quartz–white-mica–calcite schists form isolated, sometimes small outcrops on the west flank and crest of southern Kythnos, overlying the Upper Flabouria Formation; many lie within the area de Smeth (1975) marked as quartz schist (compare Figs. B & C). These schists are comparable to and are taken to be part of the quartz–white-mica–calcite schists of the Mavrianou Formation.

(iii) In the Merichas-Hora-Kolona area, de Smeth mapped a large number of isolated outcrops of blue-grey marble as mr1. In areas of flat-lying topography, essentially around Hora, associated quartz–white-mica–calcite schists were mapped separately, as quartz schists. Further west, in steeper areas, where differentiating the lithologies on the map scale used would be difficult, the quartz–white-mica–calcite schists are included in

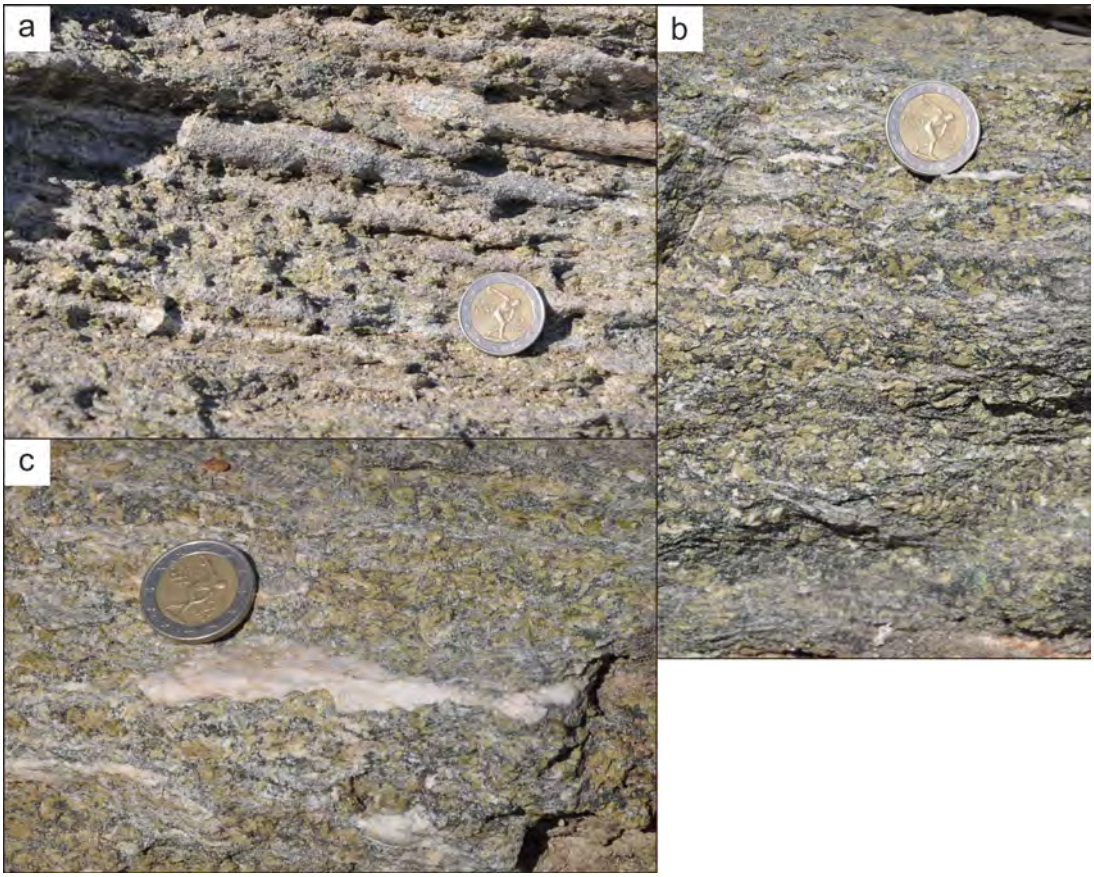

Figure D
Coarse epidote rocks of the Kanala Formation from directly north of Kanala. These are identical to the epidote schists seen in the Kanala Formation at a-Stop 5.9 and in the Episkopi Formation at Stop 1.5.

mr1. Both the blue-grey marbles and the quartz–white-mica–calcite schists are here included in the Mavrianou Formation (or in some cases these are thought to be part of the Petroussa Formation; see below; Figs. B & C). In several areas, especially between Merichas, Apokrousi and Kolona, these are overlain by epidote schists of the Episkopi Formation.

(iv) In the northeast of the island, between Loutra and Mamakos Bay, a thin but continuous layer of blue-grey marble with yellow-weathered quartz–white-mica–calcite schists crops out above the Flabouria Formation and below epidote schists (Stop 1.7). Based on preliminary lithological comparisons, these are taken to be equivalent to the Mavrianou and Episkopi Formations, respectively (Fig. C).

The Petroussa Formation was mapped by de Smeth (1975) as a continuous layer as far north as Dhryopidha, around which it was shown as several lenses of blue-grey marble (likely boudins; Fig. B); the associated yellow-weathered quartz–white-mica–calcite schists were here definitely not included in mr, as they are continuous. However, a zone of boudinaged blue-grey marble can be mapped further west than shown by de Smeth (1975), along the hillside north of the Merichas-Dhryopidha road, within a strongly deformed layer of yellow-weathered quartz–white-mica–calcite schists (blue-grey marbles lenses are shown schematically in Fig. C). This layer may link with the marble outcrops immediately east of Merichas that are also associated with yellow-weathered quartz–white-mica–calcite schists and shown as mr1 by de Smeth (1975; Figs. B & C). Thus here the Petroussa Formation is seemingly the same as the Mavrianou Formation. However, the outcrop of Kanala Formation below these outcrops of deformed marble and calc-schist (Figs. B & C) implies that the marbles directly east and southeast of Merichas must be part of the Petroussa Formation. If this is accepted, then the outcrops of mr1 (Fig. B) on the hills to the north of Merichas must also be Petroussa Formation. Essentially, there is a complexity in the geology in this part of Kythnos which, although recognised as being present, is not yet resolved.

Although it would be convenient to simply correlate the Petroussa and Mavrianou Formations (e.g. from east to west of Merichas), this is not possible. Along the southwest coast, for example at Mavrianou Bay and Stypho Bay, the Petroussa

and Mavrianou Formations are clearly separated by the Upper Flabouria Formation (Fig. C). Thus there are two marbles north of Aghios Dimitrios and, in the southwest, the upper one (Mavrianou Formation) is essentially identical to the high strain facies of the lower one (Petroussa Formation). This holds as far north as Apokrousi Bay and Kolona Bay.

How the marbles north of Kolona Bay correlate with the Petroussa and Mavrianou Formations is not known. de Smeth (1975) proposed that a normal fault northwest of Kolona Bay separated them (Fig. B). However, no evidence for such a fault structure can be seen in satellite images or from coastal observations (a-Stop 7.1), which seems unlikely, considering the throw required to place the upper border of the Mavrianou Formation in line with that of the Petroussa Formation. The tentative conclusion, in the absence of any direct observations, is that the mr of de Smeth (1975) along the northwest coast of Kythnos is, at least in some places, a low strain equivalent of the Mavrianou Formation (compare Figs. B & C); in the northwest, this unit includes very thick yellow-weathered quartz–white-mica–calcite schists (Stop 1.4).

On the south coast of Aghios Dimitrios Bay, Laner (2009) and Lenauer (2009) mapped an albite "gneiss" directly above marbles of the Petroussa Formation. The albite "gneisses" are overlain by the Upper Flabouria Formation (Stop 6.1), in turn overlain by another albite "gneiss" layer and thence by grey-brown to a blue-grey marble ultramylonites with abundant quartzite/quartz sigmoids and porphyroclasts (here the Rizou Formation; Fig. C; Stop 6.2; this marble was included in the carbonatized ?volcanic unit by de Smeth1975).

The two layers of albite "gneiss" of Laner (2009) and Lenauer (2009) join on the southern side of the peninsula south of Aghios Dimitrios Bay (Fig. C). If this lithology is equivalent to the quartz–white-mica–calcite schists found elsewhere that is here included in the Petroussa Formation, then the Rizou Formation could be an over-folded equivalent of the Petroussa Formation. Further, its position as a marble unit lying above the Petroussa Formation suggests it might be a lateral correlative of the Mavrianou Formation seen further north (Stypho Bay, Aghriolagadho Bay; Fig. C). However, these two carbonate units have markedly different appearances in southern Kythnos; the Mavrianou Formation is dominated by quartz–white-mica–calcite schists with occasional strongly disrupted boudins/lenses of blue-grey marble (ultra-)mylonite, whilst the Rizou Formation is a relatively coherent layer of often brownish marble ultramylonites with scarce quartz–white-mica–calcite schists (or albite "gneisses"; Stop 6.5).

The carbonatized ?volcanic rocks of de Smeth (1975; Table 1) in the southwest of Kythnos have been re-interpreted as a strongly brecciated quartzite (here the Aghios Dimitrios Formation) lying directly above marble ultramylonites of the Rizou Formation; these are, respectively, the immediate hanging wall and footwall of the WCDS (Fig. C; Lenauer 2009, Laner 2009, Grasemann et al. 2012).

de Smeth (1975) shows several outcrops of variably serpentinized metagabbro with relict pyroxenes (Fig. B). Schliestedt et al. (1994) stated that except for those in Flabouria and south of Kanala, these outcrops are chlorite schists and not metagabbros. Our observation of the 'metagabbro' on the road between Merichas and Dhryopidha confirms this, but mapping by Laner (2009) and Lenauer (2009) shows that metagabbro bodies, wrapped in serpentinite-talc schists, crop out on opposite sides of Aghios Dimitrios Bay, in positions that suggest they may have formed a continuous body, elongated parallel to the SSW-NNE stretching direction (Fig. C). In Fig. C the supposed metagabbro bodies of de Smeth (1975) within the Lower Flabouria Formation are shown as chlorite schists and those in the Kanala Formation as metagabbros.

Although this text seem very critical of de Smeth (1975), mapping in the 1970s was much more difficult, partly because the road network was less developed than now. With the exception of mr1 and the quartz schist in the south, the lithological boundaries were well-mapped by de Smeth (1975), although not always exactly placed, when compared to satellite images. The problems lies in correlating outcrops of the carbonate units, particularly in the north of the island, which is still difficult to access.

Chrysanthaki & Baltatzis (2003) documented three types of ferromanganoan sediments on Kythnos; (i) hematite quartzites, in the upper part of the Kanala Formation in the Kanala area or in the lower part of the Lower Flabouria Formation in the Episkopi area; (ii) mica-bearing hematite quartzites in the Kanala area along the boundary of the Kanala and Lower Flabouria Formations, interlayered with type (i) ; (iii) garnet bearing blue amphibole schists and tourmalinites at "higher levels" than the other types, in the southeast. Outcrops known to the present authors are documented in this guide (Stop 5.7); Chrysanthaki

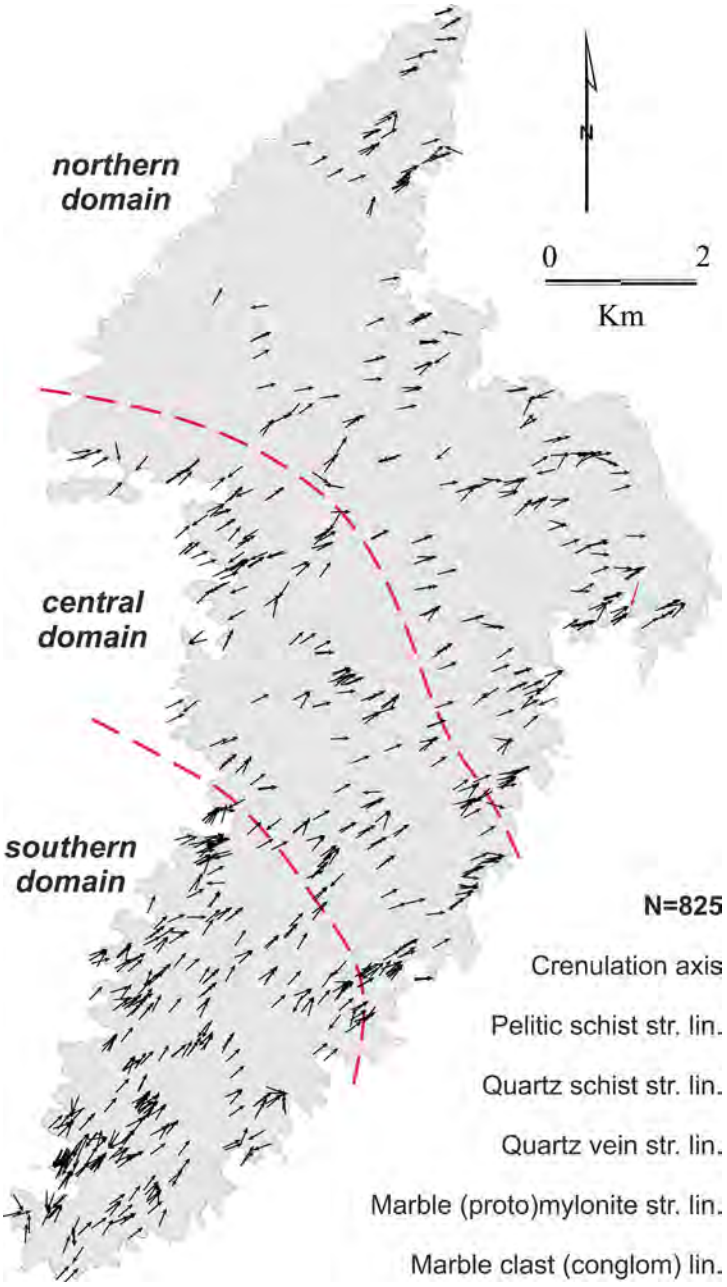

Figure E
Map showing the orientation of all ductile linear structural elements except fold axes. These define northern, central and southern domains, although the boundaries are gradational. Red arrow is movement on the Aghios Ioannis LANF.

& Baltatzis (2003) did not give detailed locations. The sediments were interpreted as products of oceanic hydrothermal alteration (Chrysathanki & Baltatzis 2003) but, since the sediments were not deposited on ocean crust, this is not possible. Nevertheless, syn-depositional hydrothermal activity leaching submarine continental basic volcanoclastic sediments would have had a comparable effect.

Keiter et al. (2008) interpreted the structural geology of the island in terms of NW-directed over-thrusting, based on the fold vergence. However, more detailed studies in the SW showed a typical Cycladic detachment system (the WCDS), with footwall ultramylonites (Rizou Formation) overlain by hanging wall cataclasites (Aghios Dimitrios Formation; Laner 2009, Lenauer 2009, Grasemann et al. 2012), a structural asymmetry diagnostic for low-angled extensional faults (LANF); stretching lineations and shear-sense indicators gave a uniform top-to-the-SSW sense of movement (Grasemann et al. 2012).

Structurally, Kythnos is intermediate to Serifos and Kea (Grasemann et al. 2012). The former underwent relatively low strains in the Cycladic Blueschist Unit during M2 low-angled normal faulting, except close (~10 m) to the documented top-to-the-SSW WCDS (Grasemann & Petrakakis 2007), whilst the latter underwent high M2 strains, with an essentially dismembered stratigraphy forming a >450 m thick top-to-the-SSW footwall shear zone, with higher strains closer to the WCDS, preserved in several klippen across the island (Iglseder et al. 2011, Rice et al. 2012).

Fig. E shows the orientation of linear structural elements (crenulations, stretching lineations, conglomerate clast long-axes, but not fold axes) across the island. These define three domains; a northern domain with E-W to ENE-WSW lineations, a central domain with ENE-WSW to NE-SW lineations and a southern domain with NE-SW to NNE-SSW lineations. Although there are exceptions in all domains, there is an overall rotation in the structural grain across the island.

Lower hemisphere equal-area stereonet plots of the linear data from the whole island (excluding fold axes; Fig. Fi-v) show clustered distributions (K=3.1-5.5; Woodcock 1977), although these are not very well defined (C=2.7-3.1). Mean orientations for stretching lineations and crenulation lineations mostly lie between 054-057°. Only stretching lineations from the marbles (mostly Petroussa and Rizou Formations) differ (mean 043°), reflecting the preponderance of data from the southern and central domains.

The variations in orientation across the island are interpreted to reflect the structural distance from the WCDS. There is no significant lithostratigraphic difference between the north of the island and the south; most of the island comprises the Upper Flabouria Formation. Hence, with a detachment dipping south relative to the lithostratigraphy, consistent with a top-to-the-south displacement, more northerly parts of the island would have been further from the detachment than southerly parts. M2 extensional strains would have been lower further from the fault zone

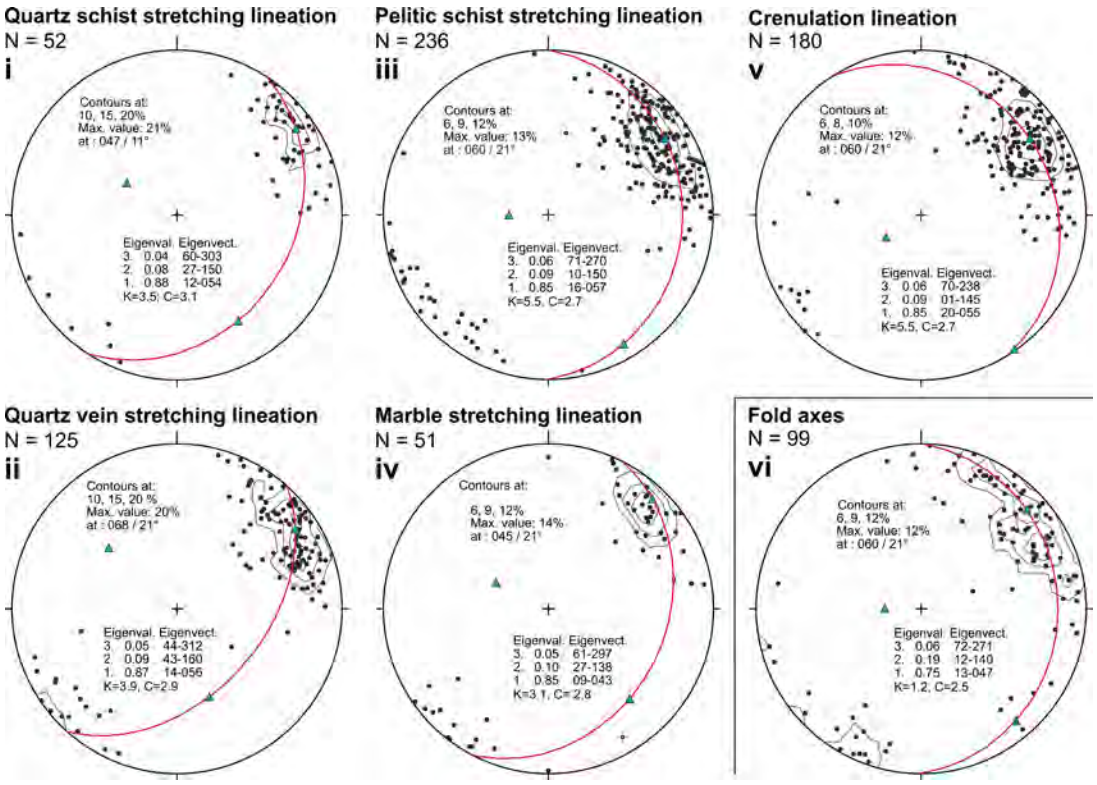

Figure F
Equal-area, lower hemisphere projections of the linear structural data. See text for details. The K parameter is a measure of the fabrics shape (K=0 is perfect girdle, K=∞ is perfect cluster, K=1 is the girdle-cluster boundary) and the C parameter is the quality of the fabric (C>4.5 indicates a tight cluster/well defined girdle, C<2 indicates a very diffuse fabric). Blue triangles are the eigenvectors and the red line is the best-fit great circle.

and so the degree of structural reworking from the M1 direction (ENE-WSW) to the M2 direction (NNE-SSW) would have been less. E-W variations in lineation direction across the island, can be explained by the detachment having a gently west dipping lateral ramp geometry. Thus the east side of the island lies further from the detachment than the west side. This is consistent with the only outcrop of the WCDS being in the extreme SW of the island.

Crenulations parallel to the stretching direction (Fig. Fv) indicate shortening perpendicular to the extension direction, typical of extensional terranes (Mancktelow & Pavlis 1994), including the Cyclades (Avigad et al. 2001, Rice et al. 2012). This is also seen in the large-scale NNE-SSW trending upright Merovighli and Kakovolo Antiforms. In the southern antiform, older rocks are exposed towards the coast, rather than in the antiform core (Fig. C), hence fold-limb dips must be less than the topographic slope of the island. Only at the western end of the bays north of Aghios Dimitrios are younger rocks exposed towards the coast; this is due to a sudden steepening of the dip, forming the here defined Kyra Leni Steep Belt (Figs. C & G; Stops 5.6, 6.1; see below). The parallelism of the stretching lineations and crenulations in the north and east, essentially the relict M1 domain, suggests that horizontal constriction also occurred during exhumation and retrogression of the early, high-pressure, M1 event.

Folds are orientated between N-S and E-W, with a mean at 047/13° (Fig. Fvi), with isoclinal recumbent to upright open geometries. All folds clearly fold an earlier fabric (except at Stop 5.6); the extent to which a new fabric formed depended on the lithology and the bulk strain, represented crudely by the fold inter-limb angle. Some folds also fold the stretching lineation (Stop a-6.9) whilst elsewhere the fold axis parallels the stretching lineation. Most folds verge to the NW (Keiter et al. 2008).

The difficulty of the Mavrianou Formation being absent on the south side of Aghios Dimitrios Bay, where the Rizou Formation crops out above the Upper Flabouria Formation and above albite "gneisses" (quartz-white mica-calcite schists), has not been properly resolved. The current working hypothesis is that the Mavrianou Formation is the same unit as the Petroussa Formation, forming the inverted limb of a large-scale recumbent isoclinal fold. This hypothesis requires that the Mavrianou Formation is the same unit as the Rizou Formation, despite their lithological differences. This is consistent with the stratigraphy seen in northern Kythnos, where the Episkopi Formation, the highest unit on Kythnos could be an inverted correlative of the Kanala Formation, the lowest unit.

Note that intermediate-scale recumbent isoclinal folds are present on Kea, where the regional outcrop pattern of the marbles might also be reflecting larger-scale isoclinal folding (Rice et al. 2012).

The WCDS is exposed only in the southwest, where Laner (2009) and Lenauer (2009) described a hanging wall of brecciated quartzites (Aghios Dimitrios Formation; Stop 6.6) lying above a low-angled, knife-sharp brittle LANF (Stop 6.8) above several metres of marble ultramylonites (Rizou Formation). Parts of these ultramylonites are relatively pure (Stop 6.5), whilst other parts contain abundant quartz porphyroclasts/sigmoids showing a top-to-the-SSW shear-sense (Stop 6.2). Late shortening perpendicular to the stretching direction resulted in the formation of outcrop-scale kink-bands (Stop 6.3) in the finely layered marble ultramylonites. At <200°C, the brittle-ductile transition for calcite, this shortening resulted in brittle thrusting and fault bend folding in the marble ultramylonites (Stop 6.3). Further details of the detachment are given in the guide.

The Kyra Leni Steep Belt (Figs. C, G; Stop 5.6) is characterized by a narrow fold hinge-zone and long planar fold limbs, similar to a kink-type fold geometry. However, the higher strains in the Petroussa Formation in the steep belt and its parallelism to the nearby WCDS suggests that they may be genetically linked.

Along part of the WCDS, a rusty-red to pink proto- to ultra-cataclasite with, in part, rounded clasts in a very fine-grained matrix occurs over a length of at least 100 m (Stop 6.4). SEM imaging of the cataclasites shows clasts-cortex structures (Rice & Grasemann 2016), similar to those described by (Smith et al. 2011), possibly suggesting an earthquake event during faulting.

In summary, the island shows evidence of significant deformation during cooling, with the rheology, and hence the structural response to stress, changing from the ductile, to brittle-ductile and then the brittle deformation field. This change, which is consistent with exhumation of the Cycladic Blueschist Unit from under an active low-angled normal fault, here the West Cycladic Detachment System, can be seen at many outcrops (for example, Stops 1.7, 2.4, 3.5, 4.5, a2.10, a4.8).

Schliestedt et al. (1994) provide the only metamorphic data from the island. The schists forming the bulk of the island underwent a HP/LT blueschist facies metamorphism, although this is only locally preserved within relict porphyroblasts in the greenschist facies overprint. Peak conditions were estimated by Schliestedt et al. (1994) to be comparable to Sifnos & Syros (P/T ~1.2-2.0 GPa/450-500°C), but this estimate is low compared to more recent work on those island and high compared to recent data from other parts of the Lower Cycladic Blueschist Nappe (400 ±20°C, 10 ±2 kbar; cf Grasemann et al. 2018). Albite porphyroblasts are interpreted by Schliestedt et al. (1994) to be the relicts of jadeite-rich pyroxenes, often preserving earlier planar fabrics. Schliestedt et al. (1994) divided the later M2 event on Kythnos into two parts; M2a at 300-400°C and 2-4 kbar, reflecting rapid exhumation under the WCDS, and M2b at 400-500°C and 5-8 kbar.

Schliestedt et al. (1994) presented two K-Ar white-mica ages. One, using paragonite from marbles in the Episkopi area (likely Mavrianou Formation), gave an age of 21.0 +/-0.8 Ma (100-500 µm grain size) and the other, using phengite from the (?Lower) Flabouria Formation in the Kanala area, gave an age of 26.1 +/-0.2 Ma (63-100 µm grain size). The younger age is comparable to five Ar/Ar white-mica ages of 18.77 +/-0.09 Ma to 21.2 +/-0.1 Ma published by Grasemann et al. (2012). (U-Th)/He data from apatite and zircon show younger ages in the central and north of the island (10-15 Ma to <10 Ma) compared to the south (>15 Ma; Grasemann et al. 2012).

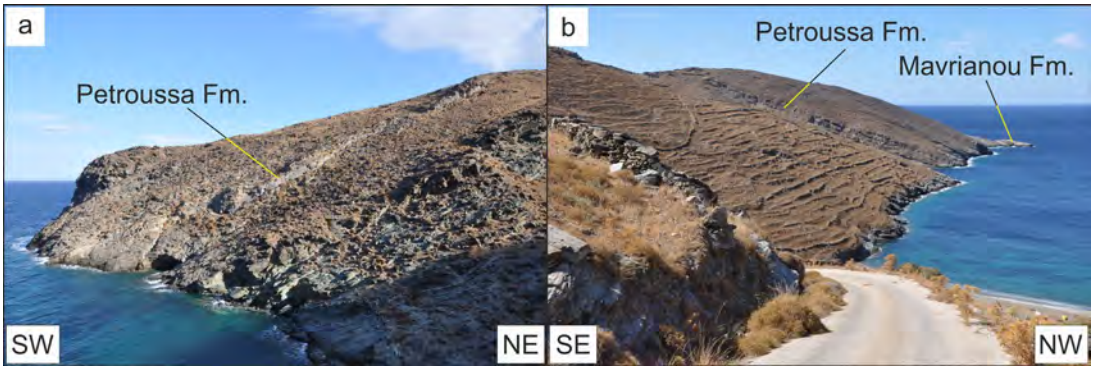

Figure G
Views of the Kyra Leni Steep Belt. (a) Looking NNW across Kyra Leni Bay; (b) Looking WSW along the south side of Stypho Bay (Fig. C).

FIELD GUIDE

Facilities on Kythnos

Some useful facilities are marked accurately (except where stated) on the *Facilities.kmz* file, available on-line with the guide.

Hire-cars can be obtained from Halivelakis Hire Car (www.halivelakis.gr) and Larenzakis Rent-a-Car & Moto (www.rentacarkythnos.gr), both in the Merichas harbour area. Make a reservation in advance. A high ground-clearance vehicle is needed for some outcrops. Petrol is sold in Merichas, Hora and on the main road east of Dhryopidha, but nowhere else. Petrol stations may close during the afternoon. An ATM outlet in Merichas lies uphill from the Larentzakis Rent-a-Car & Moto office; there is another in Hora (approximately marked). Postage stamps can only be bought at the post-office in Hora, but there is a letter-box in Merichas, on the harbour road. A good topographic map of the island (ΣΚΑΪ ΧΑΡΤΕΣ) can be bought from the small bookshop in the SE corner of Merichas harbour.

There are many restaurants serving good traditional Greek food in Loutra, Hora, Merichas, Dryopidha and Kanala. We can recommend the Gialos-Byzantico Restaurant in Merichas, the Chartino Karavi Restaurant in Dhryopidha, the Archipelago and Ophioula Restaurants in Kanala and the Milas Taverna in Aghios Dimitrios. Many other beaches have a Taverna serving excellent sfood, but these may be closed in mid- to late September. The Maestrali Café, in the southeastern corner of the harbour, is very nice. There are supermarkets and several bakeries in Merichas and likely also in Dhryopidha and Hora. A mini-market lies at the junction of the main roads directly south of Dhryopidha and in Kanala.

Simple but clean accommodation in Merichas is available from Mrs. Eleni Bouriti (Tzamaros Studios; bouritis2008@hotmail.com); we have no experience of the many other places available on the island, likely as equally good.

Excursions

The days are arranged from north to south. If only one day is spent on Kythnos, Excursion 6 is recommended. Excursion 5 is recommended for the first day if more than one day is spent on the island. All Stop locations are shown in Fig. H and in the *Excursion.kmz* and *α -Excursion.kmz* files, available on-line.

In the northern part of the island, it is sometimes unclear if a particular albite schist is the Upper or Lower Flabouria Formation; thus the general name Flabouria Formation has been given in some descriptions.

All planar orientation measurements are given as dip direction/dip angle. Linear orientations are given as plunge direction/plunge angle. The abbreviations used for structural elements are given in Table 3.

Table 3
Structural abbreviations used.

sm	main foliation;
lm	stretching lineation on main foliation;
lp	pebble long axis in conglomerate;
sc sc′	C and C′ planes;
lc lc′	stretching lineation on C and C′ planes;
lf1, lf2	fold axes of the first, second generation;
sap1, sap2	fold axial surfaces of the first, second generation;
lcr	crenulation lineation;
ses	enveloping surface of en-echelon tension gashes;
sv	vein surface;
scce	cross-cutting element in a flanking structure;
sh	fault surface;
lh	lineation on fault surface, with + or – indicating reverse or normal slip;
sj	joint surface.

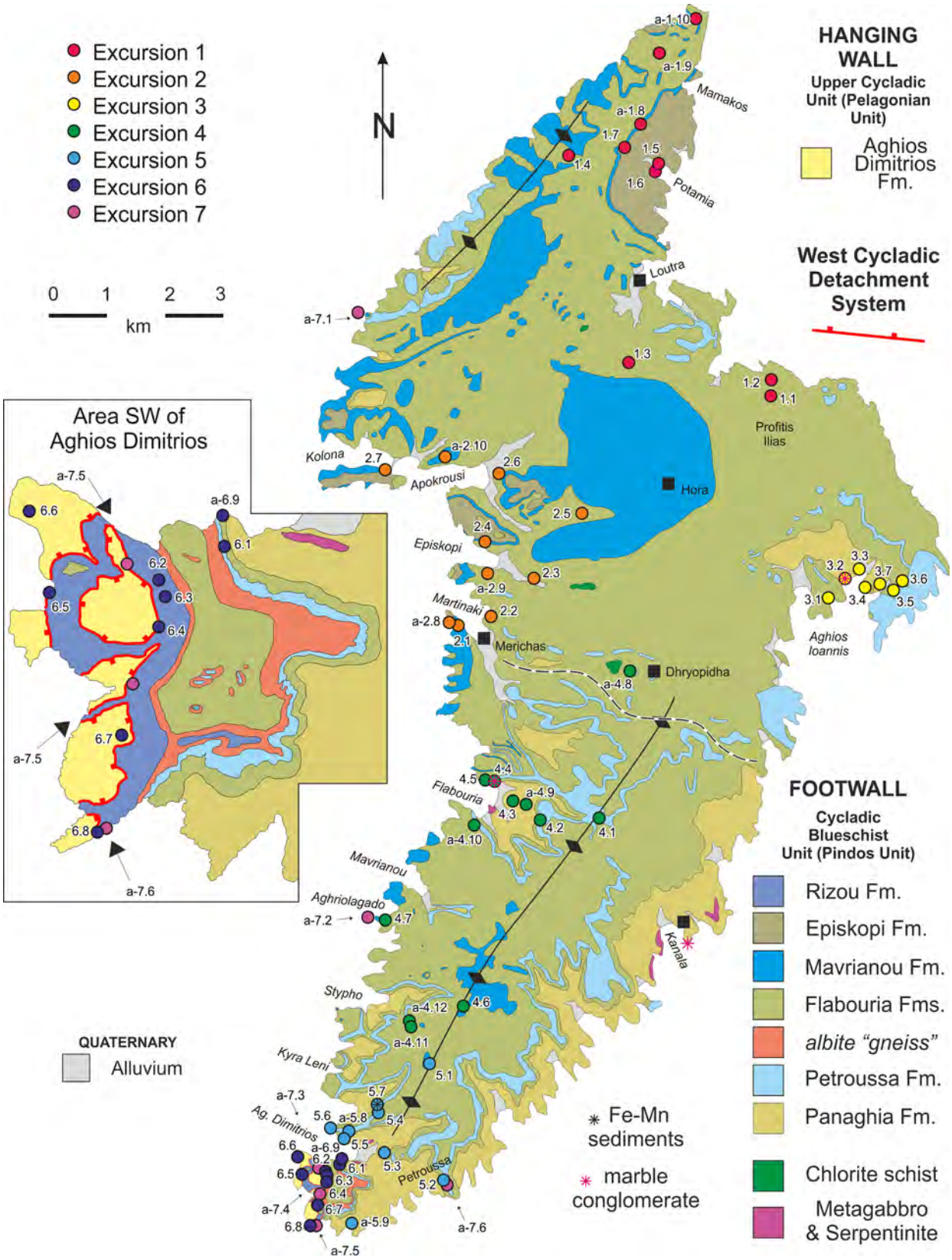

Figure H
Geological map showing positions of the outcrops documented in the field guide.

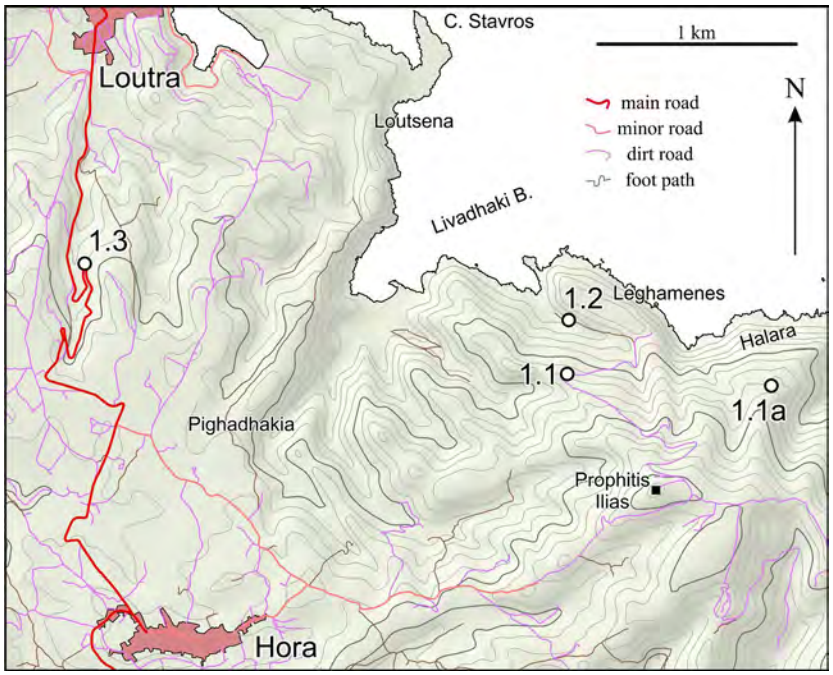

Figure 1.0a
Outcrop location map for Stops 1.1 to 1.3.

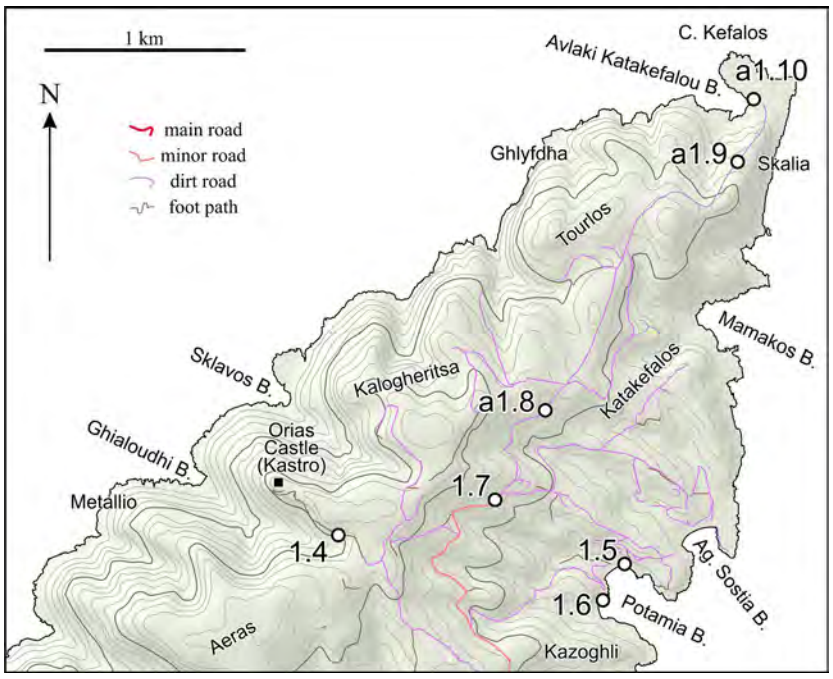

Figure 1.0b
Outcrop location map for Stops 1.4 to 1.10.

PLEASE DO NOT HAMMER THE STRUCTURES SHOWN IN THE PHOTOGRAPHS AS THIS SPOILS THE OUTCROPS FOR OTHER GEOLOGISTS.

Excursion 1: N. and NE Kythnos; *Profitis Ilias, Orias Castle and Potamia Bay*

On this excursion, two relatively short walks are described. One walk is to see particularly interesting outcrops and the other is to Kastro (Orias Castle, the main Byzantine fortification on the island) to see carbonate rocks interpreted here as the Mavrianou Formation in a relatively low strain environment, for comparison with the Petroussa Formation. Three further stops are of interest for comparing the Kanala and Episkopi Formations. All stops are shown in Figs. 1.0a and 1.0b.

Stop 1.1. Flabouria Formation. Cr-rich schist and large SC' structure.

UTM 35S 274515E 4145061N.
Fig. 1.1a, looking NE; Figs. 1.1b-d, looking SE.

Drive past Profitis Ilias and park by the gate. As you walk down to the outcrop, note the large outcrop of yellow-weathered quartz–white-mica–calcite schist that can be seen to the northeast (Stop 1.1a, Fig. 1.1a). This is shown by de Smeth (1975) as quartz schist, but it is different to some of the quartz schist marked on the map in the south of the island (Stop 5.1), which are grey metapelitic schists now included in the Upper Flabouria Formation. However, it is identical to yellow-weathered quartz–white-mica–calcite schists associated with blue-grey marbles in both the Petroussa (Stop 4.1) and the Mavrianou Formations (Stop 1.4).

At the grid-reference, an unusually thick band of bright green schist (likely containing Cr-rich white-mica or chlorite) lies within the Flabouria Formation (Fig. 1.1b), cut by a large top-to-the-SW SC' structure (sm 022/23°, lm 042/16°; sc' 252/25°, lc' 227/16°) with a thick (~20 cm) fault zone/fabric that is part wrapped around a large quartz boudin in the hanging wall of the C' surface. At its northeastern end, the Cr-rich layer has been offset by a minor high-angled flanking structure that is conjugate to and cut by the large SC' structure (Fig. 1.1c).

The northeast end of the most southwestern block of Cr-rich schist shows a lobate-cuspate geometry, with the cusps pointing into the Cr-rich

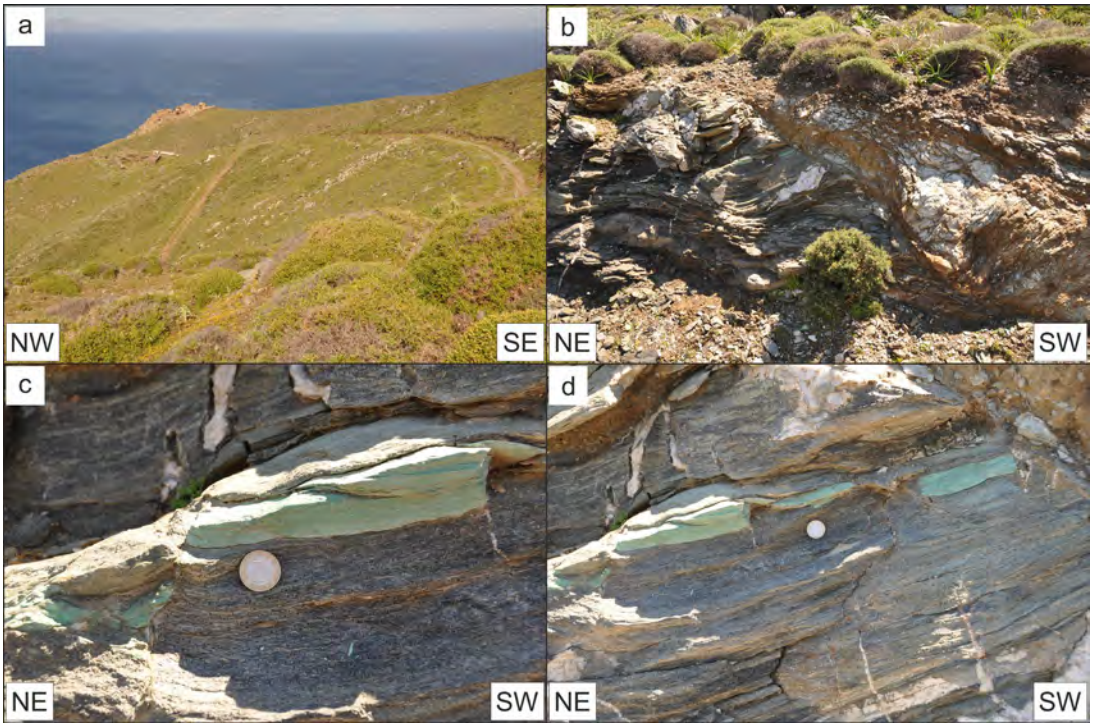

Figure 1.1
Flabouria Formation with bright green Cr-rich layer.

schist (Fig. 1.1d), indicating flattening. Although speculative, the overall geometry and thicknesses of the Cr-rich layers suggests that the southwestern block might have been derived from below the block above the coin during deformation, perhaps by boudinage, although the lack of any quartz in the inferred boudin neck suggests otherwise.

There are several generations of quartz-veins. The earliest lie parallel to the foliation and have been pinch-and-swell boudinaged. An obvious thick, pinch-and-swelled quartz-vein lies at a very low angle to the foliation, dipping NE, and is cut by the C' zone of deformation (Fig. 1.1b). Late high-angled quartz-veins are normal to the foliation in quartz-rich layers but sheared top-to-the-SW in metapelitic layers, in some cases into near parallelism with the foliation. Both the foliation and the neck of the thick quartz-vein are cut at a high angle by a thinner quartz-vein that is offset antithetically compared to the main SC' structure during formation of the reverse-drag. This suggests that the SC' structure is later than the steep quartz-veins; the almost cataclastic appearance of the fabric in the C' deformation zone also suggests it is at least partly a late, brittle-ductile structure.

Stop 1.2. Upper Flabouria Formation. Folds, refolds and axial-planar cleavages.
UTM 35S 274523E 4145327N.
Fig. 1.2, looking NNE.

Walk further downhill and take the turning to the left, along the poor conditioned road. Here, alternating grey metapelitic schists and quartz-rich layers of the Upper Flabouria Formation crop out. The schists are crenulated and contain quartz boudins with a well-developed stretching lineation.

An obvious fold (F2; Fig. 1.2a) is exposed on the north side of the road (lf2 008/09°, sap2 079/18°). In some layers, likely those with a higher quartz content, an earlier, pre-folding schistosity is still well preserved, despite the folding, whilst in other layers a new crenulation cleavage has developed, fanned around the axial surface, all but completely overprinting the earlier fabric (Fig. 1.2b), with anastomosing microlithons <2 mm thick.

Towards the base of the outcrop (Fig. 1.2a), an earlier fold structure (F1) is seen in three quartzite layers (lf1 254/18°, sap1 263/16°): the top and bottom layers have been deformed into perfect isoclinal folds, with the more metapelitic layers squeezed out almost entirely from between the quartzite limbs, while the middle layer shows a mullion fold geometry (Fig. 1.2c), with a lobate-cuspate geometry at the metapelite-quartzite boundary. The orientation of the fabric in the metapelitic layers is parallel to the axial surface of the F2 structure described above (Fig. 1.2a, c) and clearly oblique to the F1 axial surface.

No thin-section has been made from this outcrop, but the F1 structure may also be folding a

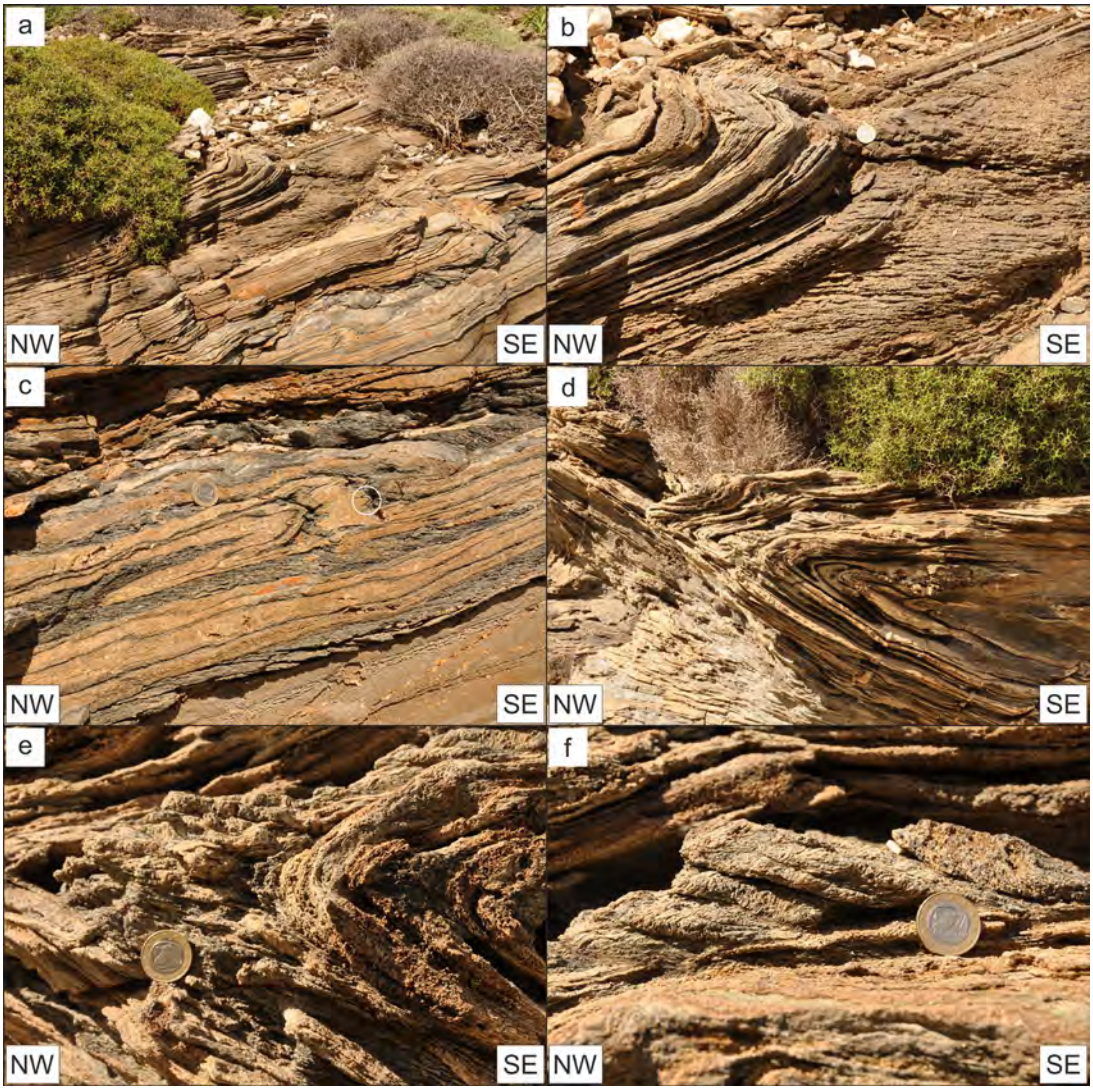

Figure 1.2
Flabouria Formation. Refolds and crenulation cleavages.

fabric; the schist adjacent to the lobate-cuspate structures appears to have a fabric parallel to the compositional layering (circled area, Fig. 1.2c), indicating that three phases of fabric development/folding occurred. However, rather than interpret the regional structural evolution in terms of three distinct phases of deformation, it is more realistic to think of a fabric being continuously developed, then folded and extended until the folding is no longer preserved and then further folded in a continuous cycle of fold formation and degradation. Thus lfn here is unlikely to be exactly coeval with lfn in outcrops far away from here.

Some 35 metres further down the hill (UTM 35S 274488E 4145332N), in similar schists (sm 291/16°, lm 025/14°), a comparable F2 structure is developed (Fig. 1.2d; lf2 164/01°; sap2 342/27°). Most of the fold preserves the earlier fabric, with evidence of refolding of F1 in the hinge-zone (and folding earlier asymmetric boudins), but one ~6 cm thick metapelitic layer has developed an up to 1 cm spaced axial-planar pressure-solution crenulation cleavage in both the hinge zone and the fold limbs (Figs. 1.2e, f). The earlier sm1 fabric is crenulated, but is clearly preserved within the microlithons. Note that several relatively thick and planar quartz-veins cut the lower limb of the fold, but these die out as the F2 axial surface is approached.

Very thin layers of Cr-rich schists are exposed in outcrops within the Flabouria Formation between the remains of the dirt road in this area.

Stop 1.3. Flabouria Formation. Fold within greenschists.
UTM 35S 272107E 4145609N.
Figs. 1.3a, c, looking NE; Fig. 1.3b, looking E.

In the sharp turn 1.5 km south of Loutra, green-

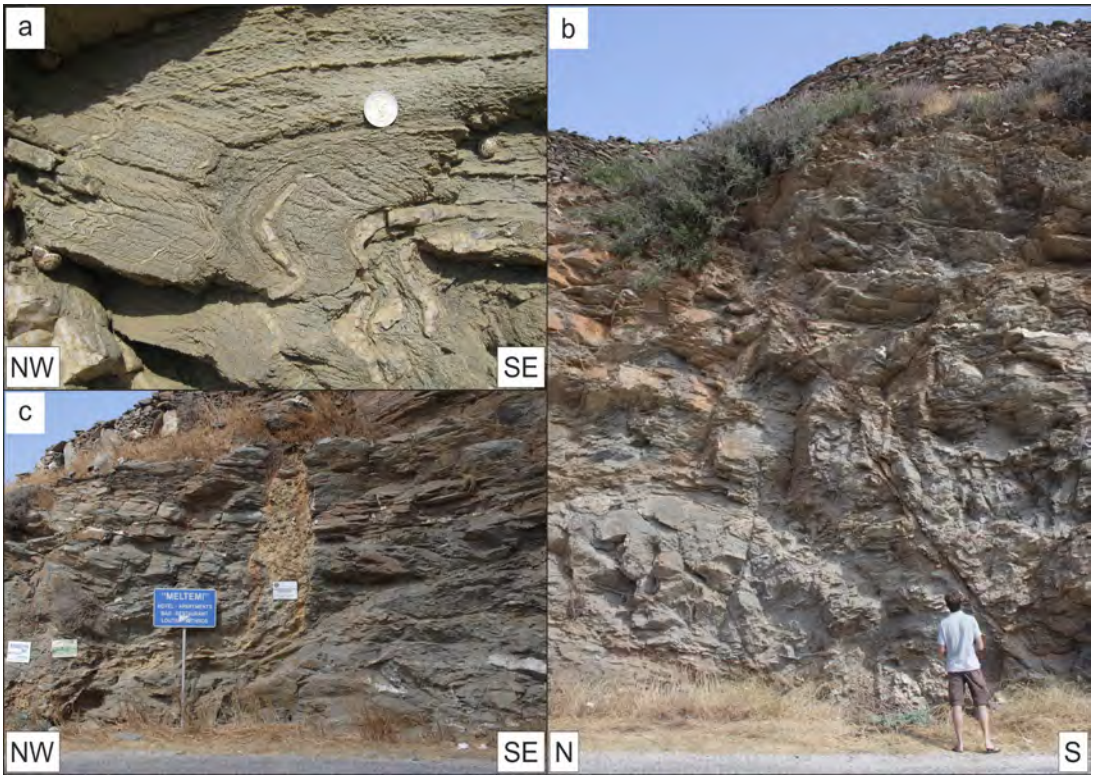

Figure 1.3
Flabouria Formation. Folding and brittle faulting.

schists within the Flabouria Formation are strongly deformed by recumbent folds, forming a strong new axial-planar cleavage in the hinge zone (Fig. 1.3a). The fold axes are roughly parallel to the stretching lineation (lm 250/01°) within the main foliation (sm 245/02° in the long fold limbs). Several quartz-veins, which were rotated into the main foliation before folding and record z- (down plunge) and m-shaped folds, have fold limbs dissolved along the axial-planar cleavage, suggesting that diffusive mass-transfer was an important deformation mechanism during folding.

Several conjugate SSW- and NE-dipping brittle normal faults with up to dm-thick non-cohesive cataclasites cut the whole outcrop (Fig. 1.3b; looking E).

Immediately west of the fold described, a thick sub-vertical vein of coarse-grained, unconsolidated breccia is exposed (Fig. 1.3c), linking to a west-dipping zone of breccia, again with a slightly browner colour than the over and underlying rocks. Slightly further west, the breccia steps down again. This structure is interpreted as the head-end of a minor landslide; the sub-horizontal zone likely developed by reactivating the west-dipping C' plane seen to the east.

Stop 1.4. Mavrianou Formation? Carbonate-filled en-echelon tension cracks.
UTM 35S 271237E 4149165N.
Figs. 1.4a-e, the discus is being thrown to the south; Fig. 1.4f, looking WNW.

Drive towards Loutra and, just before the town, turn left. After 2.2 km turn left again and drive 1.2 km uphill towards Kastro and then follow the footpath to the castle. The path lies within yellow-weathered quartz–white-mica–calcite schists, sometimes with distinct mm thick white calcite marble layers. De Smeth (1975) marked these as mr. As such, the rocks are similar to the Petroussa Formation in SE Kythnos (Stop 5.2) although here there is more schist and less marble. However, they are also similar to the Mavrianou Formation in the Merichas-Kolona area.

Towards the west end of the obvious c. 10 x 30 m platform here, the rocks (sm 345/12°, lm 061/05°) have been cut by abundant en-echelon fractures in-filled with a brown carbonate (Figs. 1.4a-c). Most of the en-echelon systems show a dextral shear-sense (Fig. 1.4a, b) but some show a sinistral shear-sense (Fig. 1.4c). The angle between the tension cracks and the enveloping surface varies, as does the degree of curvature of the

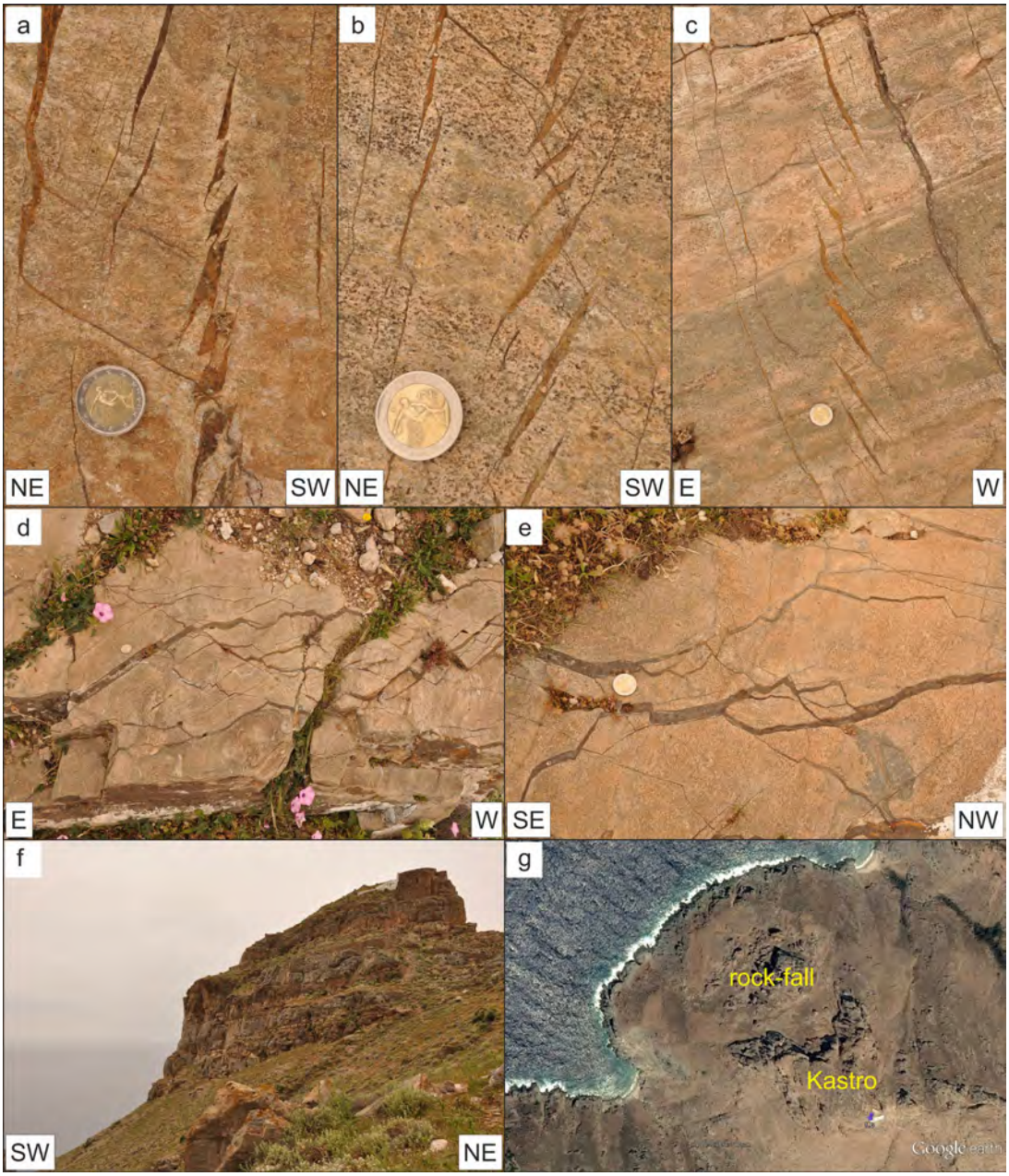

Figure 1.4
Mavrianou Formation? Carbonate filled en-echelon tension cracks, overview of the formation and rock-fall west of Kastro.

cracks. For dextral sets, the enveloping surfaces trend ~139° and for sinistral ~173°, on the foliation. Linkage of some fractures with bridge structures has occurred (Fig. 1.4a, b, c); in Fig. 1.4a, shortening either imbricated the bridge structure (brittle deformation) or bent it ductilely.

Elsewhere, multi-stage chocolate-tablet extension occurred (Fig. 1.4d, e), with both brown and later white carbonate vein fillings; the latter reactivated existing cracks. (In Fig. 1.4d, the thick vein below the coin trends 109° and in Fig. 1.4e, 140°). Chocolate-tablet extension veins cut the en-echelon tension cracks, either cutting directly across the cracks or thickening them (Fig. 1.4a, b).

From further west along the path, an excellent view of the blue-grey marbles within yellow-weathered quartz–white-mica–calcite schists is seen (Fig. 1.4f). Marbles several metres thick lie within a cliff dominated by schists. Possibly, the succession has been folded on a medium- to large-scale; thus the several bands of marble may have originally been a single layer, as seen in the low-strain part of the Petroussa Formation in SE Kythnos (Stop 5.2).

All the material visible down-hill from the outcrops at the hilltop, on the northwest side of the ruined castle and village, is part of a local downslope mass-movement (Fig. 1.4g).

Stop 1.5. Episkopi Formation. Coarse epidote porphyroblast schists.
UTM 35S 272666E 4149020N.
No Figure.

From Stop 1.4, return to the road north from Loutra and drive 0.5 km north. Take the turning to the right and drive down to the coast at Potamia Bay. On the north side of the northern beach, coarse epidote schists crop out; individual epidote-group porphyroblasts may be up to 0.5 cm long and these are randomly oriented both on and across the layering. No distinct foliation can be seen within the schists in outcrop, but a quartz boudin has a margin here presumed to be the foliation (sm 325/31°, lm 054/09°). Thin marbles occur c. 15 m SE from the north end of the beach, under a small overhang (sm 060/15°, lm 067/12°). These schist look very like those found at the lowest stratigraphic level (Kanala Formation; a-Stop 5.9; Fig. D). Whether they are the same unit, repeated by folding, or simply a stratigraphic repetition, is not yet known.

Stop 1.6. Episkopi Formation. Marble conglomerate.
UTM 35S 272558E 4148840N.
Fig. 1.6, looking NE.

Return to the vehicle and follow the footpath southwards, along the coast. Climb down from the path to the outcrops on an obvious platform ~25 m ENE of the south beach; the outcrop is not accessible from the beach. Here, marble conglomerate, identical to those found in only three other places on Kythnos, all in the Kanala Formation (Stops 3.2, 4.4), crops out in a layer ~2 m thick within greenschists (sm 083/11°). The conglomerate comprises white to grey marble clasts that are markedly prolate (Fig. 1.6), with X>>Y>Z, defining clast long-axes plunging 052/07°, identical to the stretching lineation in quartz-veins parallel to the foliation (lm 053/07°).

Figure 1.6
Episkopi Formation: Marble conglomerate.

The presence of a marble conglomerate within the Episkopi Formation, looking exactly like the marble conglomerates found in the Kanala Formation, is taken as strong evidence that the two formations can be correlated. Occam's razor indicates that the likelihood is small that both units, if not correlated, should have identical marble conglomerates, when these are not found in any other unit on the island.

Stop 1.7. Mavrianou Formation. Ductile to brittle boudinage.
UTM 35S 272020E 4149340N.
Fig. 1.7, looking NW.

Return to the main road heading north from Loutra and turn right. After ~1 km, park where the road forks. This outcrop shows a c. 2 m thick yellow-weathered quartz–white-mica–calcite schist layer within the blue-grey marble mylonites of the Mavrianou Formation (sm 065/25°, lm 064/24°), with asymmetrically boudinaged quartzite layers recording a top-to-the-SW shear-sense. The schist layer is thinned by a c. 4m long brittle-ductile shear band (boudinage) accommodated by ductile flow and the formation of a neck-fold in the marbles. Although the shear band indicates a similar top-to-the SW directed kinematic, it clearly formed after the mylonitic deformation in the marble because isoclinal folds structurally above the shear band are refolded by the neck fold (axial-surfaces of folds are shown as solid lines in Fig. 1.7). Interestingly, the marbles are affected

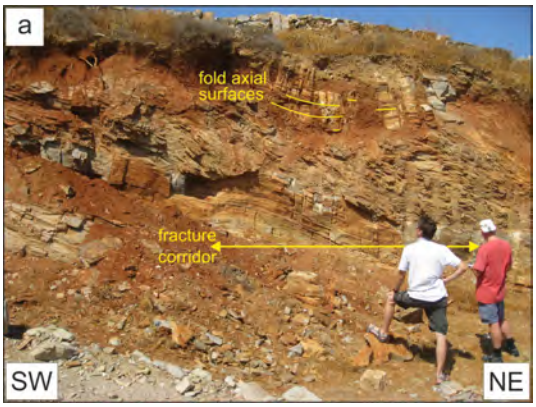

Figure 1.7
Mavrianou Formation. Ductile to brittle boudinage.

by a dm-spaced foliation-perpendicular fracture corridor exactly at the position where the neck of the shear band boudin formed (Fig. 1.7), suggesting that deformation occurred at the ductile (neck fold) to brittle (fracture corridor) transition of deformation mechanisms in calcite.

EXCURSION 2: W KYTHNOS; Merichas to Kolona Bay

Much of this day is based around the area near Merichas; several outcrops can be reached quickly by foot or in a hire-car, making them suitable for a very short trip of a few hours. Overall, the day shows many of the main geological features of the island. All Stops are shown in Fig. 2.0.

Stop 2.1. Mavrianou Formation. Refolds and flanking structures.
UTM 35S 269140E 4141359N.
Fig. 2.1a, b, looking NW; Fig. 2.1c, d, looking SW.

Drive to the west side of Merichas and stop just before the first switchback. Just south of the corner, <2 m of blue-grey marble mylonites with abundant thin quartzite layers of the Mavrianou Formation crop out. The outcrop face is sub-parallel to the stretching lineation, which shows a slight difference in orientation between the marble and quartzite layers (lm 043/12° in quartzite; 039/07° in marble). Thicker quartzite layers show brittle fracturing superimposed on a ductile, larger-scale pinch-and-swell structure (Fig. 2.1a, b). In some cases, the brittle fractures are normal to the layering, typical for stress refraction at a coupled interface between rocks with a strong viscosity contrast, whilst in other cases they are conjugate and may show symmetrical horst or graben structures. Where these fractures intersect, the separated blocks may have curious 'kinked shapes' (convex to NNE or SSW, Z or S shapes or L shapes in various orientations), possibly suggesting that the two fracture systems were essentially coeval. The different styles in deformation may be reflecting variations in confining pressure. Both sets of fractures show that a subsequent non-coaxial deformation (top-to-the-SSW rotation) occurred. Calcite deposition between some blocks indicates diffusive mass transport (Fig. 2.1a). A more detailed discussion of such structures is given at Stop 3.5.

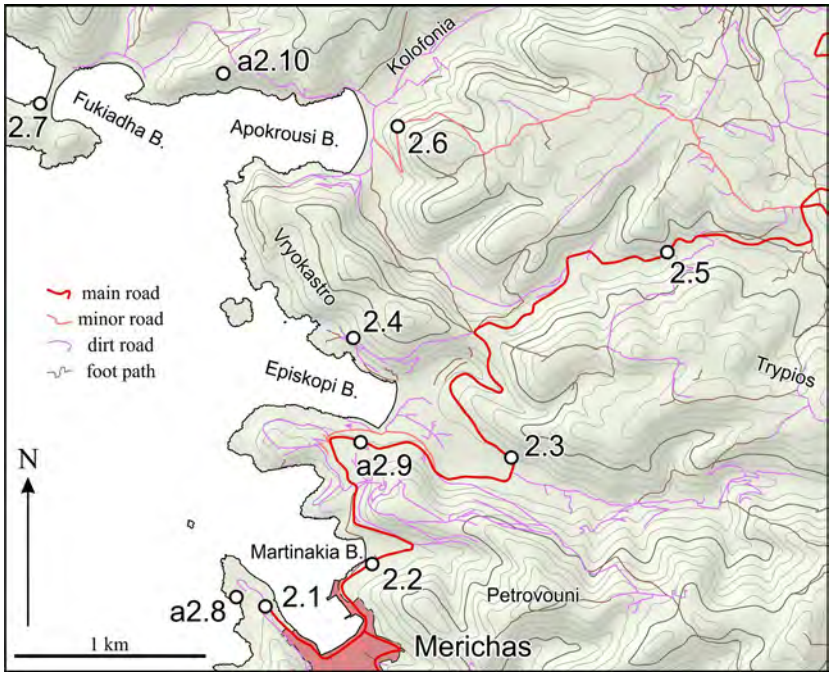

Figure 2.0
Outcrop location map for Stops 2.1 to a-2.10.

Across the road and over the dry-stone wall to the NE (UTM 35S 269147E 4141385N), where the outcrops are perpendicular to the stretching direction, yellow-weathered quartz–white-mica–calcite schists with thin interlayered marbles show Type-3 refolds (Fig. 2.1c, d). The axes from the two fold generations are parallel (lf1 237/15°; lf2 239/12°) and are also essentially parallel to the stretching lineation (lm 245/18°). The earlier generation comprises isoclinal structures with axial surfaces (sap1 261/17°) essentially parallel to the layering (Fig. 2.1d).

At the base of the outcrop, the second fold generation is an essentially upright open, symmetrical antiform (Fig. 2.1c). This is overlain by a southeast verging asymmetric fold (sap2 301/40°) that develops very abruptly in the mechanically weaker interlayered marbles and quartz–white-mica–calcite schists. The overturned middle limb of this part of the fold is cut by a high strain zone parallel to the axial surface that might offset the layers (in which case the structure can be described as a flanking structure). Where the layering abruptly changes upwards, back to relatively thick quartz-rich layers without marbles, the fold geometry progressively returns to an upright, symmetrical antiform; the middle limb is no longer overturned, the high-strain zone broadens out upwards into a number of discrete brittle or brittle-ductile fractures that die out, such that there is progressively less offset of the layering.

Downwards, the high-strain zone/fracture may

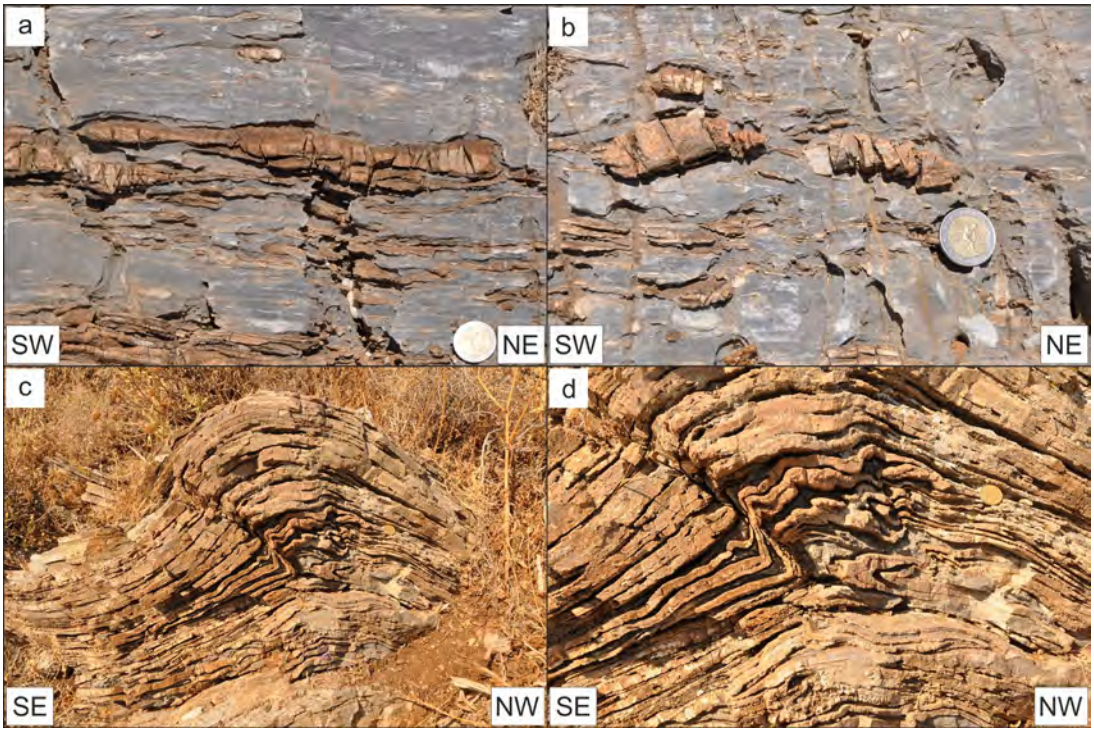

Figure 2.1
Mavrianou Formation. Ductile to brittle polyphase boudinage and refolds.

rotate into parallelism with the layering at the top of the lower upright antiform. If this is the case, the outcrop, which reflects shortening perpendicular to the transport direction, might be interpreted as a lateral ramp.

The Mavrianou Formation can be traced continuously from here southwards along the ridge to the west of Merichas for 1 km. The same lithologies can also be seen forming the west-facing hillslope when looking east from here to the hill-top across the bay above Merichas.

Stop 2.2. Flabouria Formation. Greenschists with SCC' fabric.
UTM 35S 269697E 4141580N.
Fig. 2.2, looking SE.

Drive back into Merichas and take the road going gently uphill to the north, towards Hora. Just around the corner, opposite the southern end of Martinakia beach, a road-cut for a planned house exposes greenschists within the Flabouria Formation intensely overprinted by a top-to-the-SSW SCC' fabric (Fig. 2.2). The C-planes dip at shallow angles towards 030°. On the steeper-dipping S planes, a distinct stretching lineation plunges at c. 50° towards the NNE. The C' shear planes (sc' 200/30°) deformed S-parallel quartz-veins into asymmetric pinch-and-swell boudins, confirming the SSW-directed shear-sense.

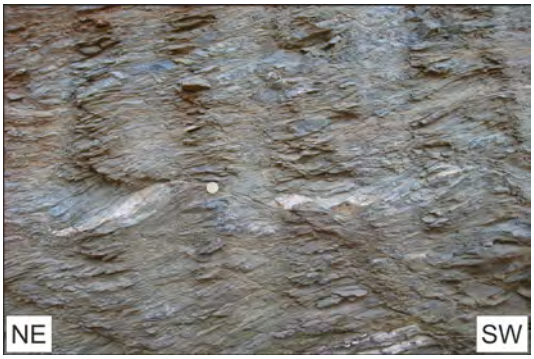

Figure 2.2
Flabouria Formation. SCC' fabrics in greenschists.

Stop 2.3. Flabouria Formation. Complex flanking fold.
UTM 35S 270423E 4142135N.
Fig. 2.3, looking NW.

Continue for 2.2 km along the road towards Hora, to Episkopi. Park at the corner, after crossing the river Episkopi, and walk uphill. The rocks are composed of grey sericite schists with black, graphitic albite porphyroblasts typical of both the Upper and Lower Flabouria Formations. A low-angled fault with cm-thick foliated cataclasites is exposed along the road-cut (the fault is visible at the base of Fig. 2.3). This is parallel to the main foliation in the schists (sm 038/08°) and records a top-to-

the-SW shear-sense. A quartz-vein that formed a complex flanking fold during SW-directed rotation, rooted into the normal fault.

Figure 2.3
Flabouria Formation. Complex flanking structure at a quartz-vein.

The rotated, fork-shaped, vein, which probably merged from two individual quartz-veins, forms an n-type flanking fold (Fig. 2.3), where the foliation close to the vein has been passively rotated, together with the vein, into the shear direction. As a result, the foliation of the attached host-rock close to the sheared veins has been deformed in a complex antiform-synform fold. However, the schists between the two quartz-veins have been antithetically sheared during rotation, forming a new foliation parallel to the vein margin.

Stop 2.4. Mavrianou Formation. Contemporary brittle and ductile extension.
UTM 35S 269600E 4142755N.
Fig. 2.4, looking NW.

Continue towards Hora, but turn at the first junction to the left, onto the road on the north side of Episkopi Bay. At the junction, note how thick the layers of blue-grey marbles and intervening yellow-weathered quartz–white-mica–calcite schists are within the Mavrianou Formation, and compare these with the much reduced thicknesses at the outcrop described here.

After 0.65 km, the road cuts through an old dry-stone wall. Close to and north of this wall, the marble and quartz–white-mica–calcite schist layers are <0.5 m thick, rather than several metres thick. This indicates a general thinning of the Mavrianou Formation to the west. Further, there are more layers of blue-grey marble here than at the road junction, suggesting extensive repetition by folding and subsequent shearing of the succession further to the west.

The outcrop shows pervasive normal faulting down-throwing to the southwest (sh ~225/dip variable°), with offsets of a few mm to several cm (Fig. 2.4a) every few cm; sometimes, the down-throw is to the east, giving horst-and-graben structures (Fig. 2.4a, b, e). This faulting has also been seen at a larger-scale in the Petroussa Formation (Stop 4.3). In one case (Fig. 2.4c), the fault has a reverse sense of displacement in one layer, down-throwing to the west, although this is not the case in adjacent layers (Fig. 2.4b, d), where the fault zone is much wider. In detail, Fig. 2.4b shows that the fault plane of the reverse fault links upwards with fault surface of an east-dipping normal fault.

Within the quartz–white-mica–calcite schists, post-schistosity forming deformation largely occurred by brittle processes, but sub-vertical arrays of tension cracks indicate a component of brittle-ductile deformation (Fig. 2.4d). In contrast, the coeval extensional deformation in the blue-grey marble mylonites was largely ductile, with extreme thinning of the layering into an oblique foliation (Fig. 2.4e, f). Nevertheless, some brittle fracturing occurred in the marble mylonites (Fig. 2.4c, e, f) indicating to either a higher strain rate coeval with essentially ductile deformation or later deformation at a lower temperature.

Stop 2.5. Flabouria Formation. SCC' structures and brittle/ductile faults.
UTM 35S 271237E 4143202N.
Fig. 2.5, looking WNW.

Return to the main road and turn left to Hora. After 1.3 km, opposite where the valley-floor begins to widen, a small quarry shows layer-parallel ductile shear zones (Fig. 2.5). Strain localized in phyllosilicate-rich layers between more competent feldspar-rich layers with albite porphyroblasts. SC, SCC' fabrics and sheared quartz-veins document top-to-the-SW kinematics. Two lineations are seen on the cleavage-planes (lm 054/22° and 009/19°). The whole sequence is cut by dm- to m-scale brittle/ductile normal faults (sf 237/23°) with a lineation dipping towards 215°. En-echelon quartz-veins cut by the faults and the precipitation of quartz along the fault planes indicate diffusive mass-transfer processes. The faults have a strong displacement gradient, resulting in bending of the fault planes and normal dragging of the main foliation. The obvious top-to-the-SW extensional

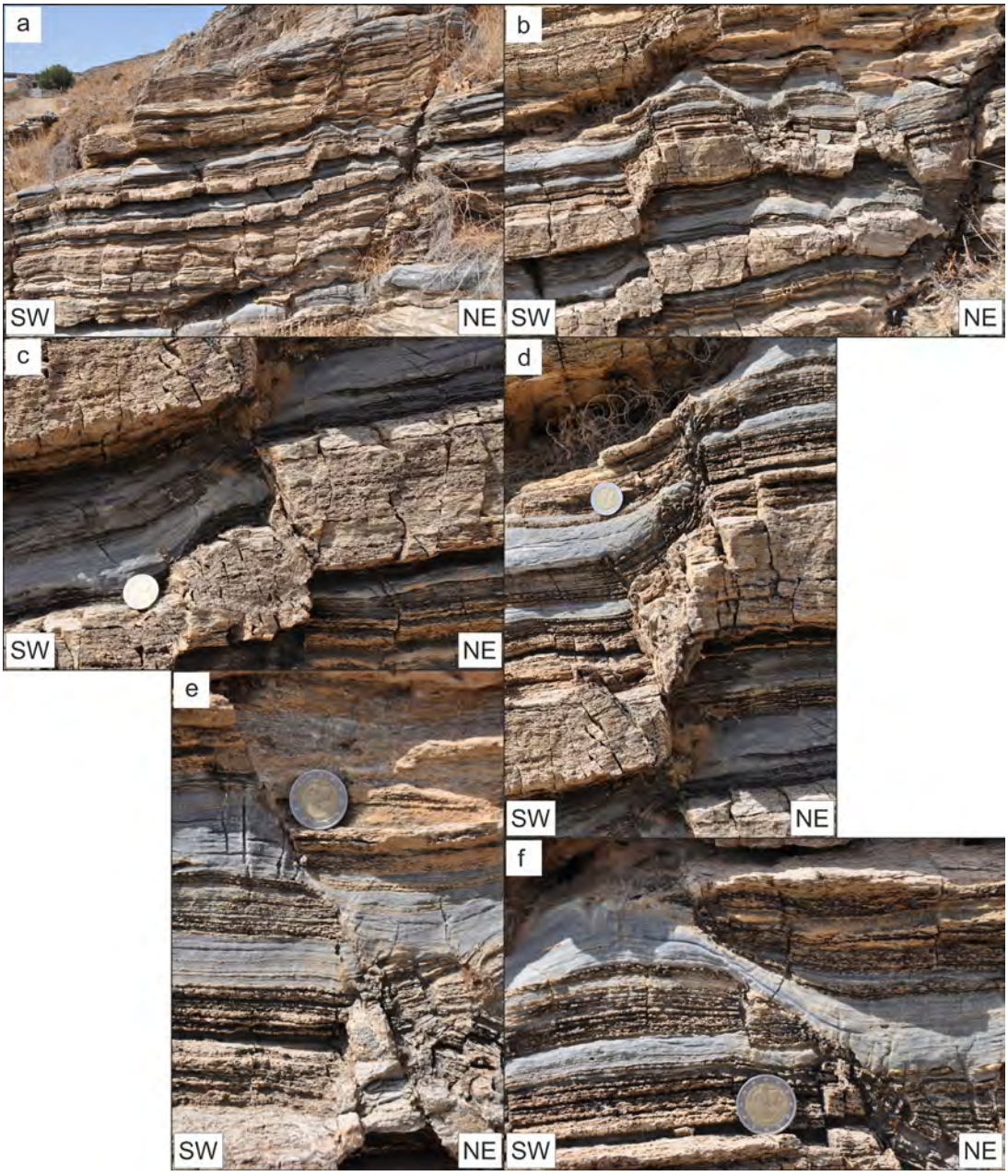

Figure 2.4
Mavrianou Formation. Contemporary ductile and brittle fracturing and faulting.

kinematics of the faults is confirmed by secondary synthetic Riedel fractures.

Stop 2.6. Upper Flabouria Formation. Grey and white marble boudins.
UTM 35S 269830E 4143858N.
Fig. 2.6, looking SE.

Continue for 1 km towards Hora; at the cross-roads, turn left to Apokrousi Bay. After 2.6 km, outcrops on the corner of the road as the bay comes into view show boudins of pale grey to white marble within the Upper Flabouria Formation (Fig. 2.6a). The zone of marbles is <3 m thick and visible for several metres along the outcrop. Parts of the boudins, which lie within chloritic schists (sm 071/20°, lm 043/15°) with top-to-the-SW SC' structures (sc' 211/38°, lc' 227/24°), have a mylonitic foliation (sm 017/20°, lm 048/18°). The boudins and schists are folded (south side of Fig. 2.6a lf 053/11°, sap 050/19°). Elsewhere, microlithons (s 070/19°) are sub-parallel to the fold axial surface (Fig. 2.6b; from the northern end of the marbles).

Such isolated marble boudins are relatively common in the Upper Flabouria Formation (see a-Stop 1.9) and, although here of a lower strain

Figure 2.5
Flabouria Formation. SCC' structures and brittle/ductile faults in greenschists.

level, are comparable in terms of their outcrop style to those exposed on the ridge forming southern Kythnos (Stops 4.6)

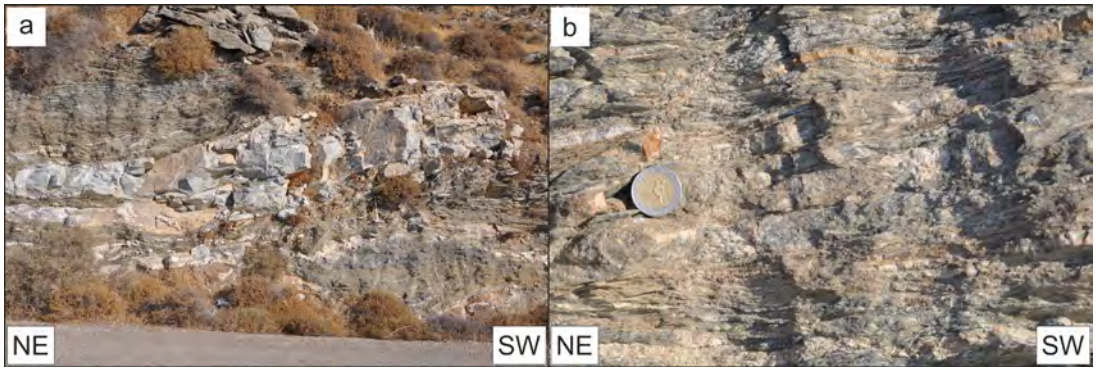

Figure 2.6
Upper Flabouria Formation. Isolated marble boudins.

Stop 2.7. Mavrianou Formation. Refolds, boudins, tension cracks and ductile-brittle SC' structures.

UTM 35S 267965E 4143977N.
Fig. 2.7, looking ESE.

Drive down to and then north across Apokrousi beach. Take the narrow road on the north side of the bay, towards Kolona. At Kolona, drive to the southern end of the sandy isthmus and go to the coastal outcrops on the west side. The outcrops comprise blue-grey mylonitic marbles and yellow-weathered quartz–white-mica–calcite schists of the Mavrianou Formation (sm 148/10°, lm 045/02°). Interesting structures occur for most of the 60 m of outcrop by the sea; Figs. 2.7a-c lie ~20 m west of the isthmus.

Early deformation in the quartz–white-mica–calcite schists was ductile; the inverted limb of the recumbent fold (lf 097/10°, sapl 079/11°) at the base of the thick schist-dominated succession in Figs. 2.7a, b has been sheared at least 0.5 m (yellow arrows). Below, a short quartz-vein between two quartz–white-mica–calcite schist layers within the blue-grey marble mylonites has been folded ductilely/ptygmatically (Fig. 2.7a, c).

Subsequent deformation was initially brittle-ductile, with arrays of en-echelon tension cracks (ses 211/63°) reflecting a downthrow to the SSW (as with the faulting at Stops 2.4, 4.5) and a blocky style of boudinage of the quartz-rich layers, which show minor necking and separation of the blocks, with calcite infilling (Fig. 2.7b; thick layer just above the blue-grey marble). The final deformation stage is seen in essentially planar brittle fractures dipping NNE (sh 031/77°). Only where intervening marble layers are thin do these fractures persist from one competent layer to the next. Top-to-the-SSW shearing is seen in the sigmoidal shape of some fractures and the co-rotation of fault blocks.

Further west, towards the end of the outcrop, a large-scale top-to-the-SW SC' structure is exposed on a west facing surface (Fig. 2.6d; sm 065/29°, lm 043/25°, sc'216/27°, lc' 210/22°). Early ductile deformation is seen in the foliation drag against the C' plane. Evidence of later brittle deformation is seen in the development of a thin C'-parallel cataclasite (white rock in Fig. 2.7e) and, lower down a polished slickenside C' surface (sc' 206/23°, lc' 204/21°) that cuts small-scale folds in quartz-rich sediments in the footwall (Fig. 2.7f, g).

Above and to the west of this SC' structure, several tight to isoclinal, gently inclined folds can be seen within the blue-grey marble mylonite with thin quartzite layers, including refold structures (Fig. 2.7h; lf2 357/05°).

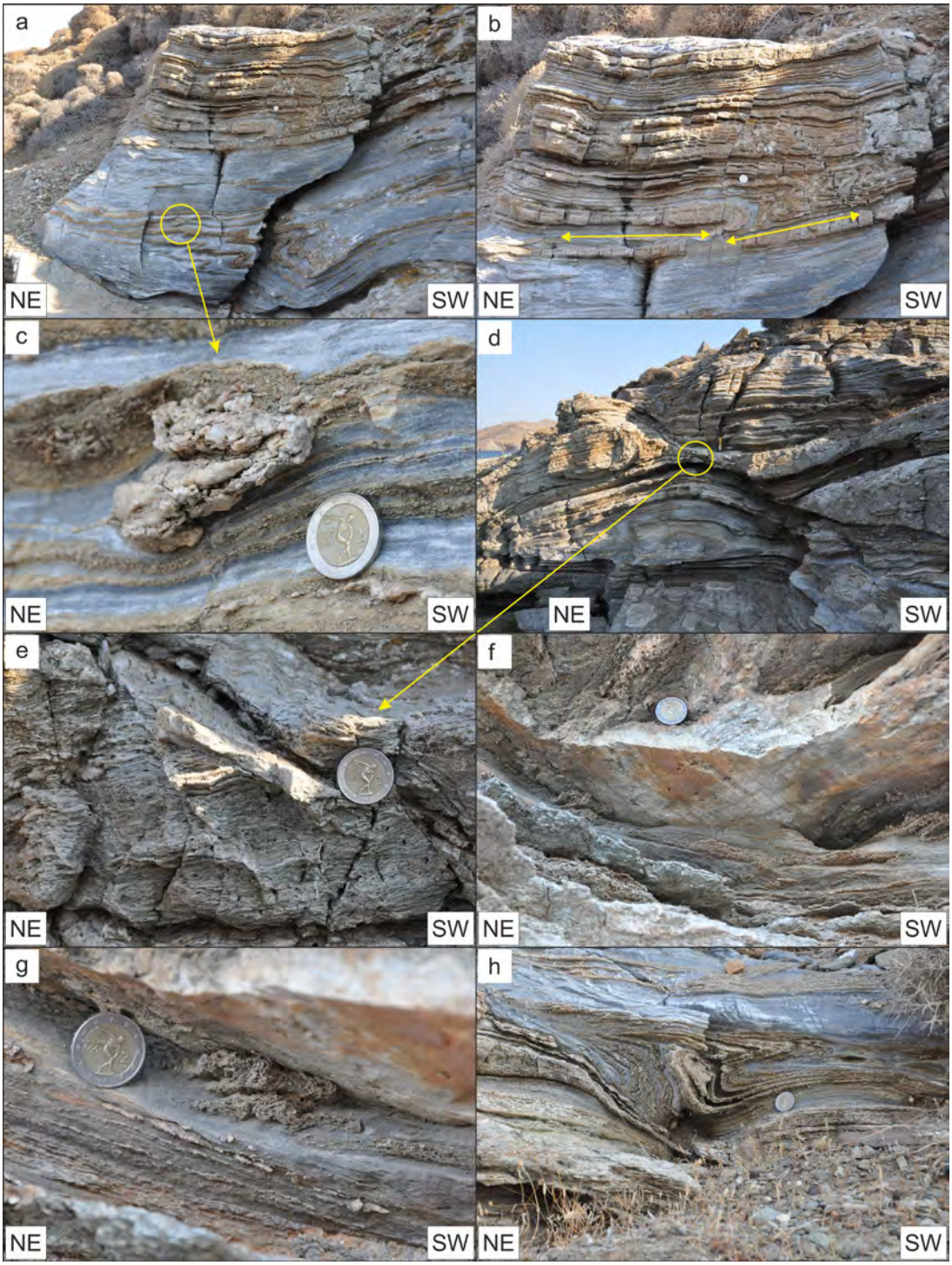

Figure 2.7
Mavrianou Formation. Ductile to brittle deformation with refolds and SCC' structures.

EXCURSION 3: E. KYTHNOS; Aghios Ioannis

This excursion shows the development of the Aghios Ioannis low-angled normal fault, a large-scale structure underlying and linking several blocks back-rotated on Riedel fractures. The area can be reached from the west, through Aghios Stefanos and then walking. The Stops described here require walking through the thorny maquis and garrigue vegetation; long trousers are recommended. All Stops are shown in Fig. 3.0.

Stop 3.1. Kanala Formation. Top-to-the-SW low-angled shearing cut by brittle high-angled faults.
UTM 35S 275415E 4141736N.
Fig. 3.1, looking SE.

Drive to the last right hand corner of the road and then walk 130 m NE to the SW corner of the beach. Here, near the shore line, chlorite-albite schists contain abundant quartz-veins that have been rotated into the shearing direction, almost parallel to the main schistosity (sm 049/20°, lm 068/18°; Fig. 3.1). During rotation, the quartz-veins were stretched, forming trains of asymmetric pinch-and-swell boudins; the monoclinic symmetry of the sigmoids suggests top-to-the-SW shearing. The rocks are cut by high-angled normal faults (mean sh 234/40°), some of which were exploit by Fe-carbonate veins (sv 231/44°). This suggests that in the brittle field of deformation, the ENE-WSW extension was accommodated by back-rotation of the high-angled faults and the formation of mineral veins with poles parallel to the stretching direction.

Figure 3.1
Kanala Formation. Low-angled ductile shearing cut by high-angle brittle faults.

Stop 3.2. Kanala Formation. Marble conglomerate.
UTM 35S 267965E 4143977N.
Fig. 3.2a, looking W; Fig. 3.2b, looking NNW.

Cross the beach and climb directly up the hill, to the NE; climb over the wall and walk NE to the outcrops in the middle of the next bay (400 m). Here, marble conglomerates, comprising white marble clasts within a greenish/impure marble matrix crop out (Fig. 3.2a, b). Similar rocks occur at three other localities on Kythnos (Stops 1.6, 4.4); the outcrop seen here is the most easterly. The long axes of the clasts (lp 071/10°) is parallel to the stretching direction in the marbles and schists; this direction is typical for eastern Kythnos. As there is no strong rheological contrast between the clasts and the marble matrix, the clast shape can be used to approximately estimate the shape of the finite strain ellipsoid. In the foliation plane of the marble conglomerate (sm 090/12°), the mean ellipticity R_{xy} is about 10. On exposures perpendicular to the stretching lineation, the clasts record a mean ellipticity R_{yz} of about 3. The finite strain ellipsoid plots, therefore, in the field of apparent constriction in the Flinn Plot, indicating prolate finite strain, i.e flattened and strongly elongated (X>>Y>Z).

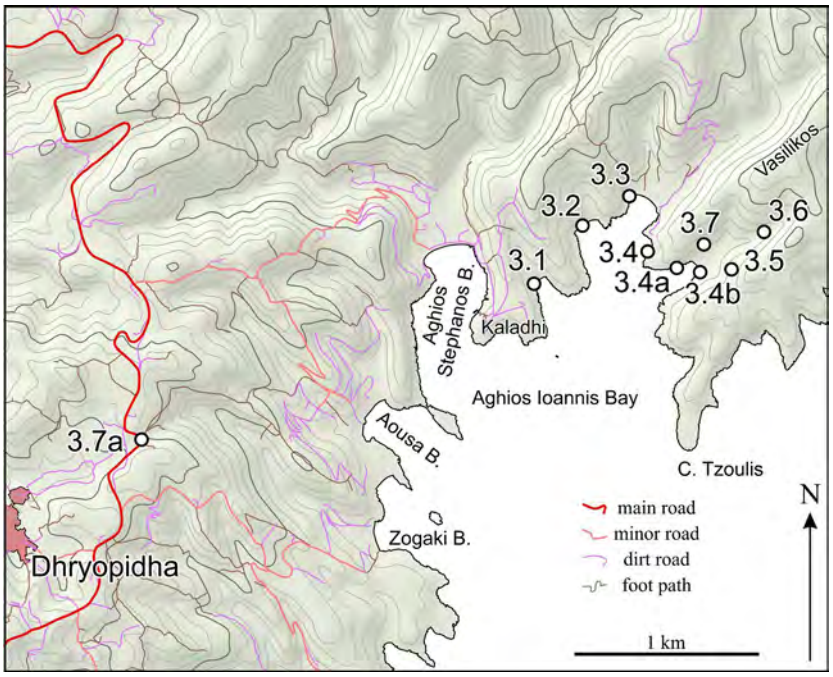

Figure 3.0
Outcrop location map for Stops 3.1 to 3.7.

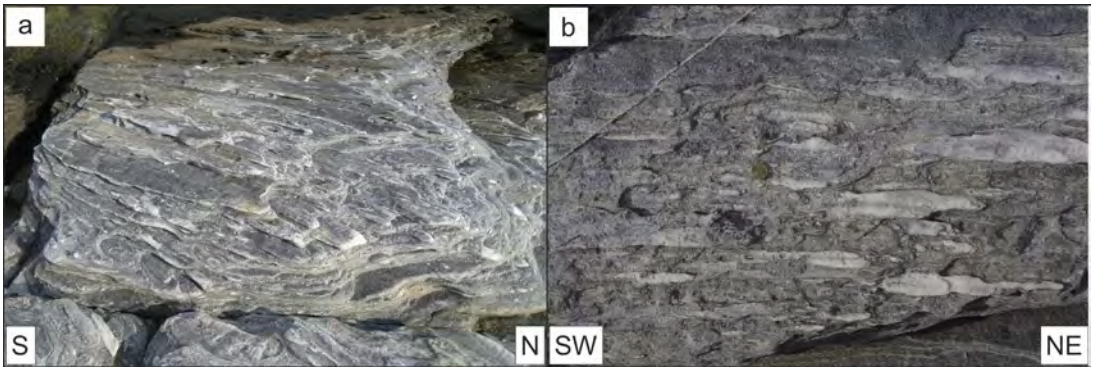

Figure 3.2
Panaghia Formation. Marble conglomerate.

Stop 3.3. Kanala Formation. Type 01 refolds and extension perpendicular shortening.
UTM 35S 275939E 4142212N.
Fig. 3.3, looking S.

Walk across the beach and then up to the obvious building. Then walk 200 m ENE and NE to the western corner of the next bay, a few metres south of the shoreline. The schists here, with cm-thick quartz and marble layers, are intensely deformed into WNW-vergent open higher-order folds (lf 020/08°, sap 109/59°), with dm-long wavelengths and amplitudes (Fig. 3.3). The folds deform the mylonitic foliation and stretching lineation, which is slightly oblique to the fold axis, and are themselves possibly sheared parallel to the fold axis towards the SSW, refolding the lineation but not changing the fold shape. These folds, therefore, might represent the rare case of a Type 01 refold structure, where the shearing direction of the superposed passive shear fold is the direction of the initial fold axis and the shear plane is perpendicular to the axial surface of the initial fold (Grasemann et al. 2004). Upright to slightly inclined folds with fold axes parallel or slightly oblique to the stretching lineation and shear direction are described from several Cycladic islands below major detachment systems (Avigad et al. 2001), including the WCDS (Grasemann et al. 2012). Commonly, this observation is interpreted to indicate a strong shortening component perpendicular to the extension direction.

Stop 3.4. Kanala Formation. Riedel to the Ag. Ioannis Low-angled Normal Fault: Mechanical interaction of high- and low-angled normal faults.
UTM 35S 276039E 4141910N.
Fig. 3.4a, looking S from the chapel; Figs. 3.4b-e, looking E; Fig. 3.4f, looking ENE; Fig.3.4g, looking WSW.

Walk 350 m SE, around the bay, to the west corner of the small chapel (Aghios Ioannis). From there, look SSW to see three obvious WSW-dipping planar fractures (Fig. 3.4a). Then walk 150 m

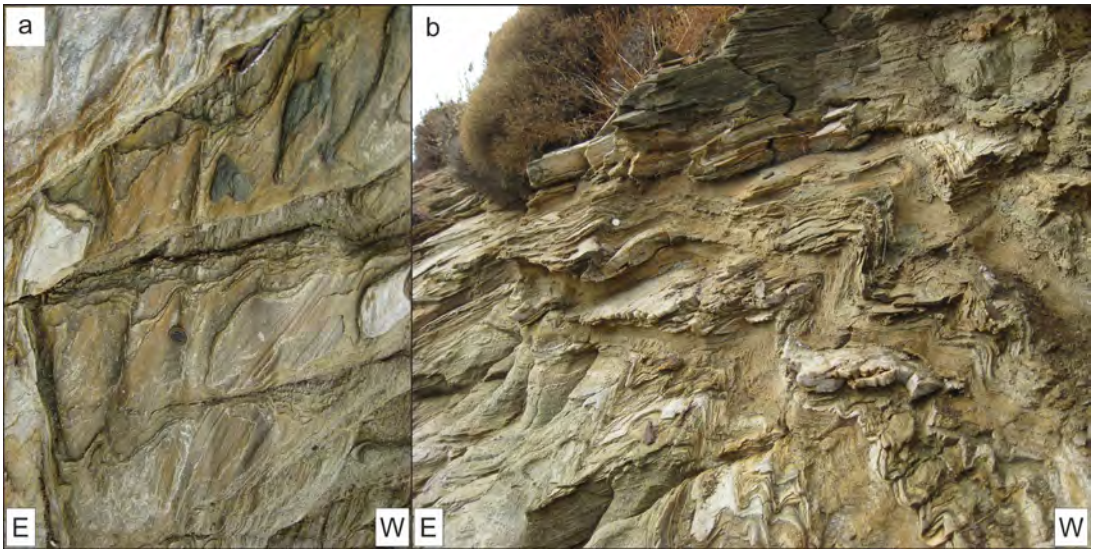

Figure 3.3
Kanala Formation. Type 01 refolds.

to the middle fracture, with an overhang, where a low-angled fault (lh 210/20°) cuts the quartz-rich host-rocks with several dm-thick marble layers (Fig. 3.4b). The metamorphic layering dips towards the NE and records a pronounced stretching lineation (footwall sm 040/30°, lm 051/21°, hanging wall sm 065/42°, lm 067/41°). The fault zone consists of an up to 3 m thick zone of cataclasites, ultracataclasites and clay gouges (Fig. 3.4c). Slip-planes at the margin of the fault zone record slickenlines dipping towards 195-200°. Dilation breccias and numerous cataclastically deformed and reworked calcite veins suggest fluid interaction during displacement along the fault. This structure, and similarly oriented faults/fractures in the area (Stops 3.4a, b) are interpreted as Riedel faults to the Aghios Ioannis Low-angled Normal Fault (LANF; Stops 3.6, 3.7).

Synthetic secondary Riedel faults (sf 185/40°) are linked to the main fault here, cutting both the cataclasites and the host-rocks (Fig. 3.4e). These indicate a top-to-the-SSW shear-sense. The shear-sense is confirmed by SCC' fabrics in both the foliated ultracataclasites and the clay gouges (Fig. 3.4c). Several high-angled normal faults mechanically interact with the low-angled normal faults and bend from the hanging wall into the low-angled fault. Kinematically, the blocks bordered by the high-angled faults in the hanging wall of the low-angled fault have back-rotated with respect to the overall SSW-directed shear-sense.

In Fig. 3.4a the main Riedel fault documented is marked with a solid yellow line; sub-parallel structures are marked with dashed yellow lines. A similar structure is exposed on the south side of the peninsula (Stop 3.4a), marked by the solid yellow line in Fig. 3.4f (picture taken from near Stop 3.4b; Fig. 3.0). The whole hillside here shows outcrop shapes controlled by fractures dipping parallel to this fault (dashed yellow lines; Fig. 3.4f). On the south side of this bay, behind the dry-stone wall, a similar structure is also well-exposed (Stop 3.4b; Fig. 3.4g; picture taken from near Stop 3.4a).

Stop 3.5. Petroussa Formation. Boudinaged, pinched-and-swelled, isoclinally folded quartz layers in blue-grey marble.
UTM 35S 276495E 4141812N.
Fig. 3.5, looking SSE.

From Stop 3.4b, walk 180 m east, uphill to the obvious marble outcrop. This shows spectacular brittle-ductile boudinage of quartzite layers in blue-grey marbles (see also Stop 2.1). The quartzite layers experienced very early isoclinal folding (Fig. 3.5a) and were subsequently deformed into elongate pinch-and-swell boudins before they were overprinted by brittle fracturing and a blocky-style boudinage (Fig. 3.5a-d). The mylonitic foliation in the marbles dips towards the ENE (sm 071/15°) and in some places is oblique to the quartzite layers (Fig. 3.5b). The general orientation of the late boudin necks trends 140-320°, almost perpendicular to the mylonitic stretching lineation (lm 051/14°), suggesting that the brittle boudinage of the quartzite layers was associated with ongoing ductile flow in the marble host-rocks. Exposures on foliation planes reveal that boudinage was roughly plane strain, with no evidence for shortening or extension in the intermediate finite strain direction. The fractures separating the boudins formed at high angles (almost perpendicular) to the foliation and rotated into the shear direction, forming book-shelf boudinage (Fig. 3.5b). The fractures propagated predominantly from one side of the quartzite layers but then, during rotation, also formed new fractures, resulting in V-shaped objects (Figs. 3.5a, c). Generally, the boudins have an unusually low width-to-thickness ratio of about 0.2-0.8. Ductile flow in the marble host-rock was accompanied by diffusive mass-transfer processes, precipitating new white calcite in the boudin necks. Some of the fractures in the quartzite layers are deformed into curved surfaces, documenting ongoing ductile deformation of the quartzite boudins. Separation of the inter-boudin surfaces with precipitation of new calcite in between, suggests a layer-parallel stretching component of strain during bookshelf boudinage, indicative for an overall general shear flow.

Stop 3.6. Lower Flabouria Formation. Low-angled high-strain zone; the Aghios Ioannis LANF.
UTM 35S 276672E 4142017N.
Fig. 3.6, looking S.

Walk 250 m north, without losing much height, so far as possible, to the dry river-bed. Then walk up the river-bed to the outcrops described, on the south side, where a distinct brittle-ductile high strain fault zone (sf 188/25°) is exposed within schists of the Flabouria Formation over several tens of metres (Fig. 3.6). The structure of the fault zone is variable, although both the foliation and included quartz-veins in the footwall and hanging wall have been rotated towards, or into, parallel-

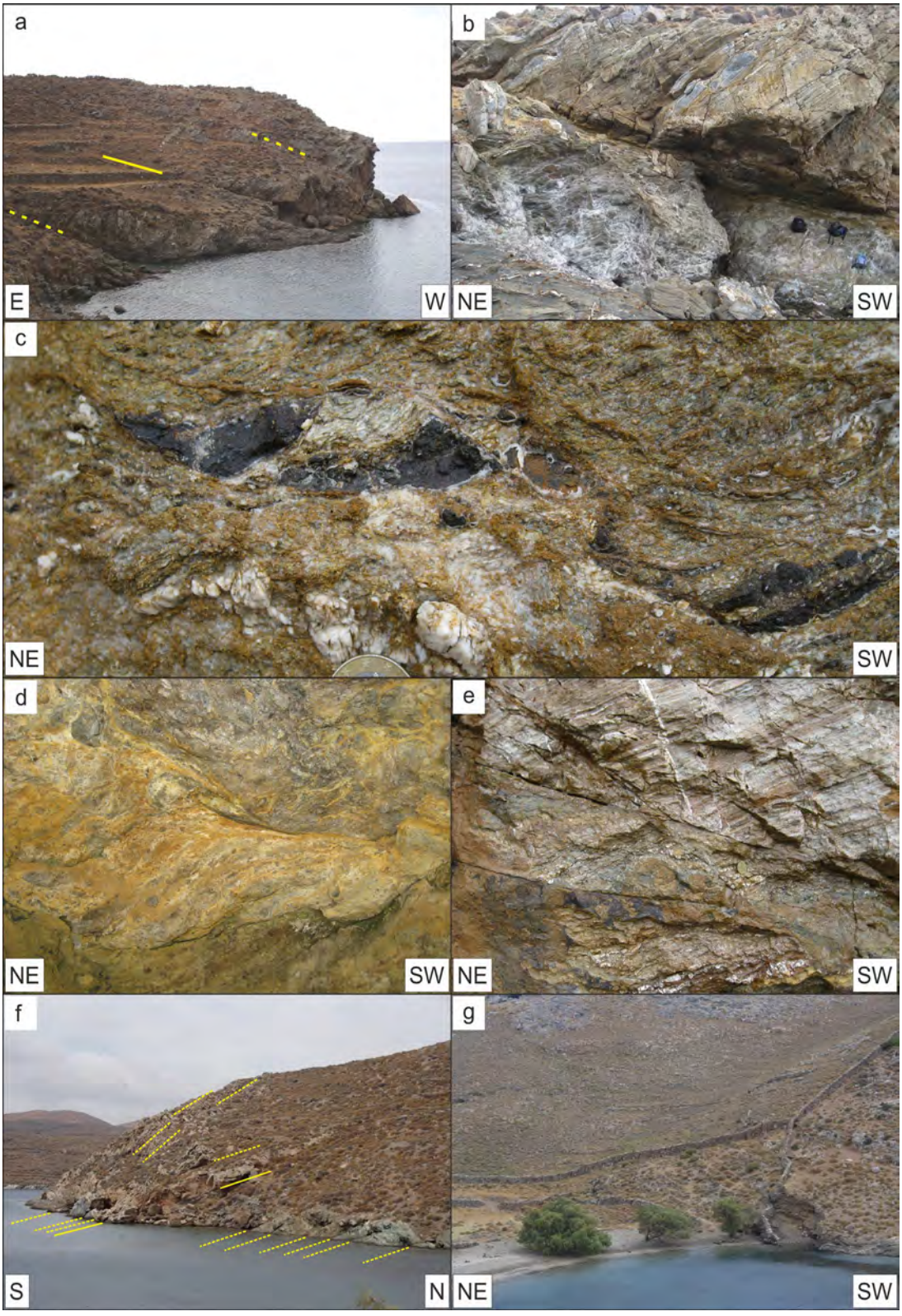

Figure 3.4
Kanala Formation. Riedel fractures linking to the Ag. Ioannis LANF .

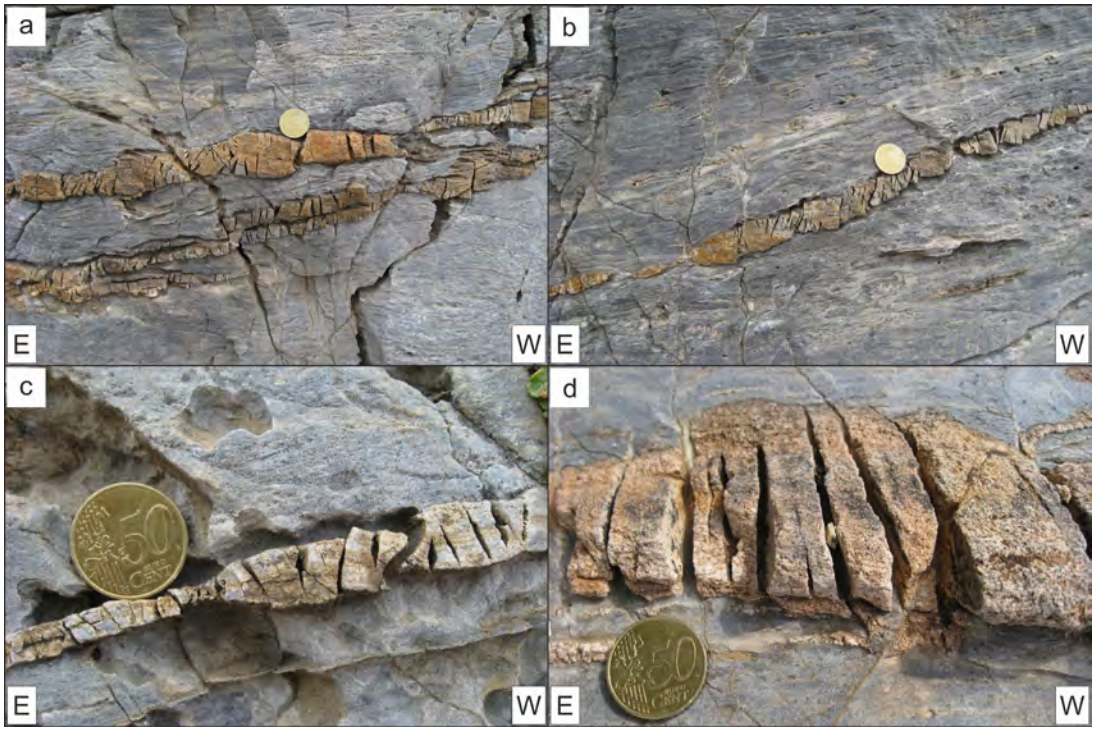

Figure 3.5
Petroussa Formation. Polyphase ductile to brittle boudinage of quartzite in marble.

ism with a zone of schist cataclasites generally <20 cm thick, within which SC' fabrics indicate top-to-the-SSW movement.

In some parts, knife-sharp contacts (principle slip surfaces) occur between the cataclasites and host-rocks (Fig. 3.6a); elsewhere, the contact is relatively gradational (Fig. 3.6b). Clasts within the cataclasite, such as that directly above the coin in Fig. 3.6c, show a top-to-the-SW sigmoid geometry. Note that the ~0.5 m thick block of schists above and to the SW of this clast is also a clast within the cataclasite, with an SC' geometry in the internal foliation indicating a top-to-the-SW movement. Including this sigmoid clast, the overall thickness of the fault zone here is ~1 m. No lineation was observed within the cataclasites.

The host-rocks are typical grey sericite schists of the Flabouria Formation (sm-hangingwall 062/34°, lcr 066/32°). The cataclasites and directly adjacent host-rocks have a green colour, likely representing chlorite growth; although this must reflect fluid circulation within the fault zone, no evidence for carbonate fluid infiltration has been seen here.

This fault is interpreted as a LANF (the Aghios Ioannis LANF) that links the high-angled top-to-the-WSW Riedel faults mapped in this area (Stops 3.4, 3.4a, 3.4b). The observed finite strain here does not seem particularly high. However, as each Riedel block is transported piggy-back by footwall imbricates, the displacement in the LANF increases to the SSW.

Stop 3.7. Panorama towards the Aghios Ioannis LANF and Riedel faults.
UTM 35S 276345E 4141948N.
Fig 3.7a, looking SE; Fig. 3.7c, looking ENE.

Walk 370m down the dry river valley and up the hill-slope on the north side of the valley, to opposite Stop 3.5. This affords a panoramic cross-section of the Aghios Ioannis LANF (Fig. 3.7a). The LANF, which underlies the valley floor, is inferred to dip gently towards the SSW. The ridges along the crest on the other side of the valley represent individual large-scale fault blocks that are separated by high-angled Riedel fractures bending into the LANF. Kinematically, each fault block has been back-rotated with respect to the top-to-the-SSW shear-sense. The abundant SSW-dipping fractures seen in the hillside behind Stop 3.4b (Fig. 3.7a, short dashed black lines) strongly suggests that there are more such Riedel fractures further to the SSW. This is consistent with the observable geology seen in satellite images (Fig. 3.7b). Note that this mechanical interaction and linkage of higher- and lower-angled normal fault can be observed at many different scales (compare Stop 3.4).

Stop 3.7c, from the main road west of Aghios Ioannis Bay, gives a more distant panorama of the

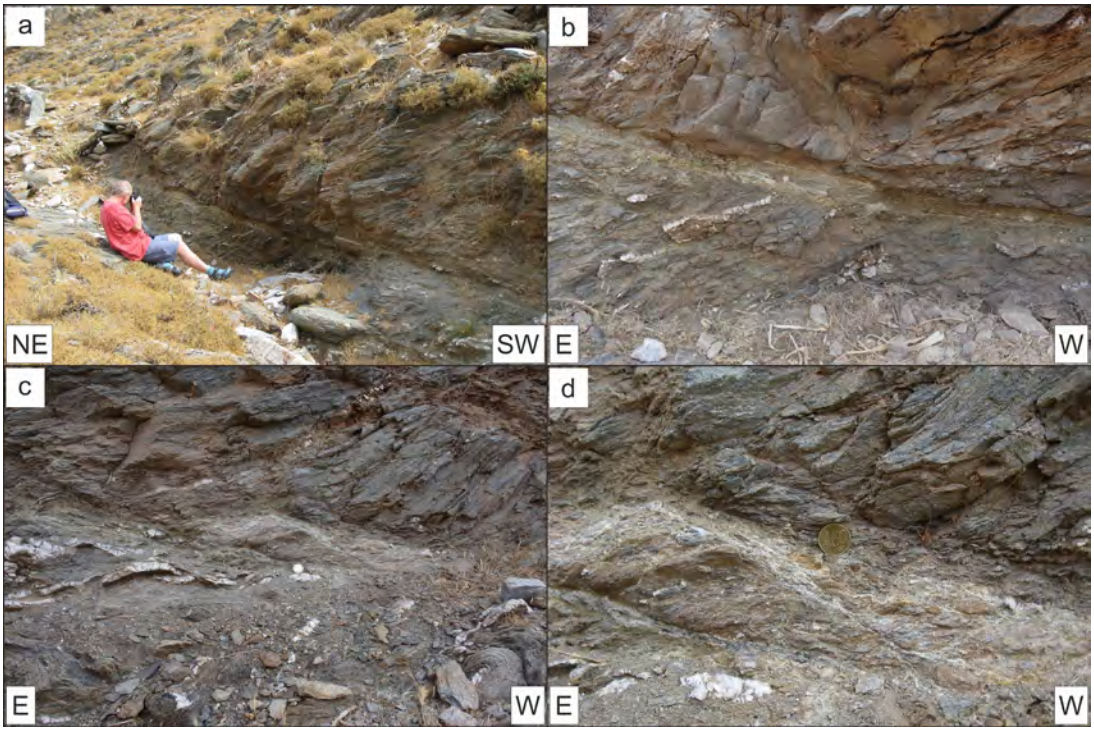

Figure 3.6
Lower Flabouria Formation. Ag. Ioannis LANF.

Aghios Ioannis LANF and associated Riedel faults (Fig. 3.7c). This, and the satellite image (Fig. 3.7b) show that the Riedel fracture seen at Stops 3.4 and 3.4a maybe the lowest on the northern side of that valley and hence that the fault seen at Stop 3.6 has an extensional lateral-ramp geometry.

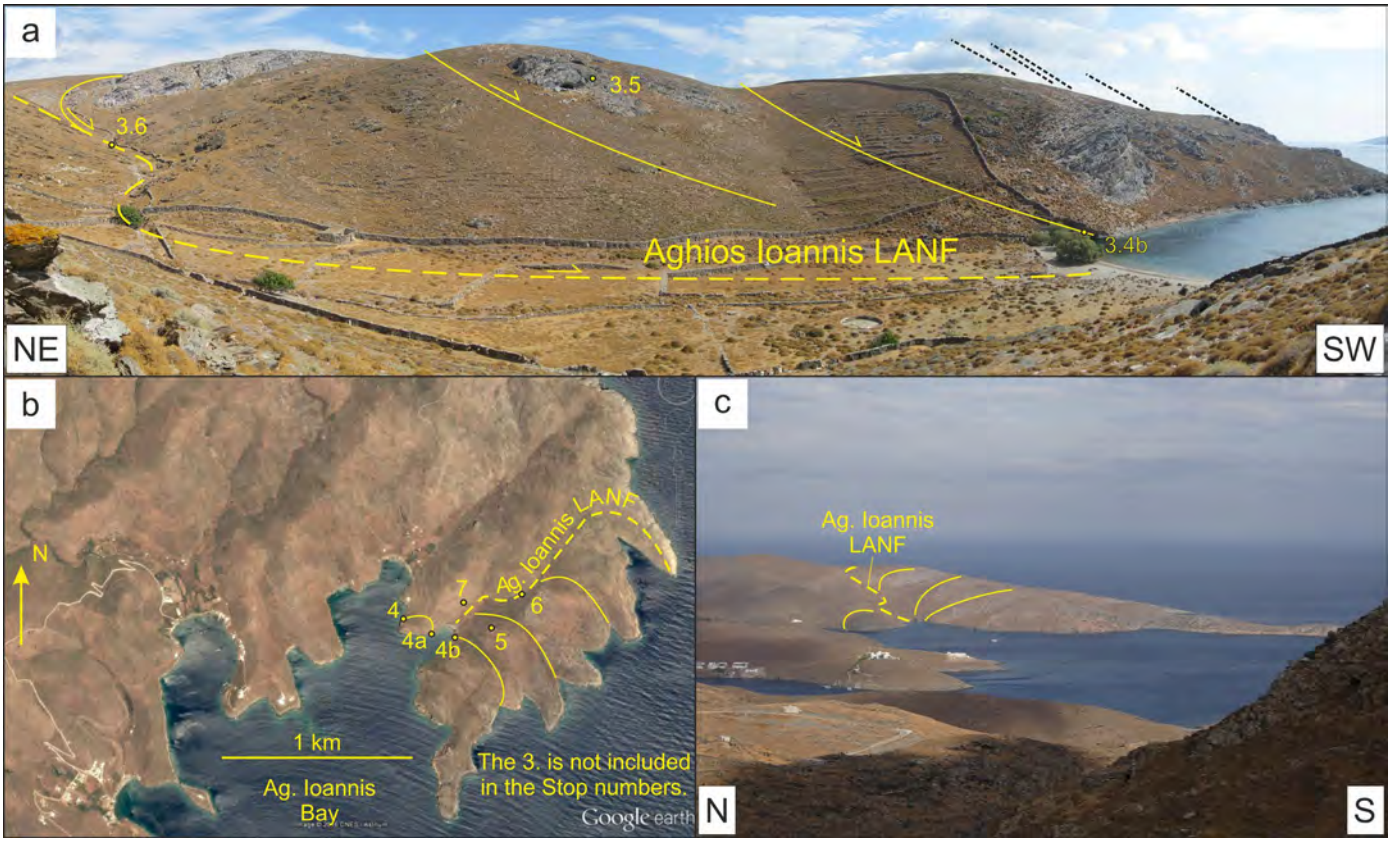

Figure 3.7
Overview of the Ag. Ioannis LANF.

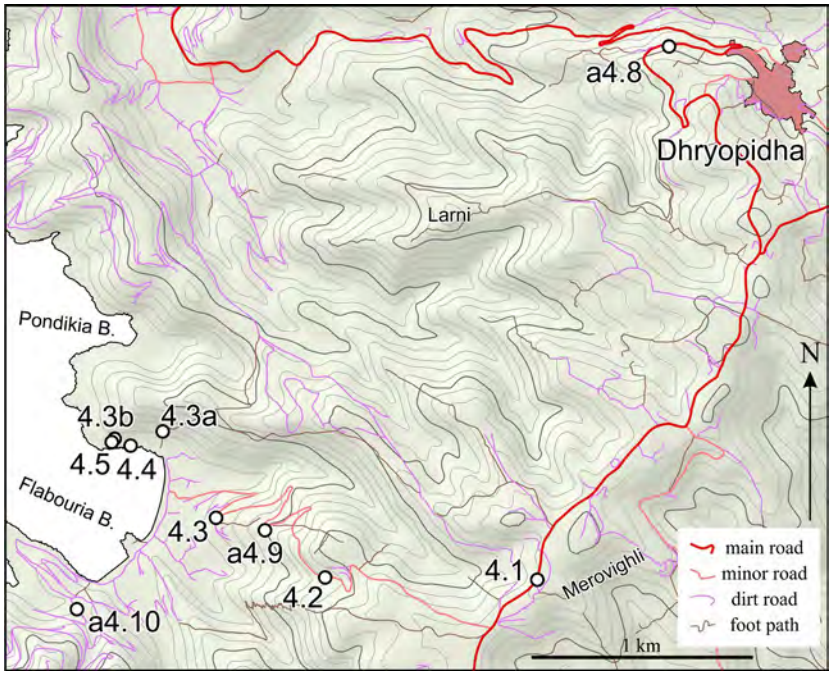

Figure 4.0a
Outcrop location map for Stops 4.1 to 4.5 and a-4.8 to a-4.10.

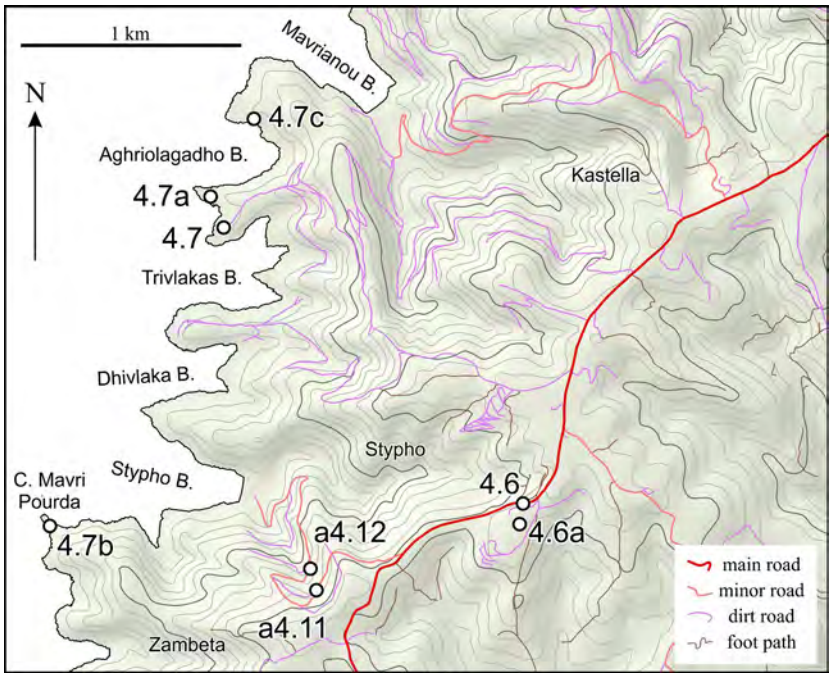

Figure 4.0b
Outcrop location map for Stops 4.6 to 4.7 and a-4.11 to a-4.12.

The development of a LANF below the Riedel imbricates indicates that there was either a strong displacement gradient associated with the faults or there must have been a similar LANF above, also linking the fractures. Whether this was the WCDS is not known, but the SSW-directed lineations in the Riedel fault at Stop 3.4 (195-200°), found in an area dominated by early WSW-directed shearing (M1; Fig. E), suggests that the LANFs were a late overprint (M2) of the earlier deformation.

A profile through a similar but intermediate-scale extensional duplex is exposed above Aghios Dimitrios, in the south of the island (Stop 5.3).

EXCURSION 4: CENTRAL KYTHNOS; Flabouria to Stypho

This excursion shows several outcrops that are important for the correlation of the marbles (Petroussa and Mavrianou Formations) on Kythnos and hence to the tentative large-scale structural interpretation of the island. All Stops are shown in Figs. 4.0a & 4.0b.

Stop 4.1. Petroussa Formation. Low strain, with boudinaged quartz–white-mica–calcite schist. UTM 35S 271455E 4138191N. Fig. 4.1, looking SE.

Drive south from Merichas and around Dhryopidha and then further south. About 1 km beyond the turning to Kanala, stop on the gentle right hand turn. This area lies at the crest of the Merovighli Antiform, which forms the large-scale structure of southern Kythnos. A long part of the road here is lined with outcrops from the Petroussa Formation; either blue-grey marble mylonites or yellow-weathered quartz–white-mica–calcite schists are exposed. Examine the roadside outcrops more extensively than just the detail outlined below, to become familiar with the lithologies.

The outcrop here is essentially parallel to the stretching lineation in the marble (sm 025/14°, lm 033/08°) and hence folds, which typically have axes parallel to the stretching lineation, although present, are not well seen. Boudins are well-developed in some quartz-rich layers within the marbles (Fig. 4.1) with the boudin neck trending 137°, essentially normal to the stretching lineation. The boudinaged layer here lies between blue-grey marble above and a thin weak layer within the quartz–white-mica–calcite schists below (now weathered out).

Figure 4.1
Petroussa Formation. Boudinage in quartz–white-mica–calcite schists.

Stop 4.2. Lower Flabouria Formation. Type 3 refold structures.
UTM 35S 270493E 4138201N.
Fig. 4.2, looking E.

Drive ca. 300 m south and then turn right, towards Flabouria. After the second switchback, quartz-veins and feldspar-rich layers are intensely folded within schists of the Lower Flabouria Formation (sm 060/11°). The fold axis of the recumbent folds (lf 071/21°, sap 009/45°) is parallel to the stretching lineation (lm 061/10°) and the axial surface is broadly parallel to the main foliation (it depends where the measurements are made). Locally, the fold hinges are significantly thickened compared to the thinned limbs; this thinning led to the formation of isolated rootless folds. A second fold generation, with a fold axis oriented sub-parallel to the first generation, led to the formation of Type-3 refold structures. The axial surfaces of the second fold generation dip steeply towards the SE and deform both limbs of the first generation folds into z-shapes folds (looking toward the NE).

Figure 4.2
Lower Flabouria Formation. Type 3 refold structure.

Stop 4.3. Petroussa Formation. View of thinning and down-faulting to the west.
UTM 35S 269994E 4138472N.
Fig. 4.3a, looking NNW; Fig. 4.3b, looking NW.

Drive further downhill to the sixth switchback. From here, the blue-grey marble mylonites of the Petroussa Formation, which crops out along the northern side of Flabouria Bay, can be seen to thin gradually towards the west, although they are still more than 2.5 metres thick where they meet the sea, and to be regularly down-faulted or down-folded to the west. Southwesterly down-faulting has also been seen at Stop 2.4, in the Mavrianou Formation. Here, this can be seen uphill, directly north of the beach (Stop 4.3a; Fig. 4.3a), with yellow-weathered quartz–white-mica–calcite schists both above and below the marble, and further west (Stop 4.3b; Fig. 4.3b). In the latter case, note that there are dry-stone walls linking the marble outcrops, giving the impression that the marble crops out continuously down the hill (i.e. that the offset of the marble is an effect of topography and erosion, not faulting or folding).

To the northeast of the beach, the Petroussa Formation climbs uphill until it forms the hilltop; in some parts, the blue-grey marble becomes thin, within thick successions of yellow-weathered quartz–white-mica–calcite schists.

Stop 4.4. Kanala Formation. Folded marble conglomerate.
UTM 35S 269610E 4138799N.
Figs. 4.4a, b, looking S; Fig. 4.4c, looking NNE; Fig. 4.4d, looking SW; Figs. 4.4e, f, looking NNE.

Drive down to the north end of Flabouria beach and walk west along the poor coastal footpath. From this, an outcrop of the marble conglomerate found at several localities on Kythnos (Stops 1.6, 3.2; Fig. C) and elsewhere in the Cycladic Blueschist Unit, can be seen. The conglomerate is particularly well exposed here, in a layer up to 2.5 m thick. Clasts are mostly prolate, with X>>Y, although some clasts have a more oblate form, with the X-Y clast plane parallel to the foliation orientation (Fig. 4.4a). The clast long axis here (lp 069/03°) is parallel to the matrix stretching lineation (lm 071/03°). In the Y-Z plane, most clasts are elliptical, but the occasional presence of relatively angular clast shapes (see large clast directly above the hammer in Fig. 4.4c), suggests that the clasts may be showing Y-Z profiles close to their original

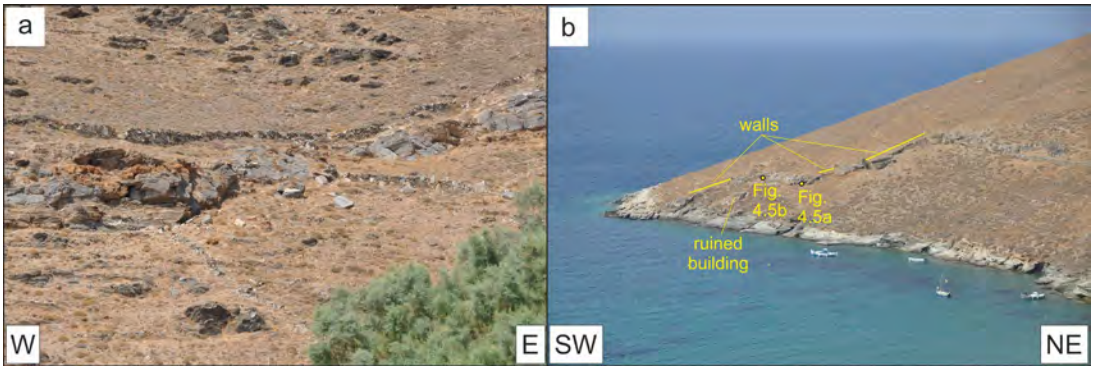

Figure 4.3
Petroussa Formation. View of the formation thinning and down faulting to the west.

sedimentary (?breccia) shape. The possibility that they are newly formed boudins is discounted by the lack of an adjacent block and by the low competence contrast between the marble clasts and the greenschist matrix, which would give a pinch-and-swell geometry.

In outcrops a few metres to the west, the foliation and conglomerate are spectacularly folded (lf 021/18°, lap 012/25°; Fig. 4.4e, f); the axial direction is parallel to a local NNE-SSW trending stretching lineation. Even where not obviously folded, the clast XY plane may be oblique to the main foliation but sub-parallel to a second, non-penetrative fabric (Fig. 4.4d), clearly indicating a top-to-the-SSW deformation. Looking down the fold axis shows that many clasts are no longer parallel to the foliation but have been rotated towards parallelism with the axial surface (Fig. 4.4e); this is particularly clear in the fold hinge zone (Fig. 4.4f). As the fold axis and stretching direction away from the fold are not parallel, this rotation was not simple.

West of the fold described, a second stretching lineation is markedly oblique to the pebble long axis direction (lm2 016/12°, lp 242/03°; Fig. 4.4b; pencil tip points to 196°). This direction is typical for M2 deformation, compared to the more ENE-WSW oriented dominant M1 lineation direction, suggesting localized high M2-strains.

Note that the marble clasts lie within a metapelitic matrix that is layered on a mm scale. Assuming that the conglomerate was deposited in a high-energy flow-regime, implying an unsorted/unlayered matrix, the observed layering must have formed by metamorphic/structurally induced recrystallization and differentiation.

Stop 4.5. Petroussa Formation. Folded, ductile and brittle boudinaged and faulted.

UTM 35S 269524E 4138815N.
Fig. 4.5a, looking NW; Figs. 4.5b, c, looking NNE; Fig. 4.5d, e, looking WNW; Fig. 4.5f, looking NNW.

Walk ~60 m further west along the coast and then go uphill to the completely ruined stone building (Fig. 4.3b). A few metres uphill from the eastern end of this, the blue-grey marble mylonites of the Petroussa Formation are underlain by yellow-weathered quartz–white-mica–calcite schists. The lineation in the schists is more easterly (sm 034/02°, lm 035/01°) than in the marbles (sm 326/16°, lm 026/07°), although this might be due to nearby small-scale folding (lf 028/12°, sap 091/11°).

A few metres west, a minor normal fault oriented essentially perpendicular to the stretching direction (sf 243/78°; Fig. 4.5a) offsets of the marble with a throw of ~0.5 m. This is a small-scale structure comparable to the major faults systematically down-throwing to the west seen on the north side of Flabouria Bay. No lineation was seen on the fault surface, but the lineation in a small stub of fibrous quartz plunges 051/02° (circled in Fig. 4.5a).

Further west, where the marble outcrop begins to go downhill, a 25 cm thick band of quartz-mylonites within blue-grey marble mylonites has been boudinaged into a gentle pinch-and-swell structure (Fig. 4.5b) that was later overprinted by high-angled, slightly curved brittle fractures showing a back-rotation sense of offset of up to 2 cm (Fig. 4.5c). A similar brittle overprinting of earlier ductile pinch-and-swell boudinage occurs at Stops 2.1 and especially 3.5. The fractures here (sf 231/68°) are more closely spaced and show a greater curvature in the neck part of the ductile structure. In a few, generally narrow, zones, fractures conjugate to the dominant set have formed, dipping steeply to the northeast, with the opposite offset, forming graben structures. Closely spaced, high-angled fractures are also present in the mar-

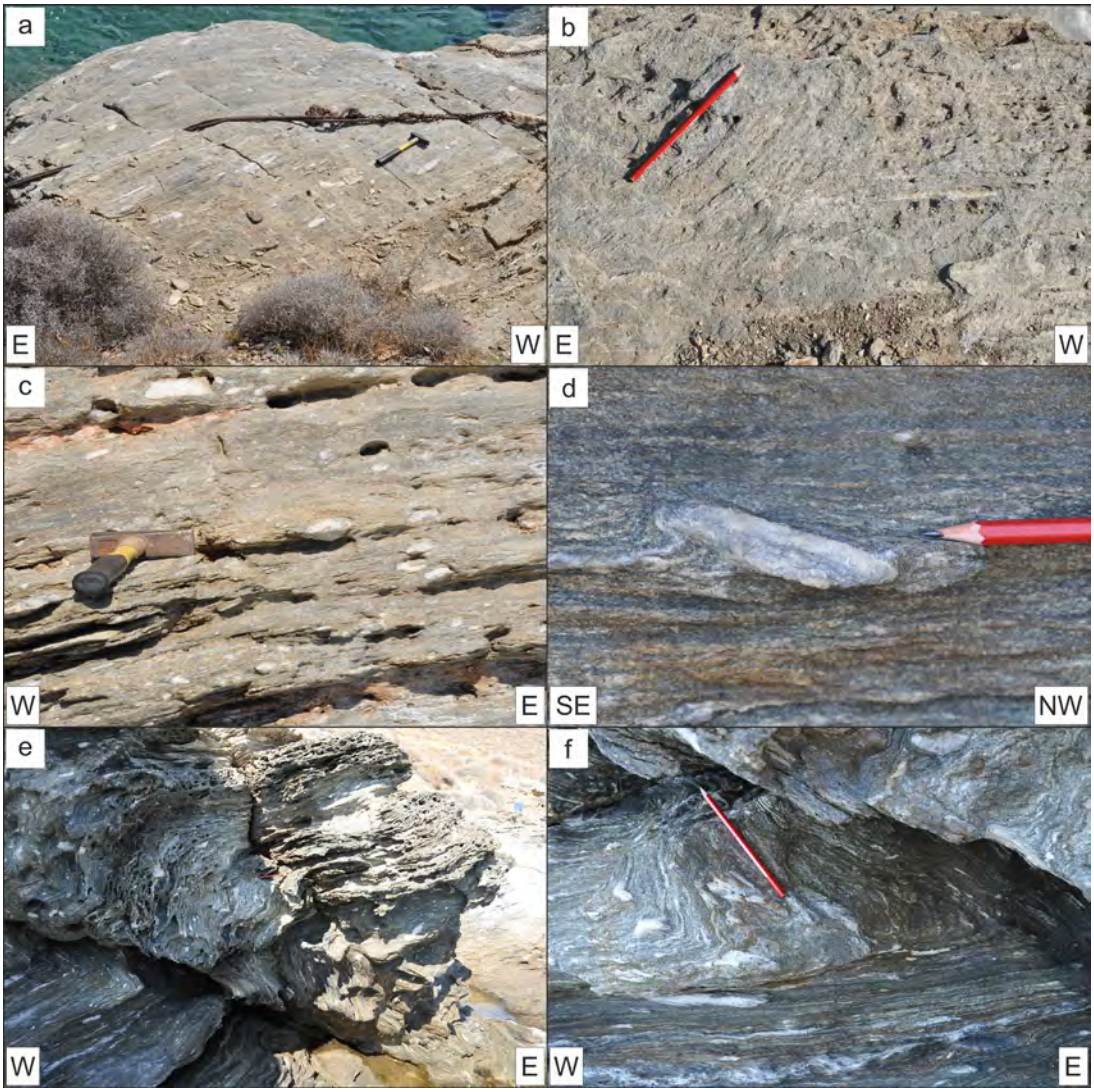

Figure 4.4
Kanala Formation. Folded marble conglomerate.

ble mylonites but these predominantly show a co-rotation sense of offset, although, again, some fractures have a conjugate orientation and the opposite offset. In both cases, as the offset increased, the fracture rotated further; back-rotation in the quartzites and co-rotation in the marbles, assuming the regional top-to-the-SW deformation. Overall, this represents a brittle overprint of earlier ductile structures, typical of the footwall to LANFs. Note also the a-type flanking structure in the marble, dipping at a low angle to the north (in the marble below the hammer handle in Fig. 4.5b). The strong displacement gradient along the cross cutting element is accommodated by reverse and normal drag in the mylonitic fabric. The shear-sense is top-to-the-SSW.

By the corner of the wall and field here, the rocks are folded on a mesoscopic scale; the marbles are folded isoclinally whilst the adjacent quartz-rich rocks form a northwest verging, slightly overturned monocline (lf 049/03°, sap 027/33°; Fig. 4.5d, e).

In the bay to the east of the headland downhill, grey metapelitic schists crop out directly under the Petroussa Formation (Fig. 4.5f); these schists have relatively abundant quartz pinch-and-swells, parallel to the foliation, with a coarse stretching lineation (sm 000/12°, lm 051/05°), similar to, but not so strongly developed as at Stop 5.6.

Stop 4.6. Upper Flabouria Formation and Mavrianou Formation. Marble mylonite layer (?mr1). UTM 35S 269126E 4135147N. Fig. 4.6, looking SE.

Return to the main road and drive 3.9 km to the south. Park in the dirt road on the left side, just before a downhill bend to the right. Then walk

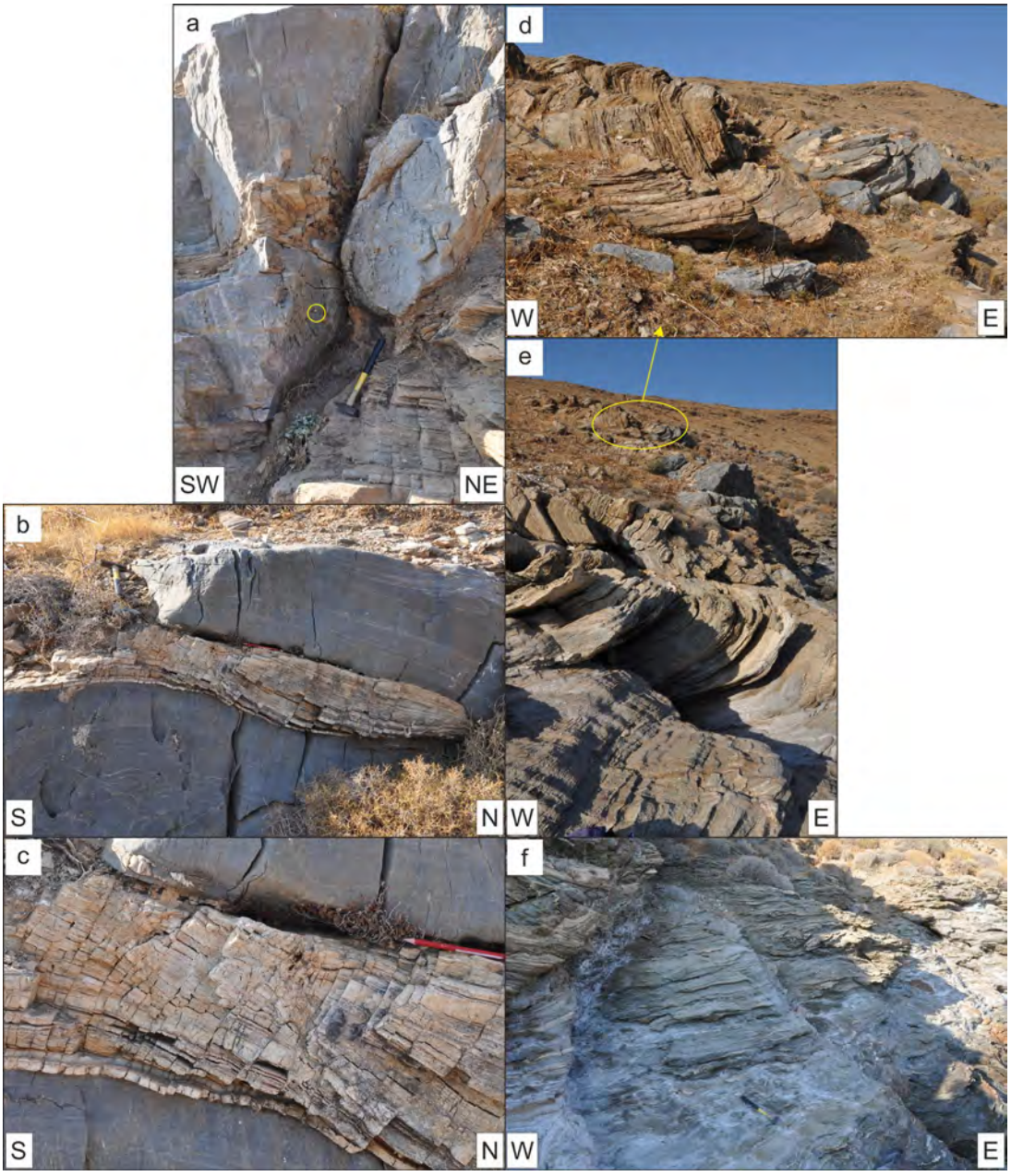

Figure 4.5
Petroussa Formation. Ductile and brittle deformation; folds and boudinage.

~70 m further south on the main road. De Smeth (1975) mapped the whole of the hill top here as mr1 (cf. Table 1). However, marbles that crop out at this level in southern Kythnos lie within the Upper Flabouria Formation. On the east side of the road, there are 5 or more boudins of grey to blue-grey marble, each with a thickness of up to 35 cm and 3 m length, in at least two layers (perhaps a fold repetition of one layer) over ca. 15 m of road outcrop (Fig. 4.6). These lie within grey metapelitic schists here included in the Upper Flabouria Formation, although albite porphyroblasts are not found (or rarely found; we have not systematically checked this). No evidence for a quartz schist comparable to those seen in the north of the island (Stop 1.1) has been found at this outcrop. The GPS point given above is the second to most northerly outcrop.

In Fig. 4.6a, the second to most southerly outcrop, two typical layers of the marble are exposed (sm 231/11°, lm 219/10°). The marble is highly strained, with layers and sigmoids of quartzite. The schist and marble at the upper contact of the northernmost boudin have been folded (Fig. 4.6b) and then cut by a thick quartz-vein, which is itself boudinaged and sheared top-to-the-SSW.

The mr1 of de Smeth (1975) seen along the west coast (Stop 4.7) and in the north of the is-

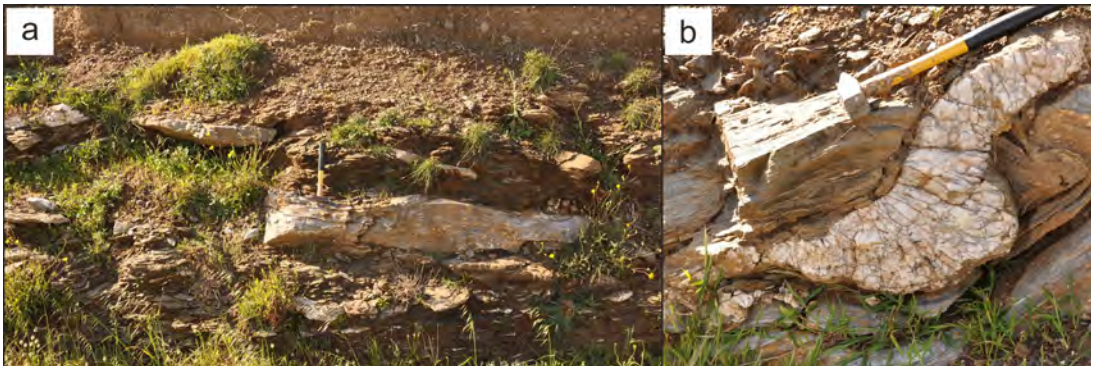

Figure 4.6
Upper Flabouria Formation. Isolated marble boudins.

land (Stops 2.1, 2.4) comprises yellow-weathered quartz–white-mica–calcite schists and occasional blue-grey marble mylonites (the Mavrianou Formation).

Return to the car and go through the iron gate to the south, into the quarry area. Walk uphill to the SW and cross the NE-SW trending wall. Follow this wall and cross over the NW-SE trending wall. In this area (Stop 4.6a; 269086 E 4135036 N), grey to blue-grey marbles with abundant quartz porphyroclasts and a well-developed stretching lineation are common (sm 10-039°, lm 08-025°), although most of the hill comprises quartz–white-mica–calcite schists. These lithologies are typical of the Mavrianou Formation (compare with Stop 4.7), which here lies in the area shown as mr1 by de Smeth (1975). Other areas, with identical rocks, were mapped by de Smeth (1975) as quartz schists; these have now been remapped as Mavrianou Formation (compare Figs. B & C).

Stop 4.7. Mavrianou Formation and Upper Flabouria Formation. High strain zone.
UTM 35S 267768E 4136395N.
Figs. 4.7a, b, looking WNW; Fig. 4.7c, looking SSW; Fig. 4.7d, looking NNE; Fig. 4.7e looking WNW; Fig. 4.7f, Stop 4.7b, looking SSW from UTM 35S 268121E 4135267N on road down to Stypho Bay; Fig. 4.7g, Stop 4.c, looking NW from UTM 35S 268059E 4136590N.

Drive north on the main road for ~620 m and take the turning to the left. After 840 m, turn right and follow the road downhill and around a switch back. Then keep to the seaward side of the luxury house and drive to near the end of the road (Stop 4.7). From there, look NNW to the peninsula (Stop 4.7a), which exposes what de Smeth (1975) mapped from here northwards to Kolona as mr1. This is here called the Mavrianou Formation, overlying the Upper Flabouria Formation. Compare these rocks with the marble at Stops 4.6a and 5.1 and with the Petroussa Formation at Stops 5.6 and 6.1.

The view towards Stop 4.7a is essentially perpendicular to the NNE-SSW oriented stretching direction (Fig. 4.7a). From here, note that the blue-grey marbles in the Mavrianou Formation are thin, strongly deformed (folded boudins) and not common at this distance and lie within yellow-weathered quartz–white-mica–calcite schists. The underlying grey schists of the Upper Flabouria Formation has numerous major sub-horizontal C surfaces, with the foliation dipping northeast (sm 033/42°, lm 047/31°, sc 303/15°; Fig. 4.7a, b). Similar, but not so well-defined surfaces are present in the Mavrianou Formation. Steeper, SW-dipping C' surfaces cut the boundary of the Mavrianou and Upper Flabouria Formations (sm 062/50°, lm 029/38°, sc' 185/37°, lc' 200/28°; Fig. 4.7a). These large-scale SC and SC' structures indicate top-to-the-SW deformation.

At the outcrop (Stop 4.7a), the abundant quartz-veins in the phyllonites of the Upper Flabouria Formation have a coarsely developed and somewhat variably oriented stretching direction (Fig. 4.7c; sm 009/57°, lm 060/33°). A new schistosity, several cm thick, has developed along the major C planes (Fig. 4.7b; 2€ coin lies within the inner circle), at least partly by rotation of sm rather than the growth of new phyllosilicates. In the overlying Mavrianou Formation, extremely thin layers of blue-grey marble mylonites are complexly refolded with the yellow-weathered quartz–white-mica–calcite mylonites (Fig. 4.7d). Both formations show abundant small-scale SC' structures indicating top-to-the-SW deformation. Small-scale and local brittle deformation occurred on discrete faults (Fig. 4.7e; sh 042/35°, lh variable 057/20°, 077/20°).

Altogether, the outcrop represents a thick zone of extremely high ductile strain, with only a minor brittle overprint. The lack of significant late brit-

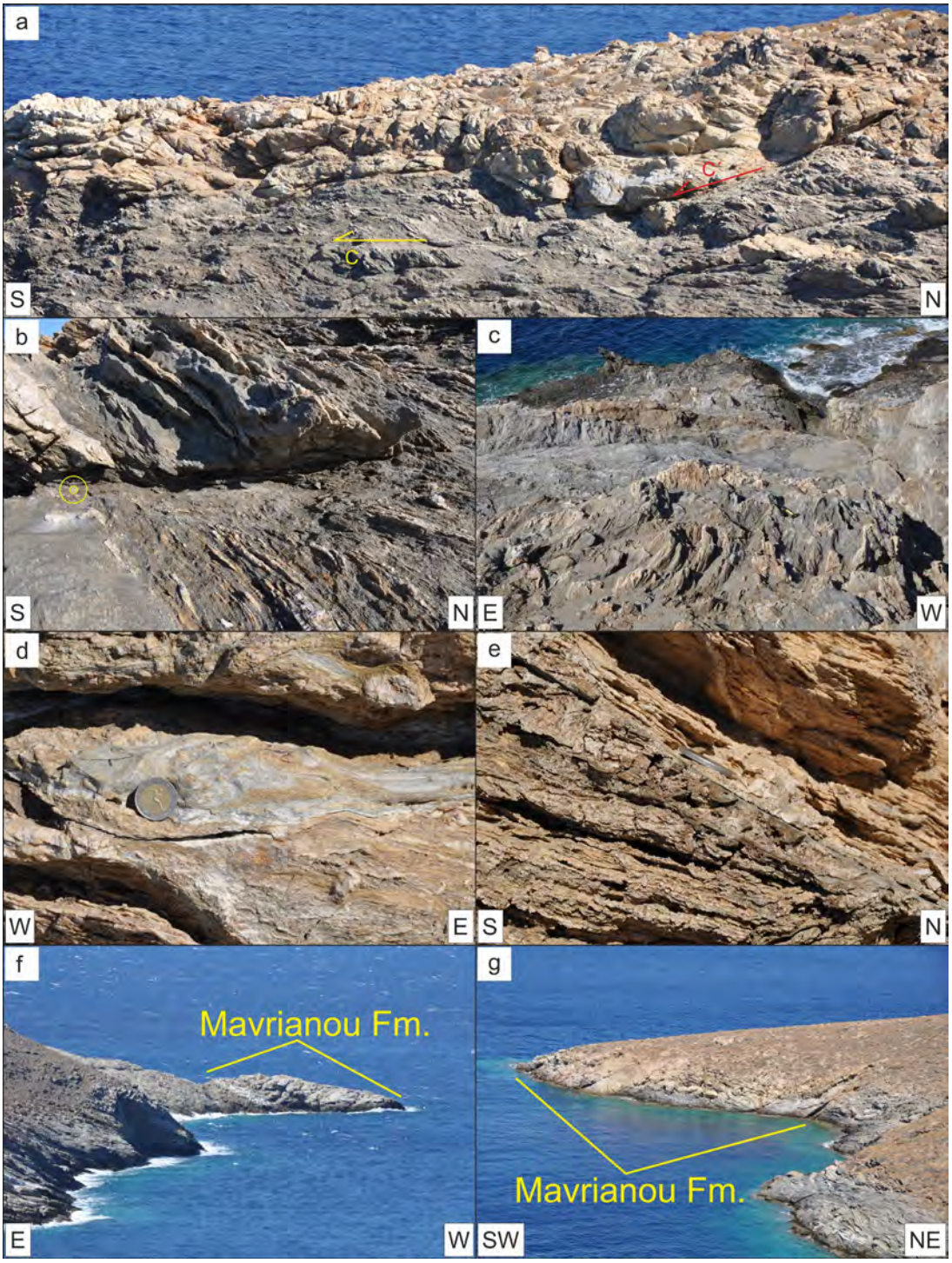

Figure 4.7
Mavrianou & Upper Flabouria Formations. High strain, SCC' structures and coarse quartz boudin stretching lineation.

tle deformation overprinting the earlier ductile deformation, which is a hallmark of rocks directly in the footwall of a LANF, including the WCDS, as they reach lower crustal levels, suggests that the high strain zone seen here is an early structure that was no longer significantly active when the CBU entered the brittle deformation field; likely, it is not linked to the WCDS.

From here, look SSW to see a similar small outcrop of highly-strained rocks of the Mavrianou Formation on the southwestern corner of Stypho Bay (Stop 4.7b, UTM 35S 266980E 4135046N, Fig. 4.7f, picture taken from the road down to Stypho Bay, at UTM 35S 268122E 4135276N). Then drive back and examine the north side of Aghriolagadho Bay from the road (Stop 4.7c, UTM 35S 267905E

4136888N, Fig. 4.7g). The same high-strain zone is exposed, with steep C' planes cutting both the phyllonites of the Upper Flabouria Formation and the overlying Mavrianou Formation. Thus, both the Mavrianou and Upper Flabouria Formation in this coastal area (Fig. C) exhibit an extremely high strain.

EXCURSION 5. S. KYTHNOS; Petroussa to Aghios Dimitrios

On this excursion, strain variations in the footwall of the West Cycladic Detachment Fault are the principal objective. The variations are particularly well shown by the blue-grey marble mylonites and associated yellow-weathered quartz–white-mica–calcite schists of the Petroussa Formation. All Stops are shown in Fig. 5.0.

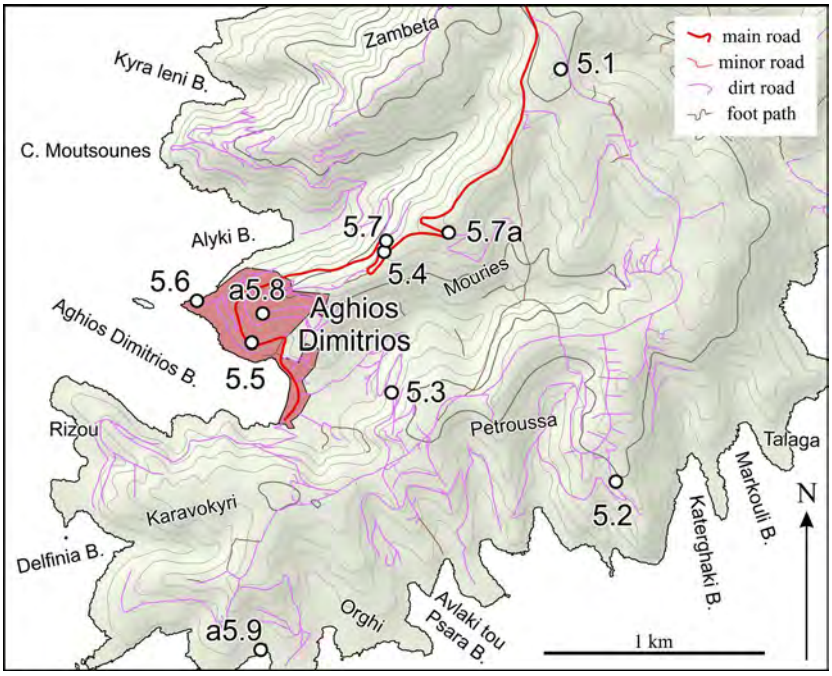

Figure 5.0
Outcrop location map for Stops 5.1 to a-5.9.

Stop 5.1. Upper Mavrianou Formation. Marble mylonites and quartz-white-mica-calcite schists.
UTM 35S 268505E 4134150N.
Fig. 5.1a, looking SSW.

Turn off the main Dhryopidha-Aghios Dimitrios road and take the dirt-road signposted towards Petroussa. Stop after 300 m. The outcrops lie a few metres west and uphill from the road, before a small cliff is reached, within the vegetation. The map of de Smeth (1975) shows that the higher parts of southern Kythnos are covered by quartz-schists overlain by mr1, equivalent to the marble-bearing unit exposed in a series of outcrops along the west coast of the southern part of the island (here the Mavrianou Formation; Stop 4.7).

Figure 5.1
Mavrianou Formation. Isolated marble boudins.

The only marble exposed in this area is ~15 cm thick, white to pale-grey coloured and contains abundant quartz-rich sigmoids and stretched-out relic layers of the same lithology, all defining a very strong stretching lineation (sm 066/15°, lm 030/14°; Fig. 5.1).

Elsewhere, along the road section, yellow-weathered quartz–white-mica–calcite schists are exposed. Similar rocks crop out on the hilltop to the south, although the exposure is very poor..

Stop 5.2. Petroussa Formation. Very thick blue-grey marble; relatively low strain.
UTM 35S 268534E 4132836.
Fig. 5.2a, looking N; Figs. 5.2b-d looking NE.

Continue along the dirt road for 1.7 km and then take the loop road heading south. After 480 m, park and walk 270 m down the poor dirt road to the southeast (around the switchbacks and then south). The road section at the coordinates provides a good view of the blue-grey marble and over- and underlying yellow-weathered quartz–white-mica–calcite schists (sm 340/35°, lcren 009/34°) of the Petroussa Formation. Although this is the thickest development of this unit (Fig. 5.2a), with > 14 m of marble, and hence the strain is relatively low, the marble is penetratively de-

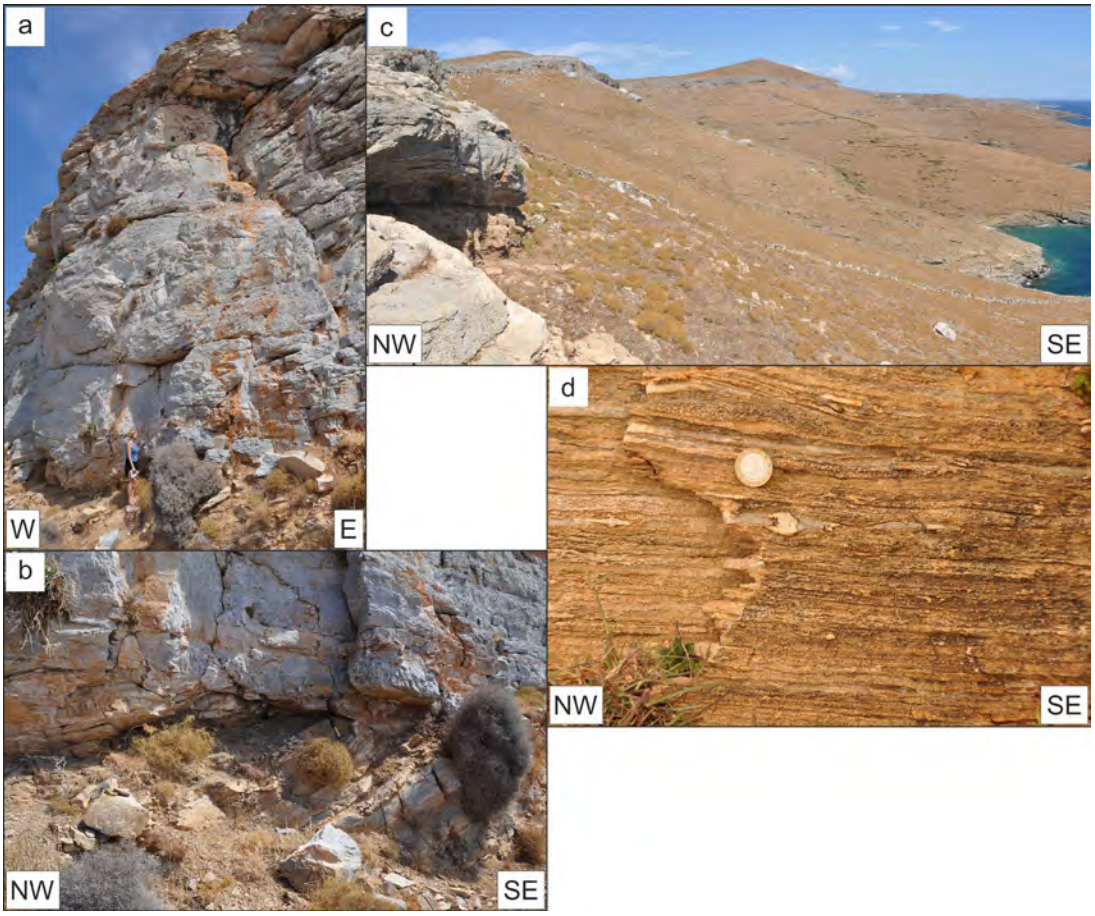

Figure 5.2
Petroussa Formation. Low strain, thick succession.

formed; the lower margin of the outcrop shows a large-scale SC' fabric at the contact of the blue-grey marbles and the quartz–white-mica–calcite schists (sc' 126/26°; Fig. 5.2b). More marble underlies the schists. Note the abundant thin layers of white carbonate within the yellow-weathered quartz–white-mica–calcite schists here (Fig. 5.2d).

From here, go further down the road until you can easily get onto the upper surface of the marble and walk east; this affords an excellent view of the blue-grey marble towards the north-east (Fig. 5.2c). Since the blue-grey marble often forms cliff outcrops, and hence would appear very narrow or non-existent in map view, capped directly by quartz–white-mica–calcite schists, mapping them separately is often not possible. Return to the vehicles by walking over the top of the marble; locally, karst deposits can be found.

Stop 5.3. Petroussa Formation. Large-scale Riedel structures and back-rotation.
UTM 35S 267739E 4132685N.
Figs.5.3, looking NNW.

Drive a further 0.75 km around this loop road, back to the dirt road to Petroussa. Turn left and drive 1.1 km and then turn right at the crossroads. Stop anywhere on this road that affords a good view of the hillside to the north of Aghios Dimitrios (Fig. 5.3). This is capped by the yellow-weathered quartz–white-mica–calcite schists of the Petroussa Formation with a thin blue-grey marble; compare this thickness to that at the previous outcrop. The hill-slope, which is oriented NE-SW and hence is sub-parallel to the NNE-SSW trending regional stretching direction, is cut by relatively regularly spaced (40-80 m) Riedel fractures dipping to the SSW (Fig. 5.3; points 5.3-west and 5.3-east, on the Excursions.kmz file, delimit the margins of the image). This marble layer is a useful marker for estimating the offset on the Riedel fractures, although, as this is due to back-rotation, little absolute downthrow of the layering occurs to the SSW. These fractures must link to an underlying local LANF, with greater displacement to the SSW, and an overlying LANF, which could be the WCDS. Stops 3.4, 3.6 and 3.7 illustrate a similar, but larger-scale structure.

Towards the eastern side of the picture, the

Figure 5.3
Petroussa Formation. Riedel fractures and back-rotation.

softer, rounded outcrops of schists of the Upper Flabouria Formation show regularly spaced fractures that are also likely Riedel fractures (indicated by yellow lines in Fig. 5.3). Similar fractures in the Upper Flabouria Formation can be examined in detail at a-Stop 5.9 and on the main road leading north from Aghios Dimitrios, between UTM 35S 267061E 4133137N and 267701E 4133376N (essentially downhill from Stop 5.4).

Stop 5.4. Petroussa Formation. Intermediate strain level; abundant shear-sense criteria.
UTM 35S 267705E 4133321N.
Fig. 5.4a, looking NE; Figs. 5.4b-e, looking ESE.

Drive on, around three switchbacks to the valley floor. Turn left to Aghios Dimitrios beach and then right. Drive through the village and then uphill for 1.6 km. Park on the corner of the switchback, SW of the outcrops (Fig. 5.4a), which are best reached from the road above. The Petroussa Formation here, which is essentially equivalent to the middle to eastern part of Fig. 5.3, is considerably thinned compared to further east (Stop 5.2) but thicker than further west (Stops 5.6, 6.1). The blue-grey marble mylonites still forms a relatively coherent layer more than 1 m thick, over and underlain by several metres of yellow-weathered quartz–white-mica–calcite schists (Fig. 5.4a). Within the marble mylonites (sm 030/17°, lm 016/10°), there are abundant layers of yellow quartzite from <1 mm to ~20 cm thick and numerous isolated sigmoids of the same lithology and also quartz (Figs. 5.4b-d). The thinner layers (mm-scale) are surprisingly persistent within the marbles, often showing very little deformation (pinch-and-swell

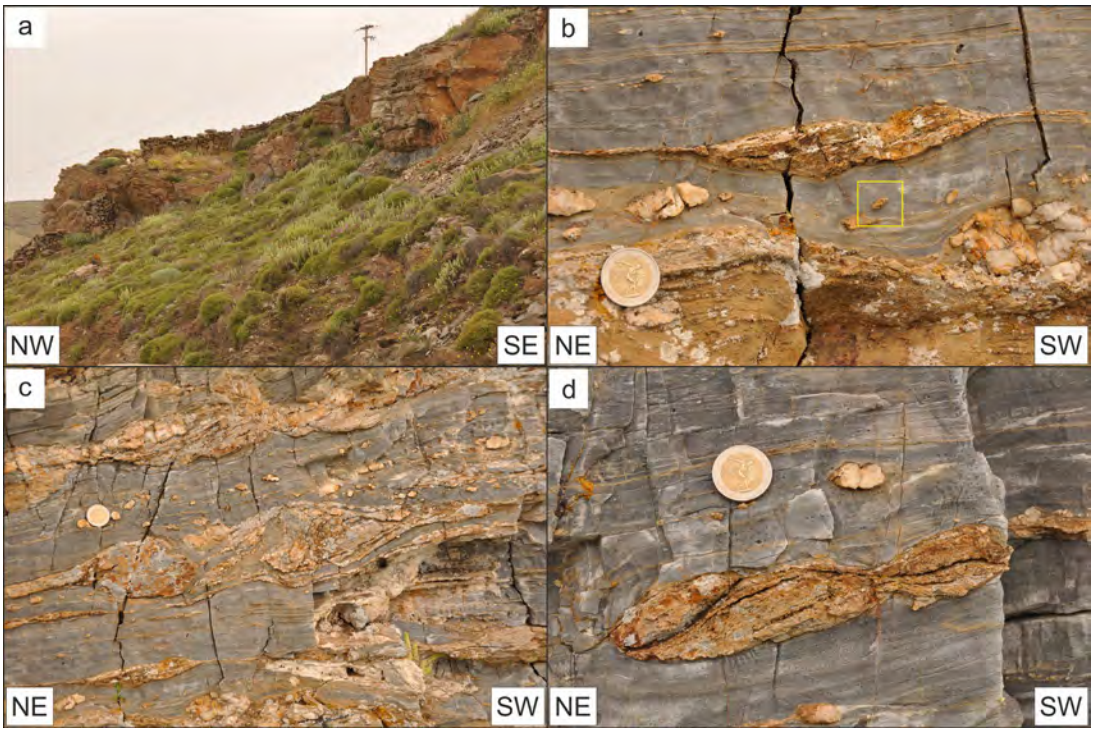

Figure 5.4
Petroussa Formation. Intermediate strain and shear-sense criteria.

or folding), suggesting that, after thinning, their rheology was not significantly different to that of the blue-grey marble mylonites.

Porphyroclasts and sigmoids show a range of geometries, with clearly stair-stepping sigma-clasts, as well as winged inclusions (yellow square in Fig. 5.4b; Hanmer 1990), which do not show stair-stepping. All indicate a top-to-the-SSW shear-sense. Thicker layers have been asymmetrically boudinaged by a combination of brittle and ductile deformation; the former often concentrates at boudin necks with the brittle fault in some cases indicating back rotation and in other cases co-rotation of the boudins.

Although folding occurred in the rocks, creating the marble-schist layering not seen in low strain areas, little evidence of this is found here, probably because the outcrop is parallel to the stretching lineation direction and most fold axes are parallel to that direction. However, some of the rather complex patterns of steep foliation within the quartz-rich layers may be oblique sections through folds.

From the corner of the main road, look eastwards, up the valley. Outcrops of marble of the Petroussa Formation from near Stop 5.2 can be traced almost continuously around the east end of the valley to the outcrops visited here.

Stop 5.5. Petroussa Formation. s-type flanking structure.
UTM 35S 267088E 4132922N.
Fig. 5.5, looking NE.

Drive 1.1 km back down the hill towards Aghios Dimitrios; note the numerous Riedel fractures developed within the Upper Flabouria Formation. These are comparable to those seen at Stop 5.3. Around the corner, park at the junction of the dirt road going back north and then walk ~70 m southeast to opposite an ugly concrete structure with an electric meter inside it (Fig. 5.5a; hammer in concrete box).

This stop is primarily to examine an s-type flanking structure developed in quartzite mylonites within blue-grey marbles of the Petroussa Formation (Fig. 5.5b; 2€ coin in square for scale). Note that the marble is brown-weathered in the middle to upper part of the picture and blue-grey coloured in the lower part; the brown to blue-grey junction in the lower left of the picture is not a lithological boundary. The view here is along the fold axis (lf 041/09°, sapl 330/15°), which is sub-parallel to the stretching direction in the marble mylonites (sm 069/08°, lm 024/07°). The

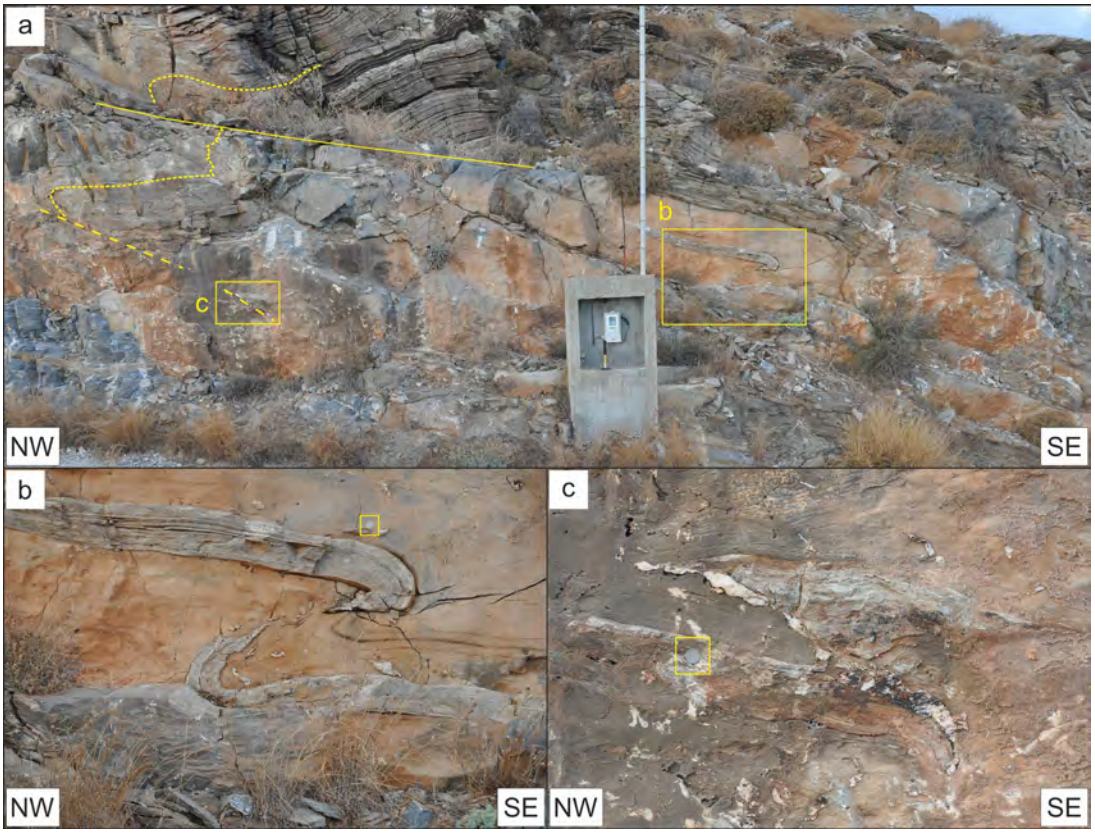

Figure 5.5
Petroussa Formation.
S-type flanking fold.

fold axial surface is parallel to the cross-cutting element in the flanking structure (scce 339/19°). A triclinic shear geometry or a non-plane strain general shear with a strong flattening component is implied by the structure, as the fold verges toward the SE whilst the regional shear is towards the SSW.

To the north, an isolated swell (as in pinch-and-swell) of quartzite within blue-grey marble (Fig 5.5c; 2€ coin in square for scale) has been deformed into an s-type flanking structure along a quartz-vein. When the quartz-vein rotated into the extensional field, it was affected by boudinage. This structure is likely continuous with the similar, north-verging structure above and to the north (dashed line in Fig. 5.5a).

Above these small-scale structures there is a larger-scale flanking structure between the quartz–white-mica–calcite schists and the underlying blue-grey marble (Fig. 5.5a; cross-cutting element is solid yellow line); this has not been studied in detail. Both the hanging wall and footwall compositional banding (dotted lines) are cut by the cross-cutting element in the structure.

Stop 5.6. Petroussa and Upper and Lower Flabouria Formations. High strain facies and the Kyra Leni Steep Belt.
UTM 35S 266857E 4133098N.
Fig. 5.6a, looking WSW; Fig. 5.6b, looking NNE; Figs. 5.6 c, d, looking SE; Fig. 5.6e, looking SSE.

Walk back to the vehicles and drive down the dirt road to the platform, essentially at sea-level, forming the point. This is a critical outcrop for comparing the high strain facies of the Petroussa Formation, well exposed here, with the Mavrianou Formation at Stop 4.7 and for understanding the

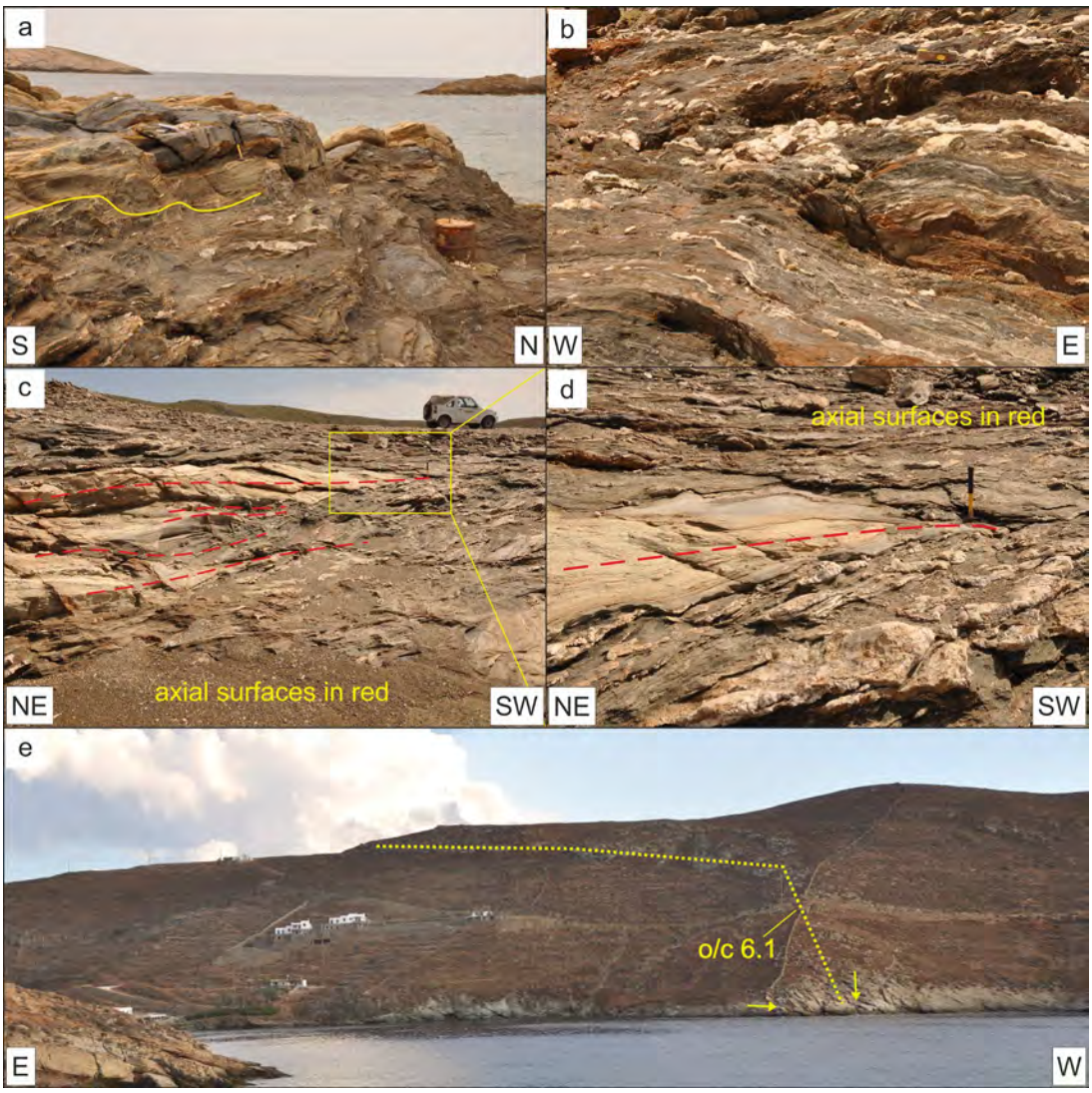

Figure 5.6
Upper and Lower Flabouria Formations and Petroussa Formation. High strain. View southwards to the Kyra Leni Steep Belt.

regional structure of Kythnos. The rocks exposed here can be confidently traced eastwards, uphill to Stops a5.8 and 5.4 and, from there, further east to the low strain facies of this unit (Stop 5.2). Thus there is no doubt that this is the Petroussa Formation, although it looks markedly different to Stop 5.2.

In the northwestern part of the outcrop, a <1m thick layer of blue-grey marble underlies obvious yellow-weathered quartz–white-mica–calcite schists (Fig. 5.6a; sm 193/27°, lm 207/26°). There is also a thin layer of quartz–white-mica–calcite schist under the marble but, as this is regularly washed by the sea, it has not developed the typical yellow colour. This is underlain by grey schists of the Lower Flabouria Formation with abundant large quartz boudins carrying a coarse stretching lineation (Fig. 5.6a; yellow line is the boundary between the two formations, recognised by the lack of quartz boudins in the Petroussa Formation). On the south side of the peninsula, outcrops of the Flabouria Formation also contain coarse quartz boudins (Fig. 5.6b).

The blue-grey marble continues to the east, within pale yellow-weathered quartz–white-mica–calcite schists, with a combined maximum thickness of ~7 m. There, the Petroussa Formation is isoclinally infolded with the Upper Flabouria Formation (lf 205/19°, 210/33°), with recumbent axial surfaces (Fig. 5.6c, d; the fold shape is again seen by the absence of quartz boudins in the Petroussa Formation). In contrast to every other fold within schists seen on Kythnos, including those this close to the WCDS, there is little macroscopic evidence for an earlier fabric (see Stop 1.2), indicating that this is a very early structure. The fold limbs are cut by later ductile SC' structures indicating top-to-the-SSW deformation.

Thus in many respects the high-strain facies of the Petroussa Formation is similar to the Mavrianou Formation at Stop 4.7. Both show likely early structures, with strongly thinned blue-grey marbles within highly deformed yellow-weathered quartz–white-mica–calcite schists. And both are associated with schists of the Lower Flabouria Formation carrying abundant large quartz boudins carrying a coarse stretching lineation.

Looking to the SSE, the Petroussa Formation can be seen clearly across Aghios Dimitrios Bay (Fig. 5.6e). The western part, including Stop 6.1 and down to sea-level, is steep, and only two thin blue-grey marble layers are visible within the yellow-weathered schists (Fig. 5.6e; yellow arrows). Higher up and towards the east, the Petroussa Formation is thicker and has a sub-horizontal dip. Effectively, the Petroussa Formation goes from an altitude of ca. 75 m down to sea-level in only ca. 120 m horizontally. On the north side of Aghios Dimitrios Bay, this steep zone starts just west of Stops a5.8 and goes down to Stop 5.5. Stop 5.6 indicates that the layering flattens out to a sub-horizontal orientation again west of the steep zone. On the south side of the Aghios Dimitrios Bay, the steep zone continues westwards to the exposures of the WCDS (Stops 6.2, 6.4, 6.7). Overall, this fold has a small hinge-zone and long planar limbs, suggesting a kink-type geometry, verging west, with a NNE-SSW trending axis. The steep zone, here called the Kyra Leni Steep Belt, can be traced as far north as the south side of Stypho Bay (Figs. C, G), with a NNE-SSW trend, suggesting it formed by shortening perpendicular to the extension direction, typical of low-angled extensional zones (Mancktelow & Pavlis 1994).

Stop 5.7. Lower Flabouria Formation. Mn-rich nodule in schists.
UTM 35S 267714E 4133371N.
Fig. 5.7a, looking E; Fig. 5.7b, looking NNE.

Drive 900 m back up the main road and stop at the first switchback. In the Western Cyclades, lenses of Mn-rich rocks have been mapped on Kythnos (Chyrsanthaki & Baltatzis 2003) and Kea (Iglsed-

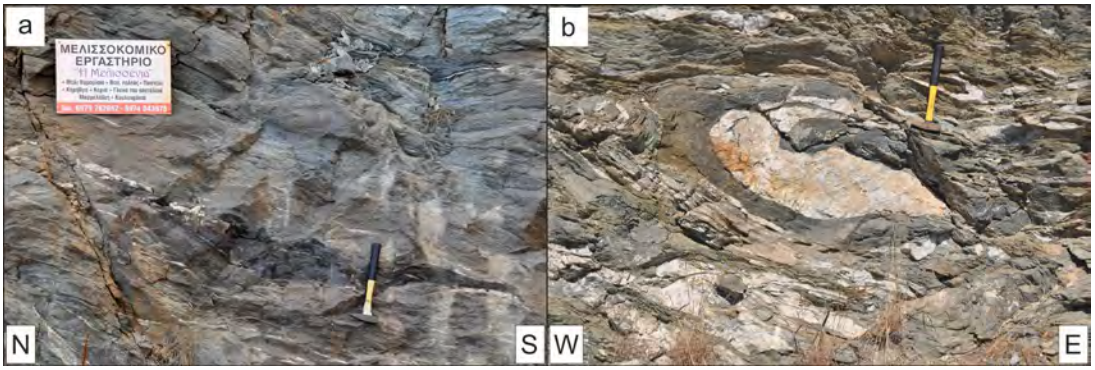

Figure 5.7
Lower Flabouria Formation. Mn-rich, garnet-bearing schists.

er et al. 2011), where they contain garnets and blue amphiboles. Here, a 2 m long and up to 15 cm thick lens of such a dark, poorly foliated rock crops out (Fig. 5.7a), pinch-and-swell boudinaged within the foliation (sm 181/09°; lm 201/09°). In thin-section, it comprises biotite, small euhedral garnets and white-micas; the presence of garnet at such low metamorphic grades suggests a Mn-rich bulk chemical composition, indicating a hydrothermally leached mafic volcanic source rock.

On the north side of the road, 645 m further up hill and around two switchbacks, a similar rock is exposed, wrapped around a large quartz-pod (Fig. 5.7b; UTM 35S 267997E 4133408N).

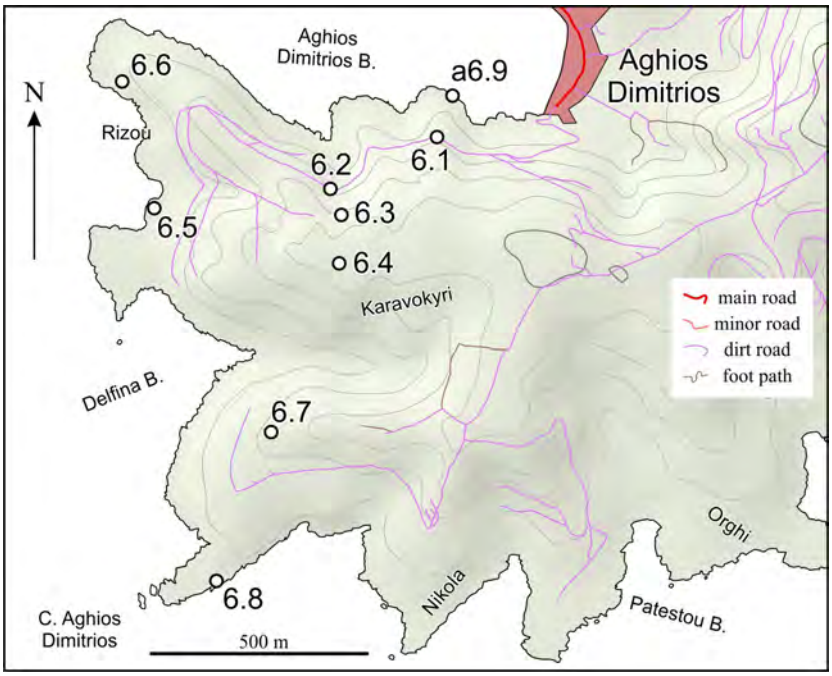

Figure 6.0
Outcrop location map for Stops 6.1 to a-6.9.

EXCURSION 6: SW KYTHNOS; Rizou and Karavokyri

On this day, a section from the footwall across the ductile and brittle parts of the WCDS to the hanging wall will be examined in the area south of Aghios Dimitrios Bay, which is the only place on Kythnos where it occurs. The profile across the WCDS shows that it has a structure comparable to that seen on Kea and Serifos: (i) Increasing strain in the footwall marbles and schists towards the detachment. (ii) Localization of the strain within tens of metres thick marble ultramylonites directly under the detachment. (iii) Complex, polyphase generation of tens of centimetres thick ultracataclasites above a knife-sharp contact to the footwall marble ultramylonites. (iv) Protocataclastic hanging wall consisting of various lithologies, partly overprinted by hydrothermal alteration. All Stops are shown in Fig. 6.0.

Stop 6.1. Petroussa Formation. Kyra Leni Steep Zone.
UTM 35S 266983E 4132492N.
Fig. 6.1, looking SSW.

From the south end of Aghios Dimitrios Bay, take the dirt road around two switchbacks and along the southern side of Aghios Dimitrios Bay for 470 m and stop at the first left-hand bend. Over most of southern Kythnos, the Petroussa Formation has a low dip-angle, defining the regional antiformal structure, and thins gradually westwards. Between Aghios Dimitrios Bay and Stypho Bay, the shallow dip is replaced by the Kyra Leni Steep Belt, bringing the Petroussa Formation down from 75 m to sea-level within a 120 metres (cf Figs. C, 5.6e).

Here, the Petroussa Formation largely consists of yellow-weathered quartz–white-mica–calcite schists, perhaps 8 m thick. Towards the top of the formation, an irregular 12 cm thick boudin of blue-grey marble mylonite crops out. No evidence of strain localisation is seen at the contact of the Petroussa Formation and the overlying Upper Flabouria Formation.

In contrast, strain localisation has occurred near the basal contact, where a ~15 cm thick pale yellow (limonitic) cataclastic zone with schist and vein-quartz fragments lies at the contact of the Lower Flabouria and Petroussa Formations, with a <8 mm thick sharp fault contact at the top (Figs. 6.1a-c; sh 246/55°; lh 209/32°, 167/04°). Downwards, the limonitic zone merges into folded schists (lf 046/08°, lapl 023/20°), with small dark albite porphyroblasts and some quartz-veins and boudins, but these do not have the prominent stretching lineation seen at Stop 5.6.

The overlying schists of the Petroussa Formation at the east end of the outcrop are folded (lf 014/16°) above an axial surface parallel fracture (sh ~270/20°, lh ~020/08°) that cuts up-section (it cuts the blue-grey marble) to the west before steepening and dying out (under red line in Fig. 6.1d).

The blue-grey marble boudins are isoclinally folded (Fig. 6.1a, c) and contain abundant angular (brittle deformed) fragments of the quartz–white-mica–calcite schist (Fig. 6.1b), reflecting ongoing ductile deformation in the calcite mylonites after brittle deformation started in the sur-

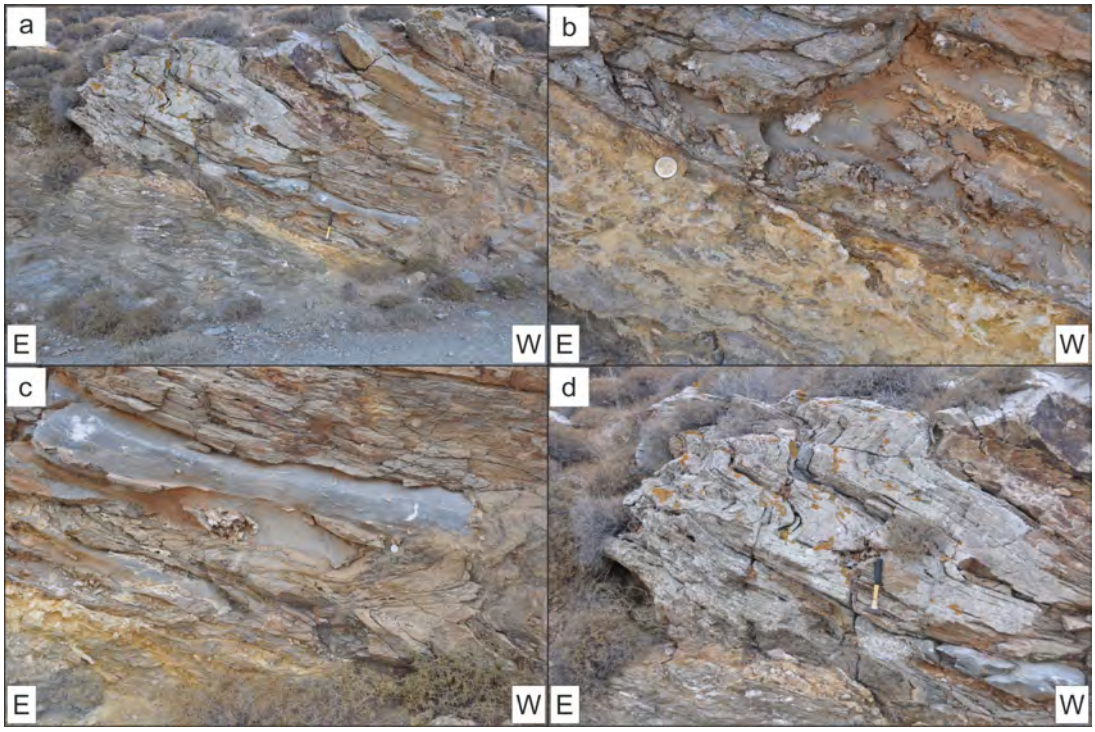

Figure 6.1
Lower Flabouria Formation and Petroussa Formation. High strain facies.

rounding quartz-rich rocks. This reflects deformation during cooling, as the footwall was exhumed from under the WCDS.

Stop 6.2. Rizou Formation. Base of the marble ultramylonites.
UTM 35S 266741E 4132374N.
Fig. 6.2a, looking SW; Fig. 6.2b, looking W.

Continue 280 m west along the road and stop at the first corner to the right. Similar to the exposures of the WCDS on Kea and Serifos (Grasemann et al. 2012), the footwall to the detachment on Kythnos comprises marble ultramylonites (Rizou Formation), exposed here.

In many places, the marble mylonites are very impure, containing abundant sub-millimetre to centimetre thick boudinaged quartzite layers (Fig. 6.2a) that record a strong stretching component parallel to the mylonitic foliation, which here dips steeply west (sm 280/40°). Although the quartzite layers are ductilely deformed into pinch-and-swell structures, the same layers were overprinted by brittle fracturing during ongoing flow of the calcite ultramylonites. This observation, together with the fact that the detachment mylonites are overlain by cataclasites with similar kinematics, suggest that shearing along the detachment happened under decreasing temperature conditions, from greenschist facies into the brittle field of the upper crust. Fig. 6.2b shows a layer-parallel stretched quartz-vein that shows evidence for ductile deformation (stretching lineation, pinch-and-swell) overprinted by brittle fracturing. Although the central segment of the boudinaged quartz-vein layer is slightly inclined and might be easily confused with a stair-stepping geometry indicative of a N-directed shear-sense, the co-rotation of the left segment together with small sigmoids in the marble mylonites clearly demonstrate top-to-the-SSW shear-sense.

Due to large-scale folding of both the footwall and hanging wall perpendicular to the extension direction, forming the Kyra Leni Steep Zone (see Stop 5.6), the WCDS here dips steeply towards the west (lf 265/49°), with a sub-horizontal stretching lineation (lm 341/15°).

Note that the Rizou Formation marbles often have a grey or reddish colour (Fig. 6.2a), rather than the blue-grey of the marble in the Petroussa and Mavrianou Formations, although relatively 'pure' blue-grey marbles also occur (Stops 6.3, 6.5). Quartz–white-mica–calcite schists (here albite "gneisses"; Laner 2009, Lenauer 2009; Fig. C) underlie the Rizou Formation but, despite the high strain, the marble has remained a coherent unit, in contrast to the extreme thinning and pinch-and-swell boudinage recorded by the blue-grey marbles at high-strain localities in the Petroussa Formation (Stops 5.6, 6.1) and the Mavrianou

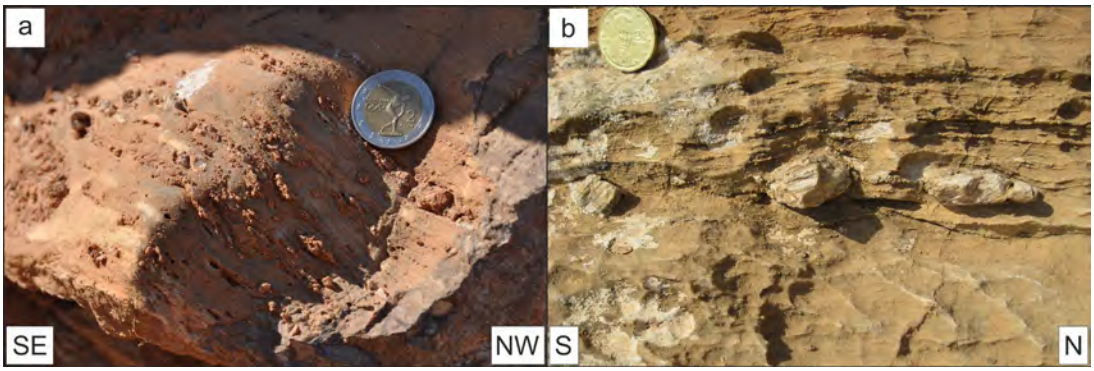

Figure 6.2
Rizou Formation. Base of the marble ultramylonites under the WCDS.

Formation (Stop 4.7). On the basis of the observations made, the Rizou Formation cannot be easily correlated with either the Petroussa or Mavrianou Formations.

Stop 6.3. Rizou Formation. Kink-bands - shortening perpendicular to extension.
UTM 35S 266766E 4132315N.
Fig. 6.3a, b, looking SSW.

Drive 0.55 km around the headland on the south side of Aghios Dimitrios Bay and park at the junction with the ruined dirt road going ESE, uphill. Walk up this road (it is no longer passable even by 4x4 vehicles) and cross over the wall at the end, to get to the outcrop 50 m further east. Here the marble ultramylonites a few metres below the detachment are strongly folded into upright folds (Fig. 6.3a: (lf 032/02°, sapl 300/66°). The s-shaped higher-order folds (looking towards the SSW) support the interpretation that the W-dipping detachment ultramylonites are the steep limb of a large-scale west-verging fold with a kink-like geometry. Although much less intensely folded, thrusting perpendicular to the shear direction overprinted by conjugate kink-bands (sapl2 305/58°, 124/60°) in the overlying marble ultramylonites suggests extension-perpendicular shortening during movement on the detachment (Fig. 6.3b; thrust tip shown by arrow). Numerous isoclinal folds with fold axes parallel to the stretching lineation (lf 211/05°) document the intense deformation of the marbles.

Stop 6.4. Carbonate/quartzite cataclasite/ultracataclasite.
UTM 35S 266761E 4132205N.
Fig. 6.4a, b, looking W; Fig. 6.4c, looking E; Fig. 6.4d, west is at top.

Climb directly up the hill and, 20 m south of the dry-stone wall at the top, go to the structurally highest outcrop of the Rizou Formation. This is overlain by a red/pink decimetre-thick zone of intense cataclastic deformation in carbonate and quartz-rich rocks. The hanging wall quartzites (Aghios Dimitrios Formation) are typically exposed several metres further west. The cataclasite zone can be traced along-strike for about 120 m to the south (See Stop 6.7), in many places comprising several discontinuous layers, distinguished by variations in their matrix colour and component type and size (Fig. 6.4a; Fig. 6.4b is a thin-section of the same rock as Fig. 6.4a). (1) A pink, ultrafine-grained unlayered carbonate matrix with up to centimetre-sized rounded components, some of quartzite (?Aghios Dimitrios Formation) and others of carbonate. Millimetre to centimetre sized

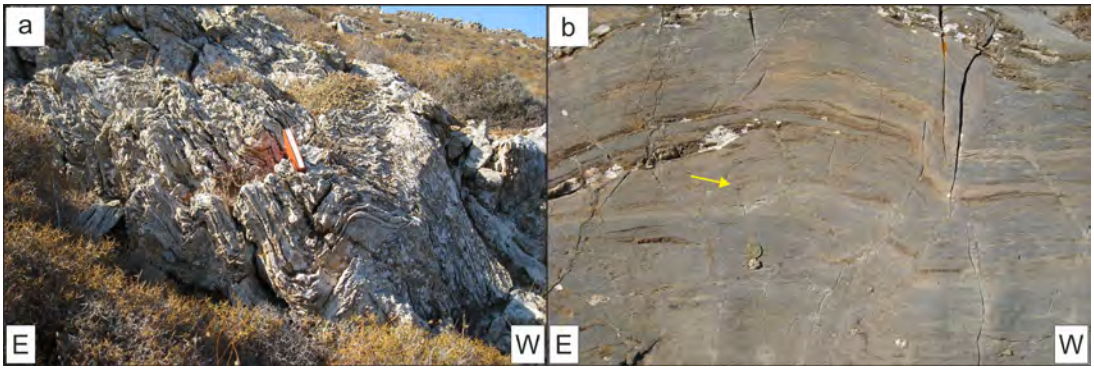

Figure 6.3
Rizou Formation. Folds, kink-bands and brittle thrusts – shortening perpendicular to extension.

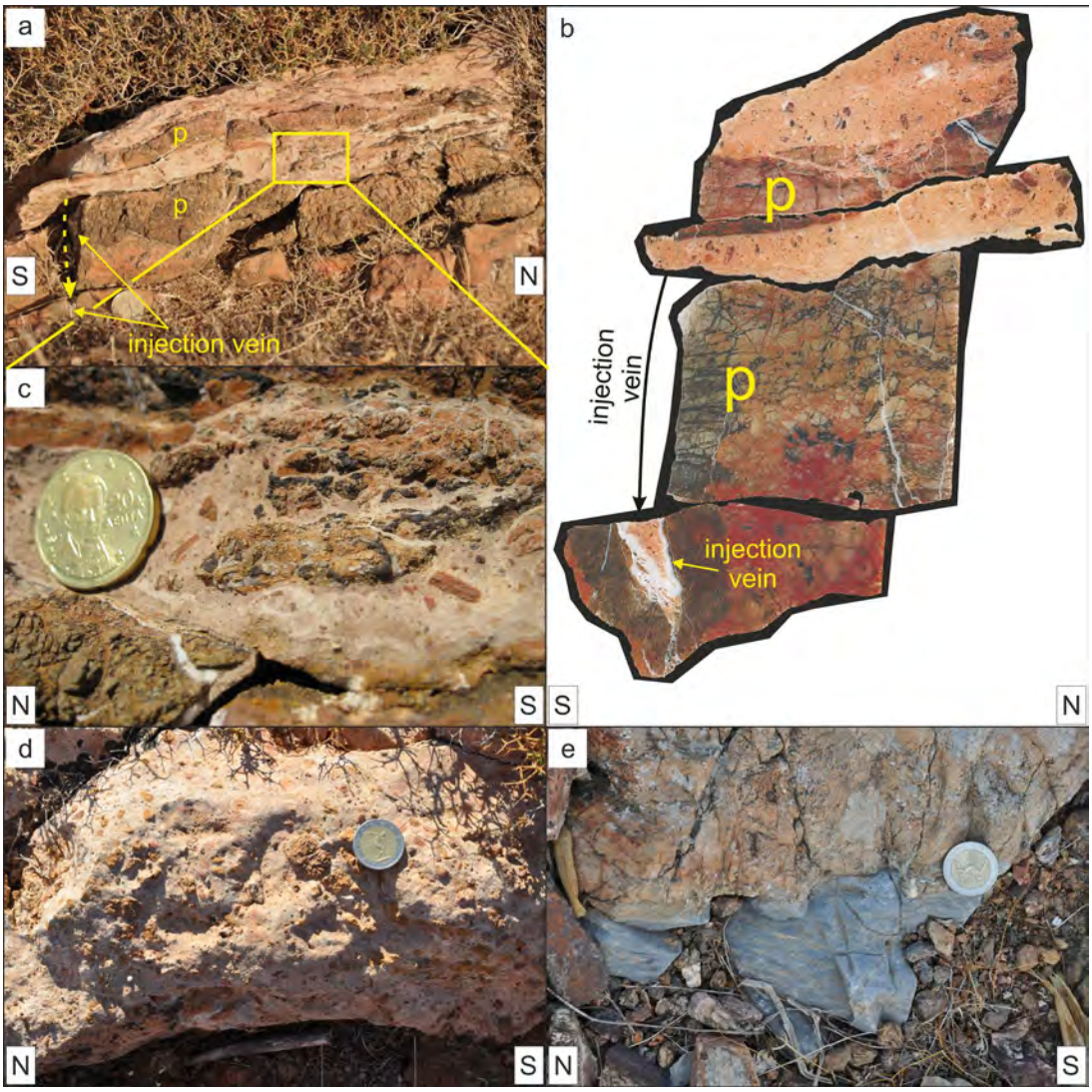

Figure 6.4
WCDS. Carbonate/ quartzite cataclasites and ultracataclasites.

platy red carbonate clasts with quartz fragments lie with a poor preferred orientation of the long axis of the components parallel to the ultramylonitic foliation (i.e. the detachment surface, lh 280/40°). The smaller clasts are markedly rounded and some are coated by thin rims of a different coloured cataclasite. Clasts of earlier cataclasite generations are also common (Fig. 6.4c). (2) Proto-cataclastic layers with grey or brownish quartzite fragments separated by a Fe-rich carbonate matrix along narrow fractures (p in Figs. 6.4a, b). All layer boundaries within the (ultra)cataclasite are irregular and no principle slip surfaces or slickensides have been observed. Injection veins up to 10 cm long cut the overall layering at a high angle and branch in several places; the indicated injection vein cannot be seen in the plane of the thin-section and only poorly in the field picture (yellow and black lines in Figs. 6a, b). The injection veins are rimmed by white calcite and barite, indicating that injection of fluidized ultracataclasites was associated with mineral precipitation.

Further south along the fault zone, a small outcrop of ultracataclasite occurs (Fig. 6.4d). This has a very fine matrix with cm-sized rounded orange clasts of quartzite proto-cataclasite and red carbonate (?ultracataclasite) clasts. Some metres further south, down the hill, below a dry-stone wall, the contact between the blue-grey marble ultramylonites and quartz-rich cataclasites crops out (Fig. 6.4e).

In general, this zone of cataclastic deformation has many similarities to the carbonate fault rocks documented by Viganò et al. (2011) from areas where earthquake-related fault slip occurred. Clasts with rims coated in different generations of cataclasite have also been used to argue for earthquake-related deformation (Smith et al. 2011).

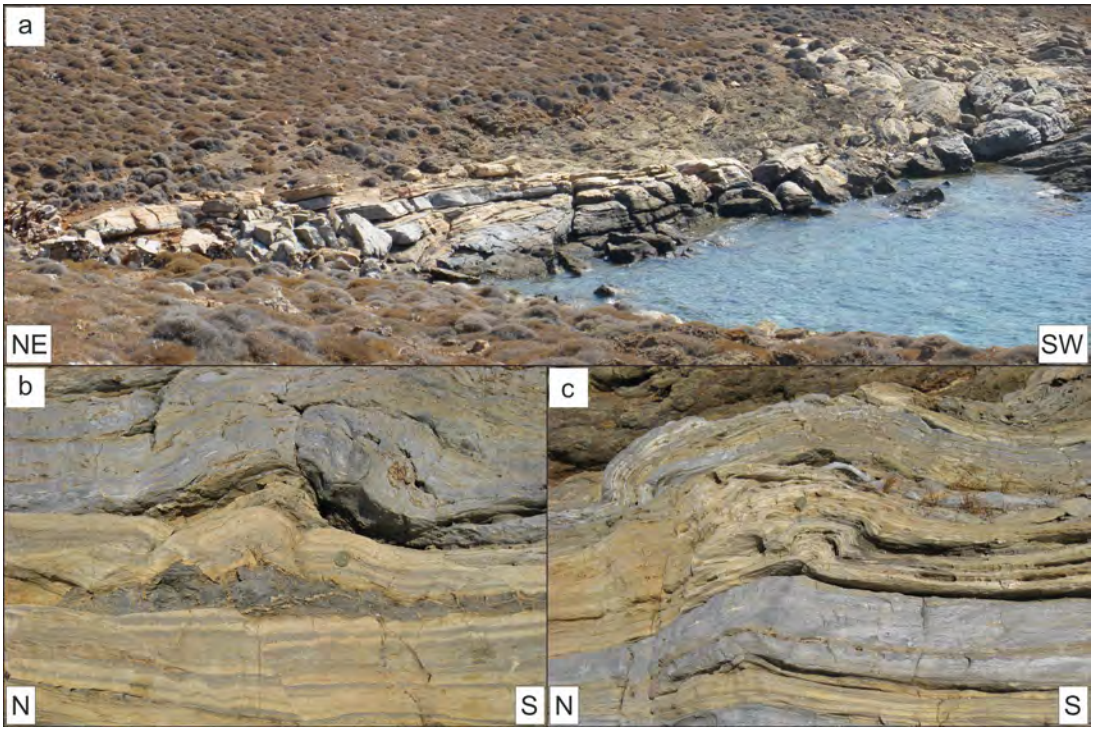

Figure 6.5
Rizou Formation. Shortening perpendicular to extension.

Stop 6.5. Rizou Formation. Shortening perpendicular to extension.
UTM 35S 266342E 4132330N.
Fig. 6.5, looking towards ENE.

Return to the vehicle and walk down to the bay to the southwest; note the yellow-weathered quartz-white-mica-calcite schists at sea level (Fig. 6.5a). The detachment marble ultramylonites, which here have a distinct yellow and grey-blue layering, are composed almost purely of calcite, with occasional small quartz clasts interlayered with schist layers only a few centimetres thick (Figs. 6.5b, c). Locally, the ultramylonitic marble is partially overprinted by Fe-rich fluids.

As at Stop 6.3, box shaped detachment folds with axes parallel to the stretching lineation (lm 020/31°) and upright axial surfaces within the marble mylonites indicate shortening perpendicular to the extension direction. Frequently, the thin schist layers acted as a layer-parallel "detachment horizon" (sm 060/38°; Fig. 6.5b). The complex evolution of the strain geometry is documented by conjugate NW- and SE-dipping high-angled normal faults overprinting the constrictional strain with apparent flattening.

The marble ultramylonites here dip to the ENE generally with a sub-horizontal dip (sm 275/12°), but are only 450 m west of the marble mylonites at Stops 6.2 - 6.4, which dip steeply west (sm 280/40°). Three different interpretations are possible. (i) The two differently dipping marble ultramylonites represent different structural horizons where the ductile strain was localized to form a complex detachment system of anastomosing shear zones. (ii) The marble ultramylonites have been reworked into the hanging wall protocataclasites by brittle deformation. (iii) Both marble ultramylonites, which have a similar trending NNE-SSW lineation, belong to a large-scale fold - in this case, they would form the lower fold-limb associated with the Kyra Leni Steep Belt.

Stop 6.6. Aghios Dimitrios Formation. Quartzites in the hanging wall of the WCDS.
UTM 35S 266269E 4132618N.
Fig. 6.6, looking E.

Drive back 190 m, park at the very sharp turn to the right and walk 190 m west. This outcrop shows the strongly brecciated, bleached and hydrothermally altered quartzitic rocks of the Aghios Dimitrios Formation that form the hanging wall of the WCDS. The protocataclastic quartzites (Fig. 6.6) crop out only on the southwestern area of Kythnos and were originally described, together with the Rizou Formation, as 'carbonatized volcanic rocks' (de Smeth 1975: Table 1). The rocks are composed mainly of quartz, and contain minor amounts of calcite and white-mica; locally, the micas show a

preferred orientation that may represent a relic original foliation. Hydrothermal alteration was associated with brittle faults (sf 150/30°) with bleaching of the host-rocks and precipitation of Fe-oxides and -hydroxides (primarily goethite and hematite) along fault planes.

Based on their structural position, they are correlated with the Upper Cycladic Unit, part of the Pelagonian Unit (Bonneau, 1984).

Figure 6.6
Aghios Dimitrios Formation. Brittle deformation in the WCDS hanging wall.

Stop 6.7. View of West Cycladic Detachment System
UTM 35S 266607E 4131823N.
Fig. 6.7, looking N.

Drive back towards Aghios Dimitrios but, opposite the end of the beach, take the right hand turn up the hill. At the junction at the top, turn right and drive 1.6 km, to 30 m before the end of the road. Walk 60 m north to the hill top. This spot affords an excellent view of the knife-sharp detachment plane of the WCDS (Fig. 6.7). A similar view, from the sea, is shown in a-Fig. 7.5. The detachment plane, which dips at ~40° towards the west, lies within the Kyra Leni Steep Belt. Ductile deformation in the WCDS footwall is localized in the ~25m thick marble ultramylonitic layer (Rizou Formation) overlain by the carbonate ultracataclasites (MUM & CUC; Fig. 6.7) documented in Stop 6.4. The yellow bar by CUC in Fig. 6.7 shows both the thickness and most southerly outcrop of the carbonate ultracataclasites recorded, so far. These are overlain by protocataclastic quartzites of the Aghios Dimitrios Formation, forming the hanging wall to the WCDS.

Stop 6.8. Rizou and Aghios Dimitrios Formations. The West Cycladic Detachment System.
UTM 35S 266483E 4131485N.
Fig. 6.8, looking NW.

Drive back 160 m, to the sharp corner to the left, and park. Walk SSW towards the coast, to ~110 m northeast of the lighthouse at the southernmost end of Kythnos. Here, the main W-dipping WCDS is exposed along steep cliffs close to the sea (Fig. 6.8; see a-Fig. 7.6). The highly deformed rocks are foliated cataclasites forming spectacular SC and SCC' fabrics consistently indicating a top-to-the-SSW shear-sense.

This outcrop also shows the brittle-ductile evolution of a complex system of extension gashes. Veins are filled with quartz, white calcite, iron-bearing red carbonates or hydrothermal iron and barite mineralization. Due to their orientations, cross-cutting relationships and their vein-fillings, four distinct generations of extension gashes can be distinguished: The oldest generation of veins comprise quartz and white calcite cements. Most of these veins have been rotated to nearly parallel to the foliation. They show ductile deformation, such as folding and pinch-and-swell boudinage. These veins are cross-cut by calcite veins that either dip towards the S or form conjugate sets of NE-SW and NW-SE striking veins, both of which record evidence of ductile deformation. All structures are overprinted by steeply SW- to SSW-dipping high–angled faults, that partly show a strong hydrothermal overprint and iron-mineralization.

ACKNOWLEDGEMENTS

AHNR thanks Christa Hofmann for assistance in the field; Eleni Bouritis, Linta Koutsi and the staff at the Gialos-Byzantico Restaurant in Merichas for their help and kindness during field-work. We thank Cornelius Tschegg for his insightful comments during initial fieldwork in 2009, the Austrian Academy of Sciences for financially supporting more recent fieldwork (Dr. Emil Suess-Erbschaft) and Kostis Soukis and an anonymous person for reviewing an earlier version of the text.

Figure 6.7
View of the WCDS. Rizou (footwall) and Aghios Dimitrios (hanging wall) Formations.

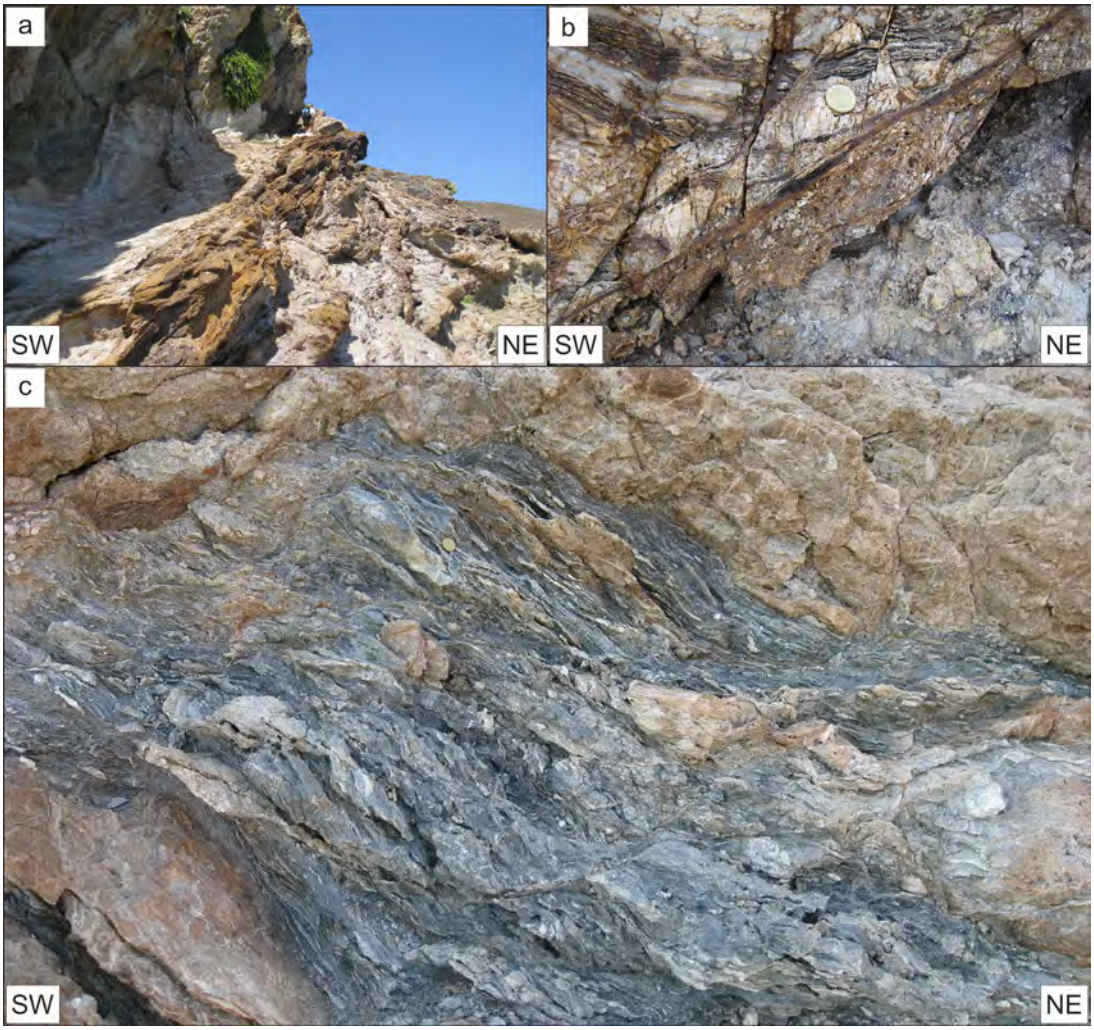

Figure 6.8
Rizou and Aghios Dimitrios Formations. Detachment contact of the WCDS.

REFERENCES

Altherr, R., Schliestedt, M., Okrusch, M., Seidel, E., Kreuzer, H., Harre, W., Lenz, H., Wendt, I., Wagner, G.A., 1979. Geochronology of high pressure rocks on Sifnos (Cyclades, Greece). Contributions to Mineralogy & Petrology 70, 245-255.

Altherr, R., Kreuzer, H., Wendt, I., Lenz, H., Wagner, G. A., Keller, J., Harre, W. & Hohndorf, A., 1982. A Late Oligocene/Early Miocene High Temperature Belt in the Attic-Cycladic Crystalline Complex (SE Pelagonian, Greece). Geologisches Jahrbuch E 23, 97-164.

Andriessen, P. A. M., Banga, G., Hebeda, E. H., 1987. Isotopic age study of pre-Alpine rocks in the basal units on Naxos, Sikinos and Ios, Greek Cyclades. Geologie en Mijnbouw 66, 3-14.

Avigad, D., Alon, Z., Garfunkel, Z., 2001. Ductile and brittle shortening, extension-parallel folds and maintenance of crustal thickness in the central Aegean (Cyclades, Greece). Tectonics 20, 277-287.

Berger, A., Schneider, D. A., Grasemann, B., Stockli, D., 2013. Footwall mineralization during Late Miocene extension along the West Cycladic Detachment System, Lavrion, Greece. Terra Nova 25, 181-191.

Bonneau, M., 1984. Correlation of the Hellenide nappes in the south-east Aegean and their tectonic reconstruction. In: Dixon, J. E., Robertson, A. H. F. (Eds.), The Geological Evolution of the Eastern Mediterranean. Geological Society, London, Special Publications, London, pp. 517-527.

Bonneau, M., Kienast, J. R., 1982. Subduction, collision et schistes bleus: L'example de l'Egée (Grèce). Bulletin de la Societe Geologique de France 7, 785-791.

Brichau, S., Thomson, S., Ring, U., 2010. Thermochronometric constraints on the tectonic evolution of the Serifos detachment, Aegean Sea, Greece. International Journal of Earth Sciences 99, 379-393.

Bröcker, M., Enders, M., 1999. U-Pb zircon geochronology of unusual eclogite-facies rocks from Syros and Tinos (Cyclades, Greece). Geological Magazine 136, 111-118.

Bröcker, M., Franz, L., 1998. Rb-Sr isotopic studies on Tinos Island (Cyclades, Greece): additional time constraints form metamorphism, extent of infiltration-controlled overprinting and deformational activity. Geological Magazine 135, 369-382.

Bröcker, M., Franz, L., 2006. Dating metamorphism and tectonic juxtaposition on Andros Island (Cyclades, Greece): results of a Rb-Sr study. Geological Magazine 143, 609-620.

Chrysanthaki, A. I., Baltatzis, E. M. M., 2003. Geochemistry and depositional environment of ferromanganoan metasediments on the island of Kythnos, Cyclades, Greece. Neues Jahrbuch für Mineralogie Monatshefte 1-17.

de Smeth, J. B., 1975. Geological Map of Greece: Kythnos Island. Institute of Geology and Mining Research (IGMR), Athens, pp. mapped during the years 1972-1973.

Gautier, P., Brun, J.P. & Jolivet, L., 1993. Structure and kinematics of upper Cenozoic extensional detachment on Naxos and Paros (Cyclades islands, Greece). Tectonics, 12, 1180-1194).

Gautier, P., Brun, J.-P., 1994. Crustal-scale geometry and kinematics of late-orogenic extension in the central Aegean (Cyclades and Evvia Island). Tectonophysics 238, 399-424.

Grasemann, B., Stüwe, K., Vannay, J.-C., 2003. Sense and non-sense of shear in flanking structures. Journal of Structural Geology 25, 19-34.

Grasemann, B., Tschegg, C., 2012. Localization of deformation triggered by chemo-mechanical feedback. Geological Society of America Bulletin 124, 737-745

Grasemann, B., Wiesmayr, G., Draganits, E., Fusseis, F., 2004. Classification of refold structures. The Journal of Geology 112, 119-126.

Grasemann, B., Petrakakis, K., 2007. Evolution of the Serifos Metamorphic Core Complex, in: Lister, G., Forster, M., Ring, U. (Eds.), Inside the Aegean Metamorphic Core Complexes, Journal of the Virtual Explorer. doi:10.3809/jvirtex.2007.00170.

Grasemann, B., Schneider, D.A., Stöckli, D. F., Iglseder, C., 2012. Miocene bivergent crustal extension in the Aegean: Evidence from the western Cyclades (Greece). Lithosphere 4, 23-39.

Grasemann, B., Huet, B., Schneider, D. A., Rice, A. H. N., Lemonnier, N., Tschegg, C. 2018. Miocene post-orogenic extension of the Eocene imbricated Hellenic subduction channel: new constraint from Milos (Cyclades, Greece). Geological Society of America Bulletin, 130, 238-262.

Hanmer, S., 1990. Natural rotated inclusions in non-ideal shear. Tectonophysics 176, 245-255.

Huet, B., Labrousse, L., Jolivet, L., 2009. Thrust

or detachment? Exhumation processes in the Aegean: Insight from a field study on Ios (Cyclades, Greece). Tectonics 28.

Huet, B., Loisl, J., Lindner, K., Grasemann, B., Rice, A. H. N., Soukis, K. & Schneider, D., 2013. Large-scale geometry and timing of the detachment systems in the Cyclades (Greece). Insight from Makronisos.Geophysical Research Abstracts 15, EGU2013-9560.

Huet, B., Labrousse, L. Monie, P., Malvoisin, B., Jolivet, L. 2015. Coupled phengite ^{40}Ar-^{39}Ar geochronology and thermobarometry: P-T-t evolution of Andros Island (Cyclades, Greece). Geological Magazine 152, 711-727.

Iglseder, C., Grasemann, B., Rice, A. H. N., Petrakakis, K., Schneider, D.A., 2011. Miocene south directed low-angle normal fault evolution on Kea Island (West Cycladic Detachment System, Greece). Tectonics 30, 10.1029/2010tc002802.

Iglseder, C., Grasemann, B., Schneider, D. A., Petrakakis, K., Miller, C., Klötzli, U. S., Thöni, M., Zámolyi, A., Rambousek, C., 2009. I and S-type plutonism on Serifos (W-Cyclades, Greece). Tectonophysics 473, 69-83.

Jolivet, L., Brun, J.-P., 2010. Cenozoic geodynamic evolution of the Aegean. International Journal of Earth Sciences 99, 109-138.

Jolivet, L., Rimmele, G., Oberhansli, R., Goffe, B., Candan, O., 2004. Correlation of syn-orogenic tectonic and metamorphic events in the Cyclades, the Lycian nappes and the Menderes massif. Geodynamic implications. Bulletin de la Societe Geologique de France 175, 217-238.

Jolivet, L., Lecomte, E., Huet, B., Denèle, Y., Lacombe, O., Labrousse, L., Le Pourhiet, L., Mehl, C., 2010. The North Cycladic Detachment System. Earth and Planetary Science Letters 289, 87-104.

Jolivet, L., Menant, A., Sternai, P., Rabillard, A., Arbaret, L., Augier, R., Laurent, V., Beaudoin, A., Grasemann, B., Huet, B., Labrousse, L., Le Pourhiet, L., 2015. The geological signature of a slab tear below the Aegean. Tectonophysics 659, 166-182.

Katzir, Y., Matthews, A., Garfunkel, Z., Schliestedt, M., Avigad, D., 1996. The tectono-metamorphic evolution of a dismembered ophiolite (Tinos, Cyclades, Greece). Geological Magazine 133, 237-254.

Keiter, M., Tomaschek, F., Ballhaus, C., 2008. The structural evolution of Kythnos Island (Cyclades, Greece) – a reconnaissance. Zeitschrift der Deutschen Gesellschaft für Geowissenschaften 159, 513-520.

Laner, G., 2009. Fluid-rock interaction in a low-angled normal fault (Kythnos, Western Cyclades, Greece). Unpub. Master thesis, University of Vienna. 87 pp.

Lenauer. I., 2009. Structural and petrological investigations along a low-angled normal fault on Kythnos, Greece. Unpub. Master thesis, University of Vienna. 88 pp.

Lenauer. I., Mörtl, G., Grasemann, B., Iglseder, C., 2009. Structural investigations along a low-angled normal fault zone (Kythnos, Greece). Trabajos de Geologá 29, 429-431.

Lister, G. S., Banga, G., Feenstra, A., 1984. Metamorphic core complexes of Cordilleran type in the Cyclades, Aegean Sea, Greece. Geology 12, 221-225.

Menant, A., Jolivet, L., Vrielynck, B., 2016, Kinematic reconstructions and magmatic evolution illuminating crustal and mantle dynamics of the eastern Mediterranean region since the late Cretaceous: Tectonophysics, v. 675, p. 103-140.

Maluski, H., Bonneau, M., Kienast, J. R., 1987. Dating the metamorphic events in the Cycladic area: ^{40}Ar/^{39}Ar data from metamorphic rocks of the island of Syros (Greece). Bulletin de la Societe Geologique de France III, 833-841.

Mancktelow, N. S., Pavlis, T. L. 1994. Fold-fault relationships in low-angled detachment systems. Tectonics 13, 668-685.

Rabillard, A., Arbaret, L., Jolivet, L., Le Breton, N., Gumiaux, C., Augier, R., Grasemann, B., 2015. Interactions between plutonism and detachments during metamorphic core complex formation, Serifos Island (Cyclades, Greece). Tectonics 34, 1080-1106.

Rice, A. H. N., Iglseder, C., Grasemann, B., Zámolyi, A., Nikolakopoulos, K. G., Mitropoulos, D., Voit, K., Müller, M., Draganits, E., Rockenschaub, M., Tsombos, P.I., 2012. A new geological map of the crustal-scale detachment on Kea (Western Cyclades, Greece). Austrian Journal of Earth Sciences 105, 108-124.

Rice, A. H. N., Grasemann, B., 2016. Carbonate pseudotachylite? from a Miocene extensional detachment, W. Cyclades, Greece. Geophysical Research Abstracts 18, EGU2016-4100.

Ring, U., Glodny, J., Will, T., Thomson, S., 2010. The Hellenic Subduction System: High-Pressure Metamorphism, Exhumation, Normal Faulting, and Large-Scale Extension. Annual Review of Earth and Planetary Sciences 38, 45-

76.
Scheffer, C., Vanderhaeghe, O., Lanari, P., Tarantola, A., Ponthus, L., Photiades, A., France, L., 2016. Syn- to post-orogenic exhumation of metamorphic nappes: Structure and thermobarometry of the western Attic-Cycladic metamorphic complex (Lavrion, Greece). Journal of Geodynamics 96, 174-193.
Schliestedt, M., Bartsch, V., Carl, M., Mathew, A., Henjes-Kunst, F., 1994. The P-T Path of Greenschist Facies Rocks from the island of Kithnos (Cyclades, Greece). Chemie der Erde. 54, 281-296.
Smith, S. A. F., Billi, A., Di Toro, G. & Spiess, R., 2011. Principal Slip Zones in Limestone: Microstructural Characterization and Implications for the Seismic Cycle (Tre Monti Fault, Central Appenines, Italy. Pure and Applied Geophysics 168, 2365-2393.
Soukis, K., Stockli, D. F., 2013. Structural and thermochronometric evidence for multi-stage exhumation of southern Syros, Cycladic islands, Greece. Tectonophysics 595-596, 148-164.
Tschegg, C., Grasemann, B., 2009. Deformation and alteration of a granodiorite during low-angle normal faulting (Serifos, Greece). Lithosphere 1, 139-154.
Viganò, A., Tumiati, S., Recchia, S., Martin, S., Marelli, M., Rigon, R., 2011. Carbonate pseudotachylytes: evidence for seismic faulting along carbonate faults. Terra Nova 23, 187-194.
Wijbrans, J.R., McDougall, I., 1988. Metamorphic evolution of the Attic Cycladic metamorphic belt on Naxos (Cyclades, Greece) utilizing $^{40}Ar/^{39}Ar$ age spectrum measurements. Journal of Metamorphic Geology 6, 571-594.
Woodcock, N. H. 1977. Specification of fabric shapes using an eigenvalue method. Geological Society of America Bulletin 88, 1231-1236.

APPENDIX EXCURSION

The days are arranged from north to south. All Stop locations are shown in Fig. H and in the a-Excursion.kmz file, available on-line.

a-EXCURSION 1: N. AND NE KYTHNOS; Tourlos

a-Stop 1.8. ?Mavrianou Formation. Non-cylindrical folds in blue-grey marble.
UTM 35S 272270E 4149788N.
a-Fig. 1.8, looking W.

From Stop 1.7, drive a further 650 m north, on the left hand road at the fork. Blue-grey marble is exposed in many places along the north side of this section of road. At the coordinates, fold hinges of isoclinally folded quartzite layers within the blue-grey marble mylonites are weathered out to show that the axes are markedly non-cylindrical (a-Fig. 1.8). Axes measured include 207/14°, 077/15° and 127/16°, all with axial surfaces at ~099/23°, essentially parallel to the foliation away from the folding (sm 076/28°, lm 064/27°).

a-Figure 1.8
?Mavrianou Formation. Non-cylindrical folds in blue-grey marble.

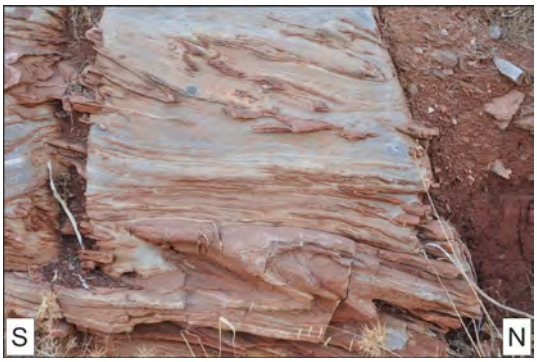

Which marble this is, is uncertain; de Smeth (1975) shows it lies between the Episkopi and Flabouria Formations and hence could be the Mavrianou Formation, as in the Episkopi area (Fig. C). Certain correlation with the marbles on the west side of the island here in the north is currently not possible (even though these are all shown as Mavrianou Formation in Fig. C).

a-Stop 1.9. Flabouria Formation. Marble layer within schists.
UTM 35S 272774E 4150774N and 273230E 4151025N.
No Figure.

From a-Stop 1.8 drive 850 m north to where the road makes a small loop. Park and walk through the gate to the north. Walk 215 m along the track to an ~1 m thick white to blue-grey marble within the Flabouria Formation that crops out in the track (sm 057/20°, lm074/16°). Then walk a further 445 m along the track to where similar marbles crop out (sm 028/18°, lm 085/14°; a-Stop 1.9a). Such marbles are relatively common (Stops 2.6) in the Flabouria Formation and are likely low-strain equivalents of the thin marble boudins found in the south of Kythnos (Stops 4.6).

a-Stop 1.10. ?Mavrianou and Flabouria Formations. High strain marble and associated rocks.
UTM 35S 273310E 4151338N.
a-Fig. 1.10, looking N.

The light house at the northern tip of the island rests on albite schists with quartz boudins parallel to the foliation (sm 029/14°, lm schist 069/11°, lm qtz vein 073/08°), typical of the Flabouria Formation.

a-Figure 1.10
?Mavrianou and Flabouria Formations View of the northern point of Kythnos.

Underlying these, downhill and to the SE, blue-grey and white marble crops out within yellow-weathered quartz–white-mica–calcite schists (sm 079/08°, lm 059/07°) that are similar to the high-strain facies of the Petroussa (Stop 5.6) and to the Mavrianou (Stop 4.7) Formations. The outcrop can be followed around to the south side of the bay. Above the yellow-weathered quartz–white-mica–calcite schists, grey schists with abundant coarse quartz-veins crop out, similar to those seen adjacent to high-strain marble units at Stops 5.6 and 4.7.

From further south, it can be seen that there are at least two thin bands of blue-grey marble within the yellow-weathered quartz–white-mica–calcite schists, offset by fractures dipping steeply to the west (a-Fig. 1.10).

a-EXCURSION 2; W KYTHNOS, Merichas to Kolona Bay

a-Stop 2.8. Mavrianou Formation. Different oriented stretching lineations but consistent shear-sense.
UTM 35S 268988E 4141407N.
a-Fig. 2.8, looking NW.

From Stop 2.1, walk west and then north around the building, down to the outcrops just above sea-level. Much of the peninsula NW of Merichas consists of interlayered blue-grey marbles and schists. The fabric in the schists is dominated by SCC' and shear-band structures that record a consistent top-to-the-SW shear-sense. In the marble layers, quartz sigmoids with a clear monoclinic symmetry confirm the SW-directed kinematics. Newly precipitated calcite grains in the wings of the sigmoids suggest that diffusive mass-transfer processes were active during shear deformation. Interestingly, the trend of the stretching lineations differ slightly between the almost horizontally oriented mylonitic foliations of the marbles (sm 221/05°, lm 219/04°) and the schists (sm 239/05°, lm 240/04°; a-Fig. 2.8). This observation may indicate that either the strain localized in different lithologies at different metamorphic conditions, with slightly different kinematic directions, or that the rheologically different layers deformed synchronously by triclinic flow.

a-Figure 2.8
Mavrianou Formation. Different stretching lineation directions in schist and blue-grey marble.

a-Stop 2.9. Flabouria Formation. High-angle fault with fault drag.
UTM 35S 269637E 4142214N.
a-Fig. 2.9, looking SE.

From Stop 2.2 drive around Martinaki beach on the main road to the junction with a concrete road, southwest of the end of Episkopi beach. At this stop, high-angle normal faults (sf 208/68°) cutting the main foliation (sm 123/21°) in the schists indicate NNE-SSW directed extension (a-Fig. 2.9). Although the faults are associated with cataclastic deformation and the formation of slickensides and slickenlines, ductile deformation in the host-rocks is demonstrated by folding and dragging of the main foliation into the fault plane. Folding is accommodated by numerous conjugate, mm-scale shear-bands in the fold hinges.

a-Figure 2.9
Flabouria Formation. Fault drag.

a-Stop 2.10. Mavrianou Formation. High strain in blue-grey marbles and quartz–white-mica–calcite schists.
UTM 35S 268920E 4144133N.
a-Fig. 2.10, looking NW.

The outcrop of the Mavrianou Formation lying southwest of the road comprises multiple layers of blue-grey marble mylonites, from less than one cm to several tens of cm thick, and yellow-weathered quartz–white-mica–calcite schists in layers up to ~1 metre thick (a-Fig. 2.10a). The whole package rests on typical crenulated schists of the Flabouria Formation (sm 340/27°, lcr 054/05°).

The fabric in marble mylonites is parallel to the margin of the marble (sm marble 339/06°, lm marble 054/01°), although often showing evidence of internal isoclinal folding; the rootless nature of some fold limbs suggests they formed as

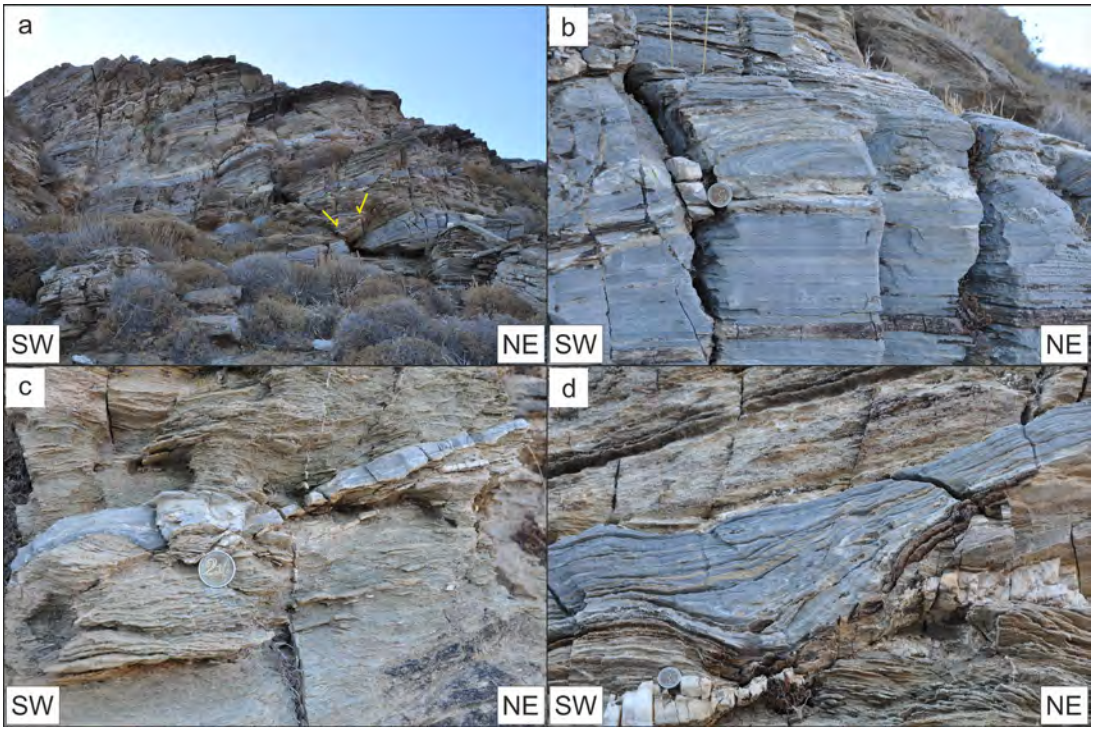

a-Figure 2.10
Mavrianou Formation. High strain with ductile and brittle structures.

a flanking structure (a-Fig. 2.10b). The fabric in the adjacent schists may be discordant to the marble-schist layering, indicating an axial-planar fabric reworking an earlier fabric in the schists that is still preserved in the marble mylonites (a-Fig. 2.10c). Since sm schist is at a lower angle than the marble-schist compositional layering, these rocks must lie in an inverted fold limb. Likely, much of the lithological repetition here is due to tight to isoclinal fold repetitions on a variety of scales.

SC' structures within the schists consistently show a top-to-the-SW shear-sense. Where such structures are developed at the margin of a marble, the marble may thicken into the SC' structure (a-Fig. 2.10c).

Conjugate brittle-ductile fractures are present on both a large-scale and a small-scale. Near the base of the outcrop, a SW-dipping fracture with a relatively large offset is conjugate with a NE-dipping fracture with a much smaller offset (arrows in a-Fig. 2.10a). Both die-out towards marble mylonite layers. On a small-scale, symmetrical brittle-ductile fractures showing a graben geometry formed in the schists under the marble mylonites that thickened, possibly due to a C' surface that cuts across a thick discordant quartz-vein (a-Fig. 2.10d). Note here the earlier pinch-and-swelled quartz-vein parallel to the foliation that is also cut by both the C' plane and the thin, late, high-angle quartz-veins.

There is much more to see here.

a-EXCURSION 4: CENTRAL KYTHNOS; Dhryopidha to Stypho

a-Stop 4.8. Petroussa Formation. SC' or back-rotated boudins of quartz–white-mica–calcite schists.
UTM 35S 272053E 4140608N.
a-Fig. 4.8a, looking SE; Fig. 4.8b, looking S.

Drive southwards around the switchback at the edge of Dhryopidha. 360 m further on, there is a very small old quarry on the left side of the road. The outcrop lies just over the dry stone wall at the north end of the quarry. Here, an 18 cm thick yellow-weathered quartz–white-mica–calcite schist layer lies within blue-grey marbles of the Petroussa Formation. The marble foliation away from structures described below dips to the northeast (sm 065/15°, lm 069/15°); within the schist layer, the foliation has a more northerly dip (sm 033/24°).

The schist layer is offset by a series of brittle-ductile fractures dipping west-southwest (sh 251/26°), with drag folds at their margins (a-Fig. 4.8a; €2 coin in square for scale). Most fractures have a normal offset, but the fracture immediately southeast of the main fracture shows a reverse sense of offset. Although the offset is over 14 cm at

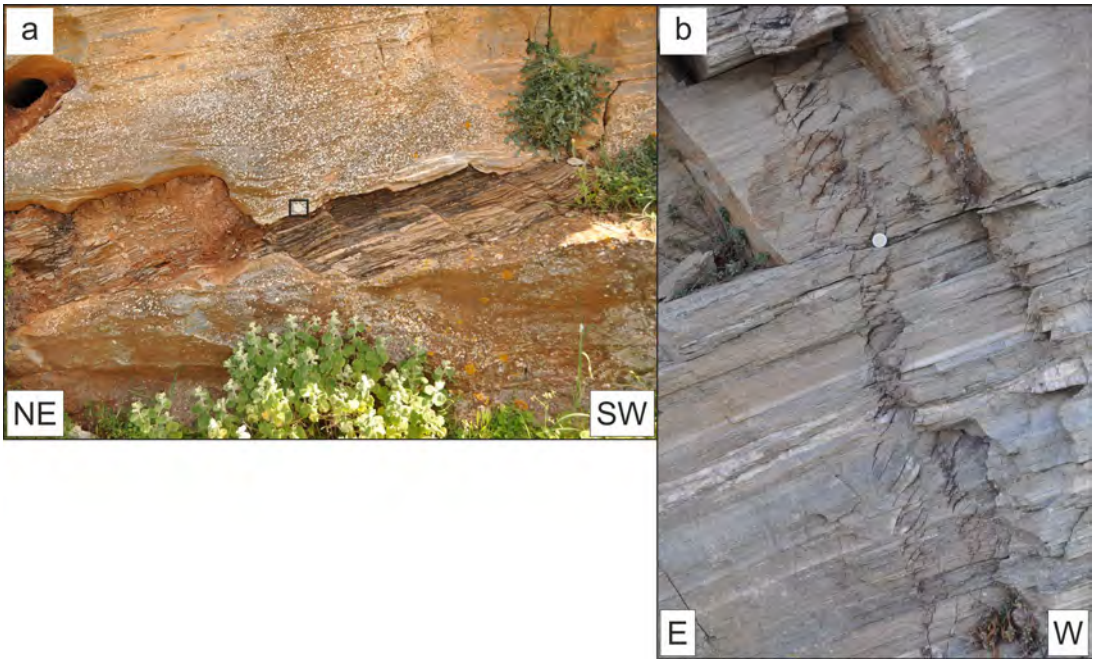

a-Figure 4.8
Petroussa Formation. Brittle-ductile deformation – fault drag and tension cracks.

one fracture, it dies out rapidly within the marble.

Some 40 m east of the quarry, several arrays of sub-vertical curved en-echelon tension-cracks are exposed within the quartz–white-mica–calcite schists (a-Fig. 4.8b). These indicate a brittle-ductile deformation with a down-throw to the south-west (~ses 234/70°); this is similar to the high-angled brittle and brittle-ductile deformation seen elsewhere (Stops 2.4, 4.3).

There are at least three thick layers of blue-grey marbles in the Petroussa Formation here, within yellow-weathered quartz–white-mica–calcite schists. Together, these form all the outcrop from here and back to the north, around the switchback.

a-Figure 4.9
Kanala Formation. Quartz-feldspar sigmoid.

a-Stop 4.9. Kanala Formation. Top-to-the-SW shear-sense in quartz-feldspar sigmoids.
UTM 35S 270219E 4138415N.
a-Fig. 4.9, looking SSE.

This outcrop lies exactly in the fourth switchback on the road down to Flabouria. Strongly deformed greenschists (sm 082/14°, lm 061/10°) contain white albite porphyroblasts (a-Fig. 4.9). Within this, several mm to cm sized crystals of feldspar in a chlorite matrix form lozenge-shaped aggregates, with shapes similar to that of σ-type mantled porphyroclast. Due to their clear stair-stepping geometry, the feldspar aggregates are interpreted to be sigmoids indicating top-to-the-SW kinematics.

a-Stop 4.10. Upper Flabouria Formation. Low-angled normal fault.
UTM 35S 269366E 4138057N.
a-Fig. 4.10, looking NE.

Drive south along Flabouria beach and turn left 60 m before end of the beach. Drive uphill around two switchbacks to the outcrop on the left side of the road. The base of the outcrop of pale green schists with abundant quartz-veins (Upper Flabouria Formation) is cut by a low-angle fault (sh 040/19°, lh 042/18°; a-Fig. 4.10a) with a top-to-the-south displacement, indicated by rare slickenside and slickencryst lineations. This is a strike-parallel view of a low-angled normal fault comparable those inferred at Stops 3.4 and 5.3, al-

though on a smaller scale. At the west end of the outcrop, the greenschists and quartz boudins are deformed into a west verging tight fold in which the thinner layers have a shorter fold wavelength (a-Fig. 4.10b). Note the lobate-cuspate structure developed within the fold hinge-zone.

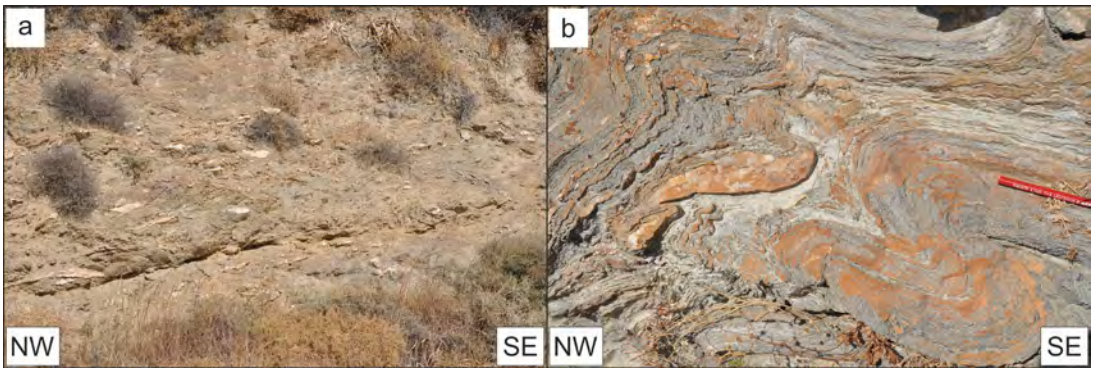

a-Figure 4.10
Upper Flabouria Formation. Low-angled normal fault.

a-Stop 4.11. Upper Flabouria Formation. Brittle-ductile conjugate C' fractures.
UTM 35S 268189E 4134754N.
a-Figs. 4.11, looking SE.

Be extremely careful when driving on the road down to Stypho Bay: the hard road surface has been undercut in many places on the outer (hill-slope) side, not necessarily visibly so from a vehicle, and likely no longer supports a heavy weight. Stay closer to the inner (outcrop) side of the road, although this is also locally undercut.

Drive back to Flabouria beach and take the road to the right, up to the main road. Turn right and drive 4.55 km southwards and then turn right, towards Stypho Bay and drive for 520 m, around the first sharp left hand bend. This outcrop lies within the Upper Flabouria Formation (sm 058/18°, lcr 056/16°), which is locally folded (lf 053/20°, sap 033/32°). The rocks show numerous shear-bands and SCC' structures, most of which record a clear top-to-the-SW kinematics (sc' 246/19°, lc' 219/16°). However, several isolated shear-bands dip in the opposing direction and suggest an apparent top-to-the-NNE shear. The existence of conjugate shear-bands (or strictly speaking, normal drag shear-bands with normal drag a-type flanking folds) has been interpreted to record a significant amount of a pure shear component during non-coaxial flow (Grasemann et al. 2003). The shear-bands are best seen where they cut quartz/feldspar veins that formed during an earlier stage of deformation and that were subsequently rotated into the shear direction. These veins are cut by shear-bands forming asymmetric shear-band boudinage structures (a-Fig. 4.11a). Penetrative SCC' fabrics form in more mica-rich layers and always record a monoclinic symmetry (a-Fig. 4.11b). Layers with SCC' fabrics indicating an opposite shear-sense have not been observed. In a-Fig 4.11c, conjugate brittle-ductile fractures offset the green-grey pelitic schists with foliation parallel (sm 051/48°) boudinaged quartz-veins. The offset is small and approximately similar on the two fractures but the south-dipping (upper) fracture is longer and is parallel to C' structures (sc' 185/21°) in the schists. The shorter fracture dies out into an asymmetric fold downwards and is cut off by the upper fracture. The offset of the lower fracture has deflected the upper fracture into a lower angle.

a-Stop 4.12. Petroussa and Upper Flabouria Formations. SCC' structures.
UTM 35S 268162E 4134852N.
a-Fig. 4.12, looking SE.

Read the warning at the start of a-Stop 4.11. Drive carefully another 520 m, around three corners. At this stop, a consistent top-to-the-SSW shear-sense can be observed from the ductile to the brittle-ductile and brittle deformation fields. The rocks lie around the boundary of the Petroussa Formation and overlying Upper Flabouria Formation (sm 072/12°, lm 041/10°). a-Fig. 4.12a shows an impure marble mylonite with calcite veins that have been strongly stretched to form isolated pinch-and-swell boudins. These isolated objects have been transformed into sigmoids during top-to-the-SSW shear deformation. The more phyllosilicate-rich layers developed SCC' fabrics.

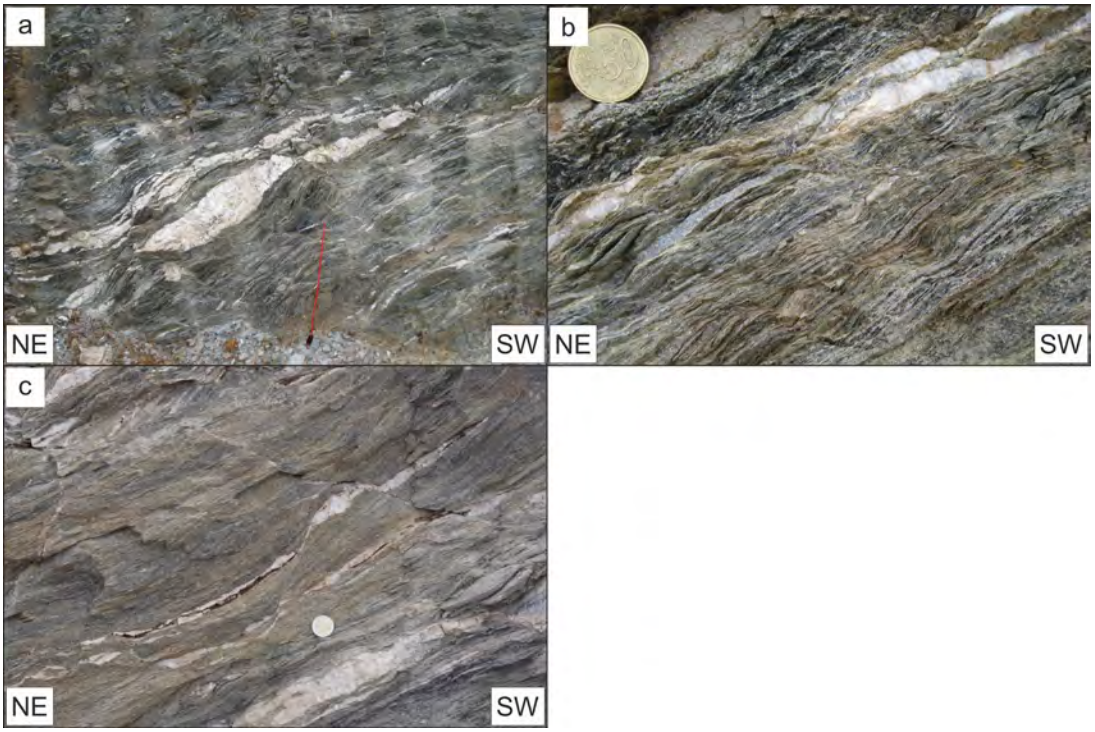

a-Figure 4.11
Upper Flabouria Formation. Brittle-ductile conjugate C' fractures.

Two closely spaced and very thin marble (mylonites) layers within yellow quartz–white-mica–calcite schists form C planes (sm 150/05°, lm 024/02°) whilst the adjacent and intervening schists develop top-to-the-SW C' planes, with the foliation back-rotated (a-Fig. 4.12d). Where the C' planes link with the C planes, the marble has flowed to fill the space created by the back-rotation, in both the hanging wall and footwall of the C' planes, such that the C plane is wholly unaffected by the back-rotation.

All structures in the outcrop are cut by several high-angle faults with several cm thick fault cores characterized by foliated cataclasites, scaly fabrics

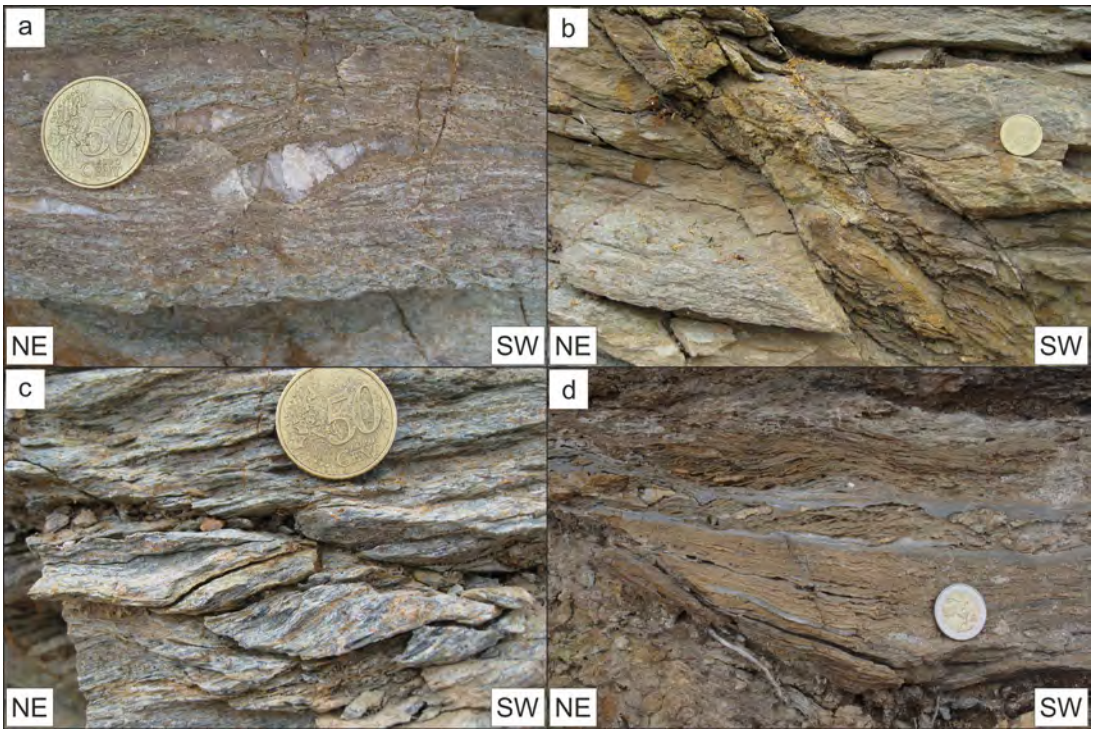

a-Figure 4.12
Petroussa and Upper Flabouria Formations. SCC' structures.

and synthetic Riedel fractures indicating top-to-the-S displacement. a-Fig. 4.12b shows such a brittle fault zone (sf 180/38°) with clear kinematic indicators for normal displacement (scaly fabric and secondary Riedel fractures). Although the border of the fault core is quite sharp, dragging of the host-rock foliation documents ductile deformation. Brittle deformation overprinting ductile structures is recorded by brittle fault zones which reactivate an earlier SCC' fabric (a-Fig. 4.12c).

a-EXCURSION 5: S. KYTHNOS; Aghios Dimitrios

a-Stop 5.8. Petroussa Formation. n-type flanking structure in mylonites.
UTM 35N 267155E 4133041N.
a-Figs. 5.8, looking N.

Drive 580 m WSW down the dirt road from the switchback at Stop 5.4 and park just around the first switchback. Essentially, this stop is to see a well-developed NW verging n-type flanking structure formed against a quartz-vein cutting across mylonites of the Petroussa Formation (a-Fig. 5.8). The vein is oriented 111/35°, parallel to the fold axial surface, with the fold axis plunging 197/13°, parallel to the stretching direction in the unfolded schists. A triclinic shear geometry or a non-plane strain general shear with a strong flattening component is implied by the structure, as the fold verges toward the NW whilst the regional shear is towards the SSW.

a-Figure 5.8
Petroussa Formation.
n-type flanking fold.

Note how the quartz-vein in the marble layer at the top of the succession is both boudinaged and folded whilst cutting through the folded mylonitic foliation in the marble (arrow in Fig. 5.8); there is little evidence of a new axial planar fabric forming.

a-Stop 5.9. Kanala Formation. Small-scale Riedel structures.
UTM 35S 267262E 4131472N.
a-Fig. 5.9a-d, looking WNW; a-Fig. 5.9e, looking NE.

From Stop 5.3, turn around, drive back, turn right at the cross-roads and proceed for 650m. Then take the left turning and after 30 m turn left again and proceed for 490 m. Then turn left and go to the end of the road. Walk 130 m west to the outcrops on the other side of the bay (a-Fig. 5.9a). Here Riedel fractures similar to those seen on the north side of Aghios Dimitrios at Stop 5.3 can be examined in detail. The host-rocks comprise green coloured coarse epidote schists of the Kanala Formation. Epidote porphyroblasts may be up to 5 mm long, idiomorphic, sometimes clustered and preferentially developed in particular layers and randomly oriented (Fig. D), despite the high strains expected of a location close to the West Cycladic Detachment System. These coarse epidote schists are also very similar to those in the Episkopi Formation (Stop 1.5).

The west side of the bay, which is oriented sub-parallel to the regional stretching direction, shows abundant Riedel fractures with a range of orientations; some are sub-vertical and others sub-horizontal (a-Fig. 5.9a) and many have thick brown (?ankeritised) fault zone rocks. Two fractures have been examined briefly (a-Fig. 5.9b); the descriptions give a flavour of the deformation seen, which is very variable in style and extent.

Fracture 1, at the northernmost end of the bay, is low-lying (sf 0163/18°; a-Fig. 5.9b) with a cataclastic 'core' zone 8-16 cm thick bounded above and below by discrete principal slip surfaces on which a lineation plunges at 189/16°, essentially parallel to the top- to-the-SSW M2 extension direction (stretching lineation in epidote schists plunges at 214/24°). Within this zone, a pelitic cataclastic fabric has been back rotated and cut by an SCC' fabric indicating top-to-the-SSW deformation (a-Fig. 5.9c; the C-planes are the principal slip surfaces and the Riedel fractures). Next to this 'core zone' are relatively narrow zones of coarser, unfoliated cataclasite, locally showing mineralisation from Fe-rich (likely carbonate) fluids. These cataclasites are also cut by discrete slip surfaces. The adjacent pelitic schists show variable degrees of cataclasis and reworking by SC' structures.

Fracture 2 (a-Fig. 5.9d), ~35 metres to the south, is steeper (sf113/49°). The fault 'core zone'

a-Figure 5.9
Kanala Formation. Small-scale Riedel structures.

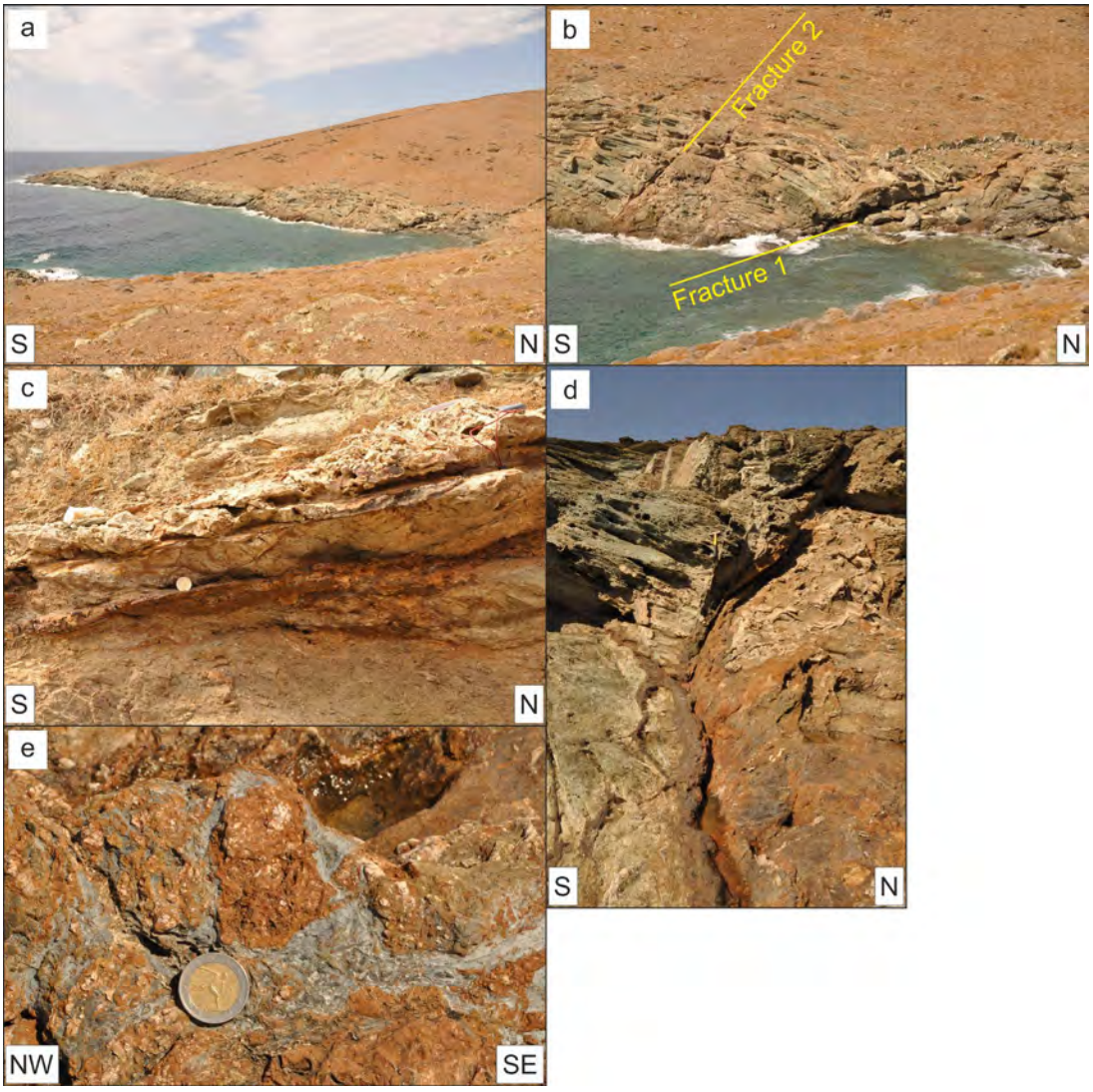

is only a few centimetres thick and has been partially affected by Fe-rich fluids; clasts of earlier generations of Fe-rich carbonate cataclasite lie within a blue-grey amorphous carbonate-free matrix (a-Fig. 5.9e). Where the fault steps right (north), up dip, abundant, relatively persistent adjustment faults formed, likely antithetic splays from the bend (by hammer, a-Fig. 5.9d).

a-EXCURSION 6: SW KYTHNOS; Aghios Dimitrios Bay

a-Stop 6.9. Lower Flabouria Formation. Folded lineation and formation of a new crenulation cleavage.
UTM 35S 267018E 4132586N.
a-Fig. 6.9, looking E.

At this outcrop the mylonitic foliation (sm 290/40°) with a strong stretching lineation (lm 235/15°) on quartz layers is deformed into isoclinal folds (lf 200/05°) with several cm-long wavelengths (a-Fig. 6.9). The folding is associated with the development of a new crenulation lineation (lcr 200/05°) and crenulation cleavage parallel to the axial surface (sap 300/10°) of the folds. On the axial planes, a new stretching lineation developed parallel to the fold axes. The folding is thought to be related to SSW-directed shearing and a result of ductile thinning of the footwall of the detachment during exhumation. A spaced joint system (sj 020/75°) developed almost perpendicular to the fold axis. The whole area, from here to the main detachment further west, is strongly overprinted by conjugate cataclastic high-angle normal faults (sf 020/60°, 210/60°) with several cm-thick fault

cores composed of foliated cataclasites with scaly fabrics, indicating NNE-SSW extension in the brittle deformation field.

a-Figure 6.9
Lower Flabouria Formation. Folded lineation and new crenulation cleavage.

Excursion 7. Sea Views

The outcrops described here show some of the important points of the geology of Kythnos seen from the ferries stopping at the island; the West Cycladic Detachment System in the southwest of the island, the extreme thinning of the Petroussa Formation across the island, from east to west, and the uncertain relationships between the Mavrianou and Petroussa Formations. Viewpoints may differ from those given, depending on the ferry route taken.

a-Stop 7.1. Normal fault in the coastal section.
UTM 35S 265329E 4145808N.
Viewed from UTM 35S 265000E 4145000N.
a-Fig. 7.1a, b, looking ENE.

De Smeth (1975) proposed that a normal fault lies in this valley (a-Fig. 7.1a), separating mr (Petroussa Formation) from mr1 (Mavrianou Formation; Fig. B), implying a significant offset. The position of this fault has been accurately superposed on a photography of the valley (a-Fig. 7.2b). No obvious sign of a fault can be seen, although this has to be checked in the field. This has significant consequences for the regional pattern of the marble units on the island and the overall structure of the island, since if no significant fault is present, all or some (see next Stop) of the marbles and quartz–white-mica–calcite schists along the west coast must be part of the Mavrianou Formation (compare Figs. B & C).

a-Stop 7.2. Uncertain affiliations in the coastal section.
UTM 35S 265329E 4145808N.
Viewed from UTM 35S 265100E 4144800N.
a-Fig. 7.2a, b, looking NE.

a-Fig. 7.2a shows a layer of yellow-weathered quartz–white-mica–calcite schists with thin mylonitic blue-grey marbles overlying grey (?albite) schists, in turn overlying yellow-weathered schists with marbles. If the upper unit is the Mavrianou Formation and the underlying schist the Upper Flabouria Formation (compare this with a-Fig. 7.3a), then the underlying marble-bearing rocks must belong to the Petroussa Formation. How these rocks link to the outcrops of 'marble' mapped by de Smeth (1975) to the east, further up the hill (a-Fig. 7.2b) is unknown; no definitive answers can be given yet, not least because the area is very difficult to access without a boat.

a-Stop 7.3. Mavrianou and Petroussa Formations; high strain facies.
UTM 35S 267660E 4136565N.
Viewed from UTM 35S 266250E 4135940N.
a-Fig.7.3, looking NE.

This shows the small but spectacular outcrop of Mavrianou Formation on the south side of Aghriolagadho Bay (a-Fig. 7.3, Fig. C; Stop 4.7). The Mavrianou Formation is here highly strained, with only thin boudins of blue-grey marble mylonite exposed towards the base of the yellow-weath-

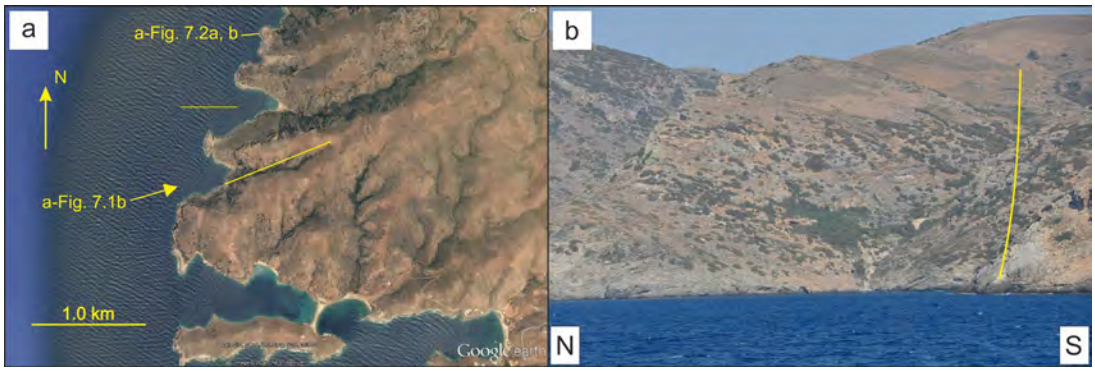

a-Figure 7.1
Fault proposed by de Smeth (1975; Fig. B).

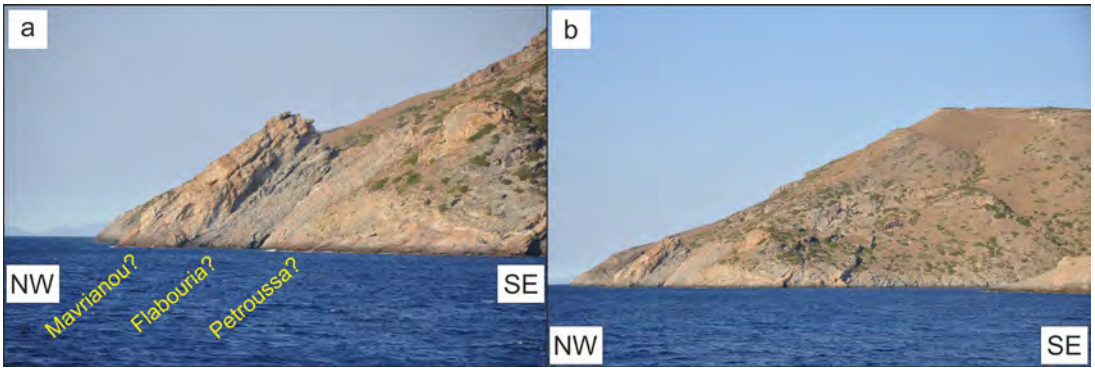

a-Figure 7.2
Mavrianou, Upper Flabouria and Petroussa Formations. High strains.

ered quartz–white-mica–calcite mylonites. These overlie grey schists with large quartz boudins and a coarse stretching lineation of the Flabouria Formation. Compare this outcrop with a-Fig. 7.2a.

a-Figure 7.3
Highly strained Mavrianou and Upper Flabouria Formations.

a-Stop 7.4. Thinning of the Petroussa Formation and the West Cycladic Detachment System.
Viewed from UTM 35S 265540 4133960.
a-Fig. 7.4a, b, looking SE; a-Fig. 7.4c.

The Petroussa Formation thins across southern Kythnos, but especially so in the Aghios Dimitrios area. The blue-grey marble mylonites at x, (a-Fig. 7.4a, c), is ~4 metres thick, forming the small cliff face; at y (Stop 6.1) only thin pinch-and-swell boudins of blue-grey marble, < 75 cm thick, can be found within the yellow-weathered quartz–white-mica–calcite schists of the Petroussa Formation. Compare these thicknesses with the 14 m thickness of blue-grey marble seen at a-Stop 7.7. The sudden steepening of the dip here (a-Fig. 7.4c) is due to the Kyra Leni Steep Belt.

From here, the WCDS can be seen on the south side of Aghios Dimitrios Bay above marble ultramylonites (MUM; Rizou Formation; line a, a-Fig. 7.4b, c). This has an apparent dip to the east in the figure, but actually dips very steeply to the west; the detachment also crops out to the west of the grey houses (line b). The footwall comprises quartzite cataclasites (Aghios Dimitrios Formation), seen in the foreground of the picture, weathered white.

a-Stop 7.5 Rizou and Aghios Dimitrios Formations. West Cycladic Detachment System.
UTM 35S 266695E 4132114N.
Viewed from UTM 35S 265800E 4131300N.
a-Fig. 7.5, looking NE.

From here, the knife-sharp boundary of the WCDS is clearly exposed (a-Fig. 7.5) between blue-grey marble ultramylonites (MUM) of the Rizou Formation in the hanging wall and quartzite cataclasites of the Aghios Dimitrios Formation in the footwall. The thin layer of calcite ultracataclasites (Stop 6.4; CUC) is also shown at the most southerly point it has been found so far. The succession seems inverted, but this is due to the oblique viewpoint.

a-Stop 7.6 Rizou and Aghios Dimitrios Formations. WCDS in profile.
UTM 35S 266479E 4131470N.
Viewed from UTM 35S 266870E 4130370N.
a-Fig. 7.6, looking NW.

This position (a-Fig. 7.6a) affords a good view of the WCDS on the southernmost part of the island (Stop 6.8), looking essentially along the strike of the detachment. Two planar surfaces are present; the upper one is the main detachment fault, separating the Rizou and Aghios Dimitrios Formations (hanging wall and footwall, respectively) with a relatively minor parallel LANF below. a-Fig. 7.6b was taken from further southwest, and hence closer to the outcrops, but the view is markedly oblique to the strike of the fault plane.

a-Figure 7.4
View of the WCDS.

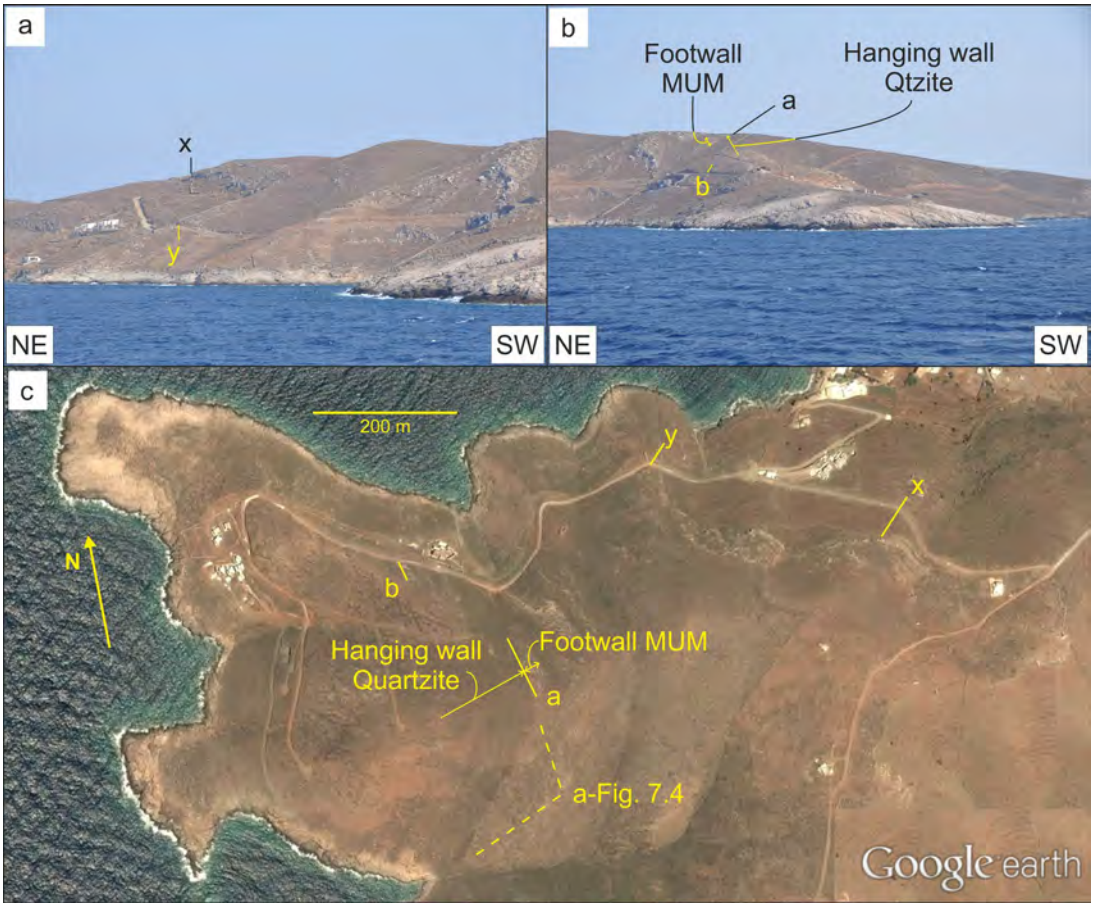

a-Figure 7.5
View of the WCDS.

a-Stop 7.7 Petroussa Formation. Thick blue-grey marble succession.
UTM 35S 268910E 4131990N.
Viewed from UTM 35S 269000E 4129000N.
a-Fig. 7.7, looking NNW.

This shows the maximum thickness (ca. 14m) of the blue-grey marble within the Petroussa Formation at Petroussa (a-Fig. 7.7a; Stop 5.2). This thins to essentially nothing on the south side of Aghios Dimitrios Bay, only 1.9 km due west of here (Stops 6.1, a-7.4).

a-Figure 7.6
View of the WCDS.

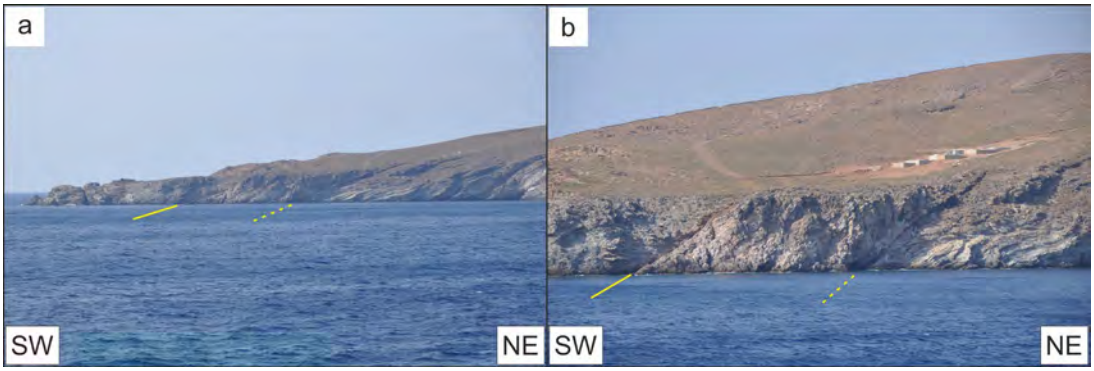

a-Figure 7.7
Petroussa Formation. Thick succession of blue-grey marble.